

THESIS

LIBRARY
Michigan State
University



This is to certify that the

dissertation entitled

An Exploration of the MALDI Experiment by Power Titrations, Mixture Analysis, and Prompt Fragmentation Analysis

presented by

Gary Nelson Lavine

has been accepted towards fulfillment of the requirements for

Ph. D. degree in Chemistry

Date 12.10.98

0-12771

PLACE IN RETURN BOX to remove this checkout from your record. TO AVOID FINES return on or before date due. MAY BE RECALLED with earlier due date if requested.

DATE DUE	DATE DUE	DATE DUE

1/98 c/CIRC/DateOue.p65-p.14

An Exploration of the MALDI Experiment by Power Titrations, Mixture Analysis, and Prompt Fragmentation Analysis

By

Gary Nelson Lavine

A DISSERTATION

Submitted to
Michigan State University
in partial fulfillment of the requirements
for the degree of

DOCTOR OF PHILOSOPHY

Department of Chemistry

1998

ABSTRACT

An Exploration of the MALDI Experiment by Power Titrations, Mixture Analysis, and Prompt Fragmentation Analysis

By

Gary Nelson Lavine

The technique of power titrations was used to study the matrix assisted laser desorption/ionization (MALDI) experiment. Power titrations are performed by irradiating a single spot on a MALDI sample and increasing the laser power at regular intervals. Component spectra are downloaded to disk so that sets of spectra with the same laser power are saved together. The resulting spectra are then displayed in the order that they were collected. By examining the results from power titrations the onset of different peaks can be compared. The onset of all of the peaks produced are very highly correlated with each other.

Power titrations have been found to be the most useful for the evaluation of MALDI samples prepared by different methods. Even small differences in the sample preparation method used can cause significant changes in the spectra that are produced. The dried droplet method, the Vorm method, the crushed crystal method, and a "combination" method were all evaluated with power titrations. Of these methods, the crushed crystal method was found to produce the best analyte signals for a wide variety of peptides. Use of the power titration procedure also highlighted the difficulty of producing reproducible samples.

Another aspect of the MALDI experiment that was evaluated was the occurrence of suppression effects in peptide mixtures. The most typical suppression occurs when an analyte that is easily detected, such as bradykinin, interferes with the detection of another analyte. In addition it is possible for an analyte that is not easily detected, such as bucalin, to interfere with the detection of other analytes. In the mixtures studied the magnitude of the suppression effect that occurred was dependent on the ratio of the analyte concentrations rather than the total amount of analytes.

Another aspect of the MALDI experiment that was studied was the formation of prompt fragment ions. The formation of prompt fragment ions was found to be matrix dependent. Bumetanide was identified as a promising matrix for prompt fragmentation analysis. The results from prompt fragmentation using bumetanide as the matrix are compared with prompt fragmentation using α -cyano-4-hydroxycinnamic acid and 2,5-dihydroxybenzoic acid. In addition a 4:1 mixture of bumetanide and α -cyano-4-hydroxycinnamic acid was evaluated. This matrix mixture produces abundant fragmentation at low laser power. With the use of this matrix mixture a very intense y_{11} prompt fragment ion of the b-chain of insulin is produced. The y_{11} prompt fragment ion was then selected for post-source decay (PSD) analysis. This is the first time that a prompt fragment ion has been successfully selected for MSⁿ analysis.

I would like to dedicate this dissertation to my parents Robert and Bylaina. My father was responsible for sparking my interest in science at a very early age. My mother has been a constant source of support ever since the first grade, when I had trouble learning to read. In return I promise to get a "real" job someday.

ACKNOWLEDGMENTS

I am deeply grateful to all of the people who in one way or the other helped me throughout my graduate career. One group of friends who provided a lot of support were my dinner group. At various times this group included Joy Heising, Sue Pasco, Shannon Majors, Tina Erickson, and Kevin White.

Throughout the first four years we managed to get together to cook each other dinner and to socialize. These get togethers were a much needed outlet. From this group the last remaining person Joy Heising deserves a special thanks as my best friend during this crazy time in my life.

I was also fortunate enough to receive some financial support through the MSU-NIH Mass Spectrometry Facility. I would like to thank both Doug Gage and Dr. Jack Watson. In addition I would like to thank Mel Micke and Nat Riddle for technical assistance over the course of my career. I also received a dissertation completion fellowship from the College of Natural Science. Finally I was also supported by Science Theatre for a semester as I worked on a book of science demonstrations. I also would like to thank my father and sister who both provided some last minute emergency proofreading.

Of course the most important person during my graduate career was my advisor John Allison. It is not an easy thing to have me as a student and JA was more than equal to the challenge. I am only now starting to realize how much I have learned under JA's guidance.

TABLE OF CONTENTS

List of Tables.	i)
List of Figures	
List of Abbreviations	xii
Chapter one. Introduction	1
1. Historical Context	1
2. Research Objectives-a Technique to Probe the MALDI System	7
3. References	12
Chapter two. The Development of Power Titrations as a Technique for S the MALDI Process	
1. Introduction	14
2. Experimental	17
3. The Usefulness of Power Titrations	32
4. References	33
Chapter three. Evaluation of Sample Preparation Techniques	34
1. Introduction	34
2. The Standard Method of Sample Preparation	36
3. Alternative Sample Preparation Procedures	43
4. References	60
Chapter four. Suppression Effects of Peptides and Proteins Using α -cyahydroxycinnamic Acid as a matrix for MALDI	
1. Introduction	61
2. Results and Discussion	65
2 Peferences	04

Chapter five. Prompt Fragmentation (PF-MALDI)	83
1. Introduction	83
2. Results and Discussion	85
3. Chemistry of Fragmentation	99
4. Combining Matrices	106
5. Prompt Fragmentation-Post Source Decay	107
6. Conclusion	111
7. References	112
Appendix	114

LIST OF TABLES

Table 4.1	Peak heights of bradykinin under different conditions	
Table 4.2	Peak heights of the b-chain of insulin under different conditions	
Table 5.1	Effect of type of residues on fragmentation	

LIST OF FIGURES

Figure 1.1	Three dimensional representation of a typical MALDI experiment
Figure 1.2	Three dimensional representation of a typical power titration
Figure 2.1	Diagram of the Vestec 2000, linear MALDI-TOF instrument
Figure 2.2	Power titration of angiotensin in a-cyano-4-hydroxycinnamic acid
Figure 2.3	Matrix region of the power titration spectrum of angiotensin
Figure 2.4	Theoretical spectrum of C₄H₃N⁺
Figure 2.5	Region of the protonated analyte peak in the power titration of angiotensin
Figure 2.6	Region of the Na ⁺ peak in the power titration of angiotensin
Figure 2.7	Three component spectra of the power titration of angiotensin in $\alpha\text{-cyano-4-hydroxycinnamic}$ acid
Figure 3.1	Power titration spectrum of the seven component mixture, prepared by the analyte first dried droplet procedure
Figure 3.2	Power titration spectrum of the seven component mixture, prepared by the matrix first dried droplet procedure
Figure 3.3	Power titration spectrum of the two component mixture, prepared by the dried droplet procedure
Figure 3.4	Matrix region of the power titration spectrum of the two component mixture, prepared by the dried droplet procedure
Figure 3.5	Power titration spectrum of the two component mixture, prepared by the Vorm procedure
Figure 3.6	Matrix region of the power titration spectrum of the two component mixture, prepared by the Vorm procedure
Figure 3.7	Power titration spectrum of the two component mixture, prepared by the crushed crystal procedure
Figure 3.8	Matrix region of the power titration spectrum of the two component mixture prepared by the crushed crystal procedure

Figure 3.9	Power titration spectrum of the two component mixture, prepared combo procedure
Figure 3.10	Matrix region of the power titration spectrum of the two componen mixture, prepared by the combo procedure
Figure 3.11	Comparison of the component spectra taken at a laser power of 1450 for the different preparation procedures
Figure 3.12	Expanded view of bradykinin in the comparision of the component spectrum taken at a laser power of 1450 for the different preparation procedures
Figure 3.13	Comparision of the component spectra taken at a laser power of 2500 for the different preparation procedures
Figure 3.14	Power titration spectrum of the two component mixture, prepared by the pure crushed crystal method
Figure 3.15	Matrix region of the power titration spectrum of the two component mixture, prepared by the pure crushed crystal method
Figure 4.1	High power spectrum of six component mixture
Figure 4.2	MALDI spectrum of 5 pm cytochrome C
Figure 4.3	Low power spectrum of six component mixture
Figure 4.4	Spectrum of 1:1 mixture of bradykinin and b-chain of insulin
Figure 4.5	Spectrum of 1:9 mixture of bradykinin and b-chain of insulin
Figure 4.6	3 consecutive spectra of a 1:1:1 mixture of bradykinin, b-chain of insulin and insulin
Figure 4.7	3 consecutive spectra of a 3:1:1:1 mixture of bucalin, bradykinin, b chain of insulin, and insulin
Figure 5.1	Structure and ultraviolet-visible absorption spectrum of bumetanide
Figure 5.2	MALDI mass spectrum of bumetanide as a matrix
Figure 5.3	Prompt fragmentation spectra of dynorphin with a) DHB, b) HCCN and c) BMN

- Figure 5.4 Prompt fragmentation spectra of MSH with a) DHB, b) HCCN, c) BMN (karat symbol above two peaks represents pairs of a_n and a_n NH₃ ions)
- Figure 5.5 Prompt fragmentation spectrum of the b-chain of insulin in a) HCCN, b) DHB (square brackets represent pairs of y_n and Z"_n ions)
- Figure 5.6 Prompt fragmentation spectra with a) BMN, b) HCCN and b) 4:1 BMN:HCCN
- Figure 5.7 Post source decay of the y₁₁ prompt fragment ion of the b-chain of insulin

LIST OF ABBREVIATIONS

A/D	Analog-to-digital conversion
A	Alanine
AH ⁺	Protonated angiotensin
B	Bradykinin, Cysteic acid
b-chain	
BH ⁺	
BMN	
CAD	
C	•
CH ⁺	
CH ₂ ²⁺	Doubly protonated cytochrome C
CH ₂ ²⁺	Triply protonated cytochrome C
Cu ⁺	
D	
Da	•
DHB	
Dyn	• • • • • • • • • • • • • • • • • • • •
E	
F	
Н	• • • • • • • • • • • • • • • • • • •
H ⁺	
HCCN	
I	
IH ⁺	
IbH ⁺	
J	
K	
K ⁺	
L	
M	
M/z	•
MALDI	
MeH ⁺	······································
MS	
MS ⁿ	Mass spectrometry to the nth newer
MSH	
MW	
MyH+	Protonated myoglobin
MyH ₂ ²⁺	
Na+	
ns	
0	
Q	Glutamine

Proline	P
Prompt Fragmentation	
Post source decay	
Arginine	
Serine	
time	
Time-of-flight	
Volt	
Tryptophan	Y

Chapter one. Introduction

1. Historical Context

Laser Desorption

Laser desorption mass spectrometry (MS) was one of the earliest methods used to analyze thermally labile molecules. Laser desorption has been performed with a large number of analytes. These analytes include alkali salts, oligosaccharides, oligionucleotides, peptides and polymers¹. In this work I will be concentrating on the analysis of peptides. For peptides the upper mass limit of laser desorption is approximately 2000 Da².

Laser desorption MS is performed by dissolving an analyte in a volatile solvent such as methanol or ethanol. A drop of the sample solution is then placed on a stainless steel surface and the solvent is allowed to evaporate. A thin layer of the analyte remains on the surface after the solvent has evaporated. This layer is typically too thin to be seen by the unaided eye². The sample is then placed in the mass spectrometer. A variety of types of mass spectrometers have been used for laser desorption; these instruments include dual sector mass spectrometers, time-of-flight mass spectrometers, and Fourier transform mass spectrometers. The sample is then irradiated by the laser and the analysis begins. The most common laser that is used with peptides is a CO_2 laser. This type of laser produces photons at a wavelength of 10.6 μ m and a pulse width of 40 ns.

Few results have been reported using this technique for the analysis of peptides. The first spectrum of a peptide was reported in 1978³. This experiment was performed with a double-focusing mass spectrometer. In this experiment the laser was fired to produce the desorption, then there was a delay of 500 μs before an extraction pulse was applied to accelerate the ions. A custom made array detector detected a range of m/z values in a single pulsed acquisition. An octapeptide with a molecular weight of 718 Da was analyzed with this instrument. The resulting spectrum consisted of Na⁺ and K⁺ adducts of the intact peptide, and a single fragment that was also a metal adduct.

Time-of-flight mass spectrometry has also been used for laser desorption of peptides^{4,5}. In this experiment the sample was irradiated with light from a CO₂ laser. There is then a delay time of 10-20 μs before the extraction voltage is applied. In this work a short delay produced poor resolution and multiple cleavages of the peptide backbone, while longer delays produced higher resolution and little fragmentation. The peaks corresponding to the analyte were the sodium and potassium adducts^{4,5}.

Another type of mass spectrometry that has been used in the analysis of laser desorption products is Fourier transform mass spectrometry. In this technique the analyte is desorbed and ionized by the laser. The products are accelerated into a sample cell. The cell is contained in a homogenous magnetic field and an electrostatic potential is applied to the end plates of the cell so that the ions are forced into circular trajectories based on their mass-to-charge ratio. An excitation pulse is then used to force all of the ions of a given m/z value to

bunch together in space and orbit together. A pair of receiver plates detects the current from these orbits. The time data is converted into data in the frequency domain. The frequency of an ion packet in a circular orbit is inversely proportional to the m/z of the ions in the packet⁶. After the analyte is desorbed the analytes are allowed to stay in the cell for 3-10 seconds before the detection is done. Using this method, a protonated analyte is typically detected along with sodium and potassium adducts. In addition there are very intense peaks from fragmentation products. The fragments tend to occur from breakage of the peptide bonds⁷.

There are two main theories about the mechanism of laser desorption. When energy is introduced into a solid analyte two processes it can undergo are desorption and decomposition. Desorption is a high energy fast process, while decomposition is a low energy slow process. In general the desorption of thermally labile molecules is thought to occur when enough energy is put into the molecule so that the rate of desorption exceeds the rate of decomposition. The laser provides a very efficent means to heat the sample quickly. A wide array of lasers are used in this work with laser powers that from 50 kW to 100 MW and wavelength that range from 151 μ m to 10.6 nm⁸. These lasers include both continous wave and pulsed lasers. The laser raises the temperature of the stainless steel surface at a rate of $10^8 - 10^{12}$ K/s ⁸. Energy then flows through the surface adsorbate bond to heat the analyte. The energy from the laser is transferred to the peptide at a relatively slow rate, from the substrate, so the

bonds between the substrate surface and the peptide break before the bonds in the analyte break⁸.

Matrix Assisted Laser Desorption/Ionization (MALDI)

In 1987 Hillenkamp modified the typical laser desorption experiment by adding a matrix of nicotinic acid in a large excess to the analyte⁹. This technique greatly increased the mass range of analytes that could by detected. This first work was done with a Nd/YAG laser at a wavelength of 266 nm. Nicotinic acid has a high molar absorbtivity at this wavelength. The technique was soon adapted to UV lasers by the use of different matrices. UV lasers have the advantage of being inexpensive and compact. Much of the work that is being done currently in this field uses nitrogen lasers, which emit light at a wavelength of 337 nm¹⁰. This technique is referred to as matrix assisted laser deorption/ionization (MALDI).

The MALDI experiment is typically performed by mixing together a matrix solution and an analyte solution and letting the combined sample dry. Typical matrices include cinnamic acid derivatives such as caffeic acid, sinnapinic acid, and α -cyano-4-hydroxycinnamic acid¹¹. In addition 2,5-dihydroxybenzoic acid has also found use as a MALDI matrix¹².

Matrix assisted laser desorption/ionization has become a very powerful technique for the analysis of peptides and proteins. Using this technique the mass range is well in excess of 100,000 Da and attomolar amounts can be detected 13,14. The predominant analyte related peak is from the protonated

analyte. However there are also minor peaks representing metal ion adducts. The majority of work with this technique is performed using time-of-flight mass spectrometry. MALDI is typically considered a "cool" desorption technique since peaks from fragmentation products are typically not observed. However metastable decay does occur after the acceleration out of the ion source¹⁵.

Current Models of the MALDI Process

The mechanisms that have been proposed for the desorption process in MALDI are similar to the mechanisms proposed for Laser desorption. The matrices used in this technique are always strong absorbers in the wavelength region in which they are used. The matrix absorbs energy from the laser as a first step. The most prevalent model for the desorption process is that the matrix heats up very quickly without heating the analyte. The high temperature causes the matrix to quickly sublime. As the matrix quickly sublimes the analyte is entrained into the gas phase. The analyte does not have a lot of internal energy because energy is slow to transfer from the matrix to the analyte. This model is called the bottleneck model 16. Another possible model for the desorption process is that as energy is deposited into the matrix a pressure gradient is set up in the matrix. Once this pressure gradient exceeds a threshold value a pressure pulse is created which causes the matrix to suddenly expand 17. The rapidly expanding matrix would have analyte entrained within it.

The ionization in the MALDI process could be occurring by a number of means. One of the processes that could be involved is excited state acid-base

chemistry. In this model, laser irradiation of the matrix produces excited state acids, which could then react with the analyte or other matrix molecules ¹⁸. According to this mechanism the proton transfer could occur in the solid state or in the gas phase. If the protonation occurred in the gas phase it would be similar to chemical ionization. The ionization process could also proceed through the steps of photoionization of the matrix and proton transfer to the analyte ¹⁹.

The majority of current theories on the mechanism of ionization rely on either photoionization or photoexcitation of a single matrix molecule to give rise to the proton transfer²⁰. However other possibilities are also being proposed. Multiply excited matrix aggregates, formed by photoexcitation, may also serve as the source of protons for protonated analytes ^{21,22}. One other possibility is that matrix excitation occurs through fast heating of the matrix. It has been shown that for peptides under 3000 Da a protonated analyte peak can be detected by quick heating of a model sample on a filament ²³. The relatively low mass limit of this experiment could be explained by the fact that the filament heat the matrix and sample at a much slower rate than laser irradiation. The one area of general agreement in the field is that a variety of ionization processes are occurring in the MALDI experiment ^{19,20}.

2. Research Objectives-a Technique to Probe the MALDI System

The variables that can be controlled; during a MALDI experiment include the number of acquisitions, the laser power, and the position of the laser spot. These parameters can be used to define a three dimensional space. We define the acquisition number as our abscissa. Component spectra are acquired at a constant rate throughout the experiment, so the total number of component spectra is directly proportional to the length of the experiment. The ordinate corresponds to the position of the laser spot on the surface. The laser power is defined as the Z value in this representation of the MALDI experiment. Finally, in our instrument the sample is placed on a round sample pin that has a radius of 1 mm, these pins are inserted into a carousel which is inserted into the instrument. The laser irradiates the sample with a laser spot that is much smaller than the surface of the sample pin. Turning the carousel moves the sample, as the carousel turns the individual pins spin in place. The laser spot position is fixed at an edge of the pin and the pins rotate to allow different parts of the sample to be irradiated. The position value of the laser spot actually corresponds to the amount that the sample has been rotated. The actual amount that the sample pin rotates varies from experiment to experiment, for this reason no attempt is made to quantitate how much the pins rotates.

In a typical acquisition in the MALDI experiment the sample position and laser power are varied with the number of acquisitions, and are averaged together. This type of experiment is represented on the axes system in Figure

1.1. In this example the experiment is started at a laser power of 200 and then raised to a laser power of 250 over the course of 5 acquisitions. The laser power is then increased to 275 over the next 15 acquisitions. During the first 20 acquisitions the same spot on the sample is irradiated. Over the course of the next 40 acquisitions laser spot position and the laser power are both varied. As illustrated in Figure 1.1 the typical MALDI experiment does not represent an orderly trip through the range of possibilities that we have defined. The only goal of the typical MALDI experiment is to produce a high resolution, high signal to noise spectrum.

In order to reproducibly study the effects of different variables on the MALDI experiment a reproducible spectrum acquisition protocol must be developed. Power tirations were developed in order to fill this need. A power titration is simply a method to systematically explore the variable space that we have defined. In order to study the effects on a given spot the laser position is always held constant. During this experiment, the laser power is increased at regular intervals. Typically the experiment is continued for a large number of total acquisitions so a wide range of laser powers can be explored. The representation of this type of experiment in the previously defined variable space is shown in Figure 1.2. In order to observe the changes that occur during the experiment a spectrum is always saved to disk just before the laser power is increased. A new spectrum is then started at a higher laser power.

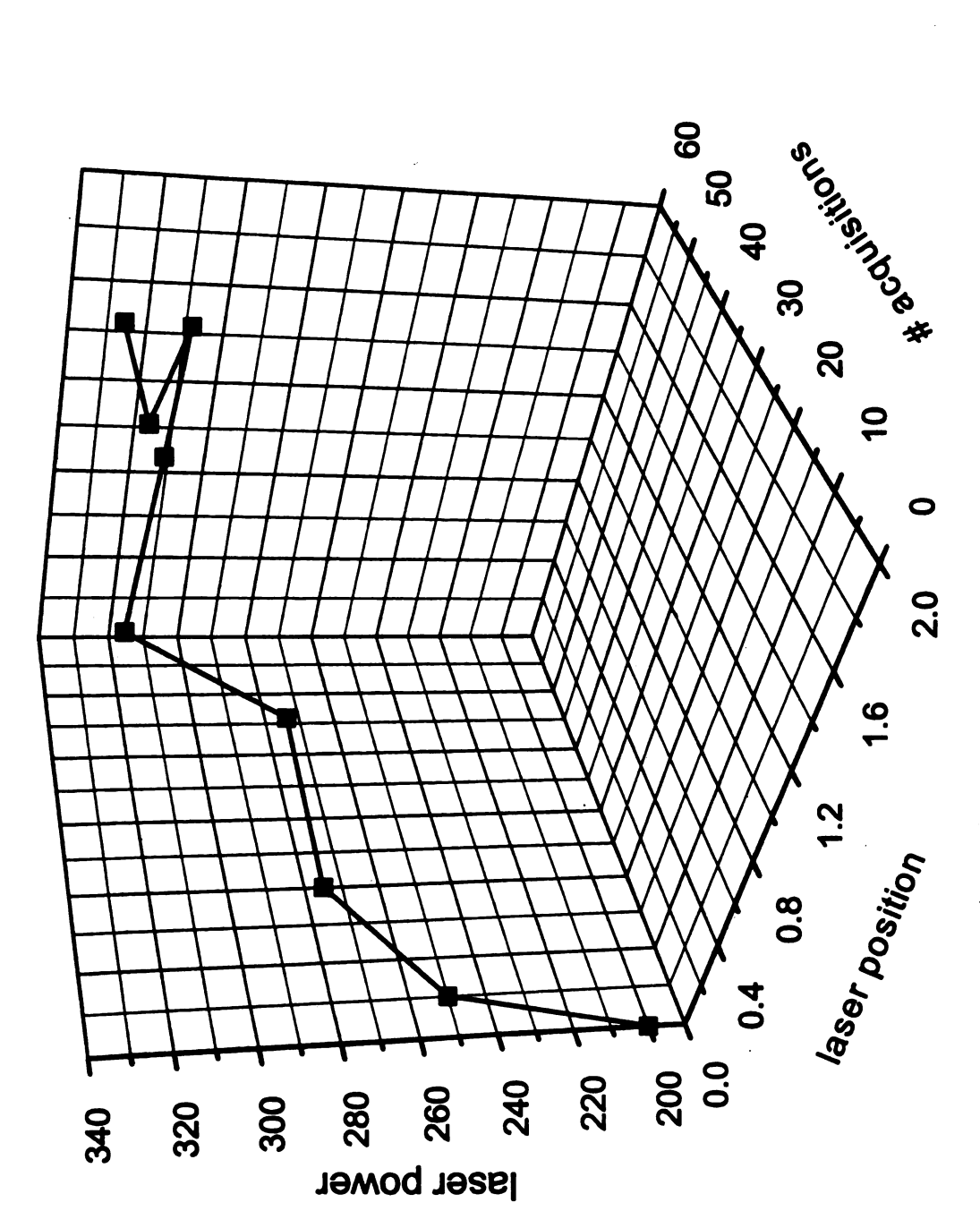


Figure 1.1 Three dimensional representation of a typical MALDI experiment

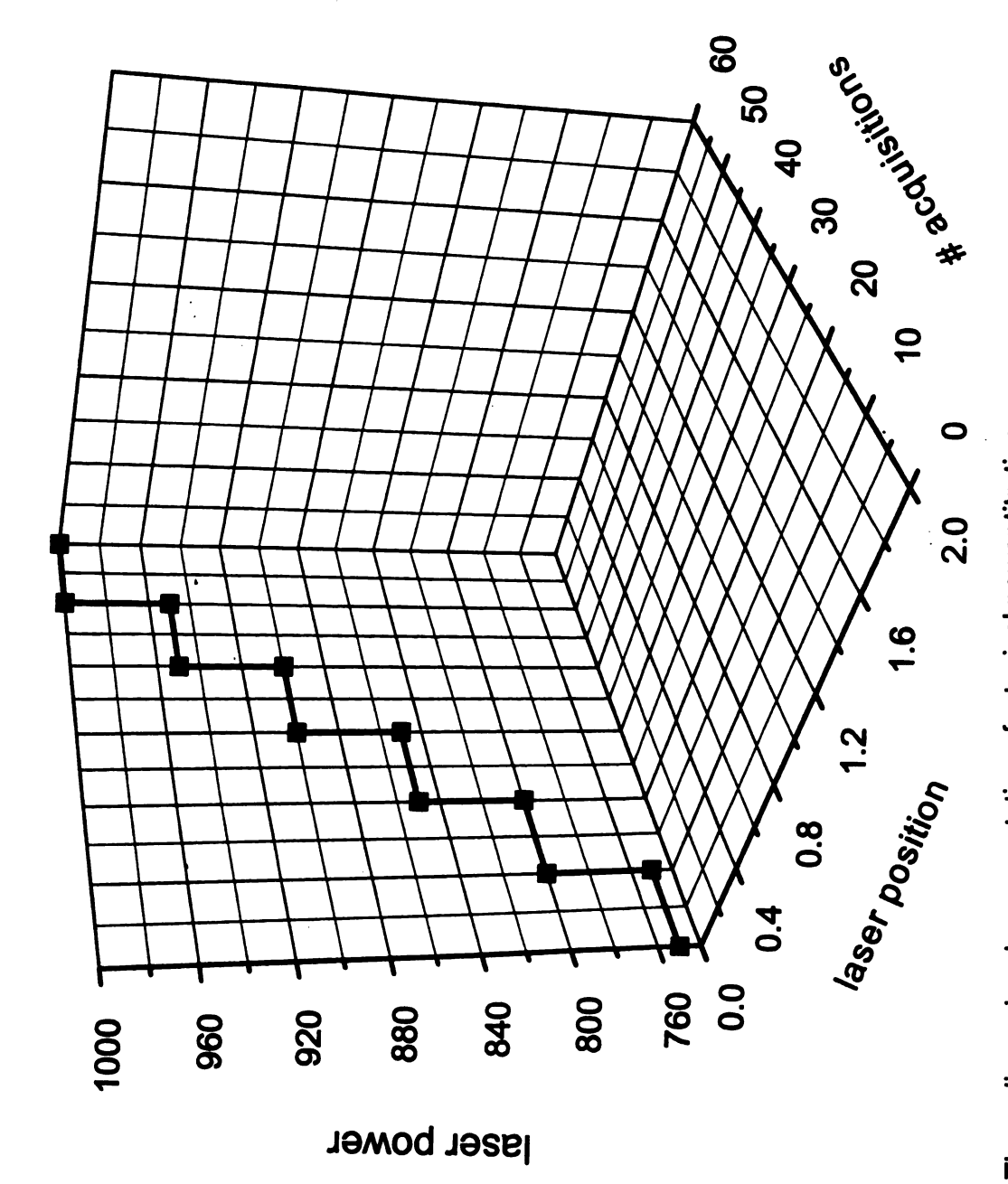


Figure 1.2 Three dimensional representation of a typical power titration

By performing a series of power titrations under slightly different conditions, much can be learned about the MALDI experiment. Power titrations can be used to study the effect that repeated laser shots have on the sample surface. Since the laser spot is held constant, one spot is subjected to a large number of laser shots. In addition the power titration technique can be used as a standardized acquisition method to study different types of MALDI samples. One example of different samples that can be compared is MALDI samples that are prepared by different techniques. The effects of power titrations on mixtures of different analytes has also be studied.

By using power titrations with mixtures prepared by different sample preparation techniques the best methods for analyzing mixtures were identified.

MALDI is a very quick and easy method to analyze mixtures of peptides and proteins. By optimizing mixture analysis I hope to make the technique even easier. In addition I will evaluate the likelihood of selected components of a mixture not being detected.

At very high laser power in power titrations peaks sometimes appear corresponding to peptide fragments. These fragments are forming in the ion source and are not a result of metastable decay. These fragments could be useful for obtaining structural information about peptides. In addition these prompt fragments provide an opportunity to study the fragmentation of peptides under a different set of conditions.

3. References

- 1)Conzemius, R. J.; Capellen, J. M. *International Journal of Mass Spectrometry and Ion Physics* **1980**, *34*, 197-271.
- 2)Cotter, R. J. Analytica Chimica Acta 1987, 195, 45-59.
- 3)Posthumus, M. A.; Kistemaker, P. G.; Meuzelaar, H. L. C.; Brauw, M. C. T. *Analytical Chemistry* **1978**, *50*, 985-991.
- 4) Tabet, J. C.; Cotter, R. J. Analytical Chemistry 1984, 56, 1662-1667.
- 5)Stoll, R.; Rollgen, F. W. Organic Mass Spectrometry 1979, 14, 642-645.
- 6)Buchanan, M. V.; Hettich, R. L. Analytical Chemistry 1993, 65, 245A-258A.
- 7) Wilkins, C.; Weil, D.; Yang, C. L. C.; James, C. F. *Analytical Chemistry* **1985**, *57*, 520-524.
- 8) Levis, R. J. Annual Reviews in Physical Chemistry 1994, 45, 483-518.
- 9) Karas, M.; Hillenkamp, F. Analytical Chemistry 1988, 60, 2299-2305.
- 10)Beavis, R. C.; Chait, B. T. Rapid Communications in Mass Spectrometry 1989, 3, 342.
- 11)Beavis, R. C.; Chaudhary, T.; Chait, B. T. Organic Mass Spectrometry 1992, 27, 156-158.
- 12) Karas, M.; Ehring, H.; Nordhoff, E.; Stahl, B.; Strupat, K.; Hillenkamp, F.; Grehl, M.; Krebs, B. *Organic Mass Spectrometry* **1993**, *28*, 1476-1481.
- 13)Doktycz, S. J.; Savickas, P. J.; Krueger, D. A. Rapid Communications in Mass Spectrometry 1991, 5, 145-148.
- 14) Vorm, O.; Roepstorff, P.; Mann, M. Analytical Chemistry 1994, 66, 3281-3287.
- 15) Spengler, B.; Kirsch, D.; Kaufmann, R. Rapid Communications in Mass Spectrometry 1991, 5, 198-202.
- 16) Vertes, A.; Gijbels, R. Rapid Communications in Mass Spectrometry 1990, 4, 228-232.
- 17) Johnson, R. E.; Sundqvist, B. U. R. Rapid Communications in Mass Spectrometry 1991, 5, 574-578.

- 18) Dikler, S.; Kelly, J. W.; Russell, D. H. *Journal of Mass Spectrometry* **1997**, *32*, 1337.
- 19) Ehring, H.; Karas, M.; Hillenkamp, F. Organic Mass Spectrometry 1992, 27.
- 20)Liao, P.-C.; Allison, J. Journal of Mass Spectrometry 1995, 30, 408-423.
- 21)Knochenmuss, R.; Dubois, F.; Dale, M. J.; Zenobi, R. Rapid Communications in Mass Spectrometry 1996, 10, 871-877.
- 22)Knochenmuss, R.; Karbach, V.; Wiesli, U.; Breuker, K.; Zenobi, R. Rapid Communications in Mass Spectrometry 1998, 12, 529-534.
- 23)Karbach, V.; Knochenmuss, R.; Zenobi, R. *Journal of the American Society for Mass Spectrometry* **1998**, 9, 1226-1228.

Chapter two. The Development of Power Titrations as a Technique for Studying the MALDI Process

1. Introduction

Goals

The technique of matrix-assisted laser desorption/ionization has greatly expanded the range of analytes that can be detected with mass spectrometry. However the mechanism of this technique is poorly understood. At this time even the effects that different parameters have on the experiment are poorly mapped out. Power titrations were developed in an attempt to better understand the multidimensional nature of data acquisition in the MALDI experiment.

Once reliable data are obtained the data can be used to help answer questions that are fundamental to the MALDI experiment. Power titrations provide a means to study the effect of continued irradiation of the sample. The development of some guidelines could be useful for comparing the results between different laboratories and provide rules for obtaining a standard MALDI spectrum.

The results from power titrations can also be used to help probe mechanistic aspects of the MALDI experiment. The most obvious experiment would be to determine which matrix peaks correlate the most highly with the formation of the protonated analyte peak. Any peaks that have a strong correlation with the protonated analyte could be incorporated into proposed mechanisms of the desorption/ionization process. In addition by observing the laser power onset of the various matrix peaks, reactions in the matrix could be potentially identified.

The Power Titration Procedure

There are a number of variables that are carefully controlled in the power titration experiment. The entire experiment is performed at a single spot on the sample. Our instrument has been modified so that the focus of the laser spot can be controlled by changing the distance between the focussing lens and the sample. Although the effect of spot size is poorly understood, the size of the laser spot has been found to affect the MALDI experiment¹. As the lens is moved further away from the sample a larger area of the sample is irradiated. The position of the lens can be characterized by a vernier scale on the stage on which the lens is mounted. Unfortunately the numbers on the scale have not been calibrated to actual laser spot sizes. The difficulty lies in the measurement of the laser spot size on the sample surface. We simply use the scale values as a relative indication of the laser spot size. A value of 65 corresponds to the lens being positioned up against the source housing to produce the smallest spot possible. This is the standard position for the lens and produces a spot with a radius on the order of .1 mm. A position of 40 is the largest spot that we found to be practical for MALDI analysis. With this lens position the laser spot has a radius of about .4 mm. As the laser spot gets bigger, higher laser powers are necessary to achieve the fluence 2 to perform the MALDI experiment.

The next component of the power titration experiment is to select an initial laser power. The laser power is best discussed relative to the threshold for a given sample. I define a sample's threshold as the laser power at which the

protonated analyte peaks have a signal-to-noise ratio of 3:1. The initial laser power can either be above or below the threshold laser power. Using an initial laser power that is above the threshold laser power produces a power titration, which contains signal throughout the experiment. By using an initial laser power that is below the threshold laser power, the appearance laser powers of matrix and analytes can be detected and compared.

In the MALDI experiment the number of spectra that can be recorded at a given spot with a single laser power is limited. The higher the laser power that is used the more spectra that can be recorded before the analyte signal decays ³. The amount of material (matrix and analyte) that is ablated from the sample, per laser shot, is also increased at higher laser powers⁴. The amount of material that is ablated in a typical MALDI experiment is 1 x 10¹³ – 1 x 10¹¹ particles per laser shot ⁴. When the signal is depleted at any laser power the power can be increased to produce more signal⁵. These trends indicate that photochemistry is occuring on the matrix at laser powers used in the MALDI experiment. The types of photochemistry that could be occurring are photodissociation and solid state dimerization. Products that could be from photodecomposition and dimers are detected in the matrix spectrum. Solid state dimerization of cinnamic acid derivatives has also been reported⁶.

In order to determine if any chemistry is occurring below the laser power necessary to produce desorption/ionization, a sample can be irradiated below the threshold laser power prior to the power titration. The results from a pre-irradiated sample can then be compared with the results from a standard power

titration. If the MALDI threshold values are shifted then the matrix is undergoing photochemistry at laser powers that are lower than required for the MALDI experiment.

Finally the number of laser shots that are acquired in a single spectrum needs to be determined. The advantage of averaging together a small number of laser shots is that subtle changes in intensities can be detected. In contrast averaging together a large number of spectra allows for spectra with less noise.

2. Experimental

Instrumental Setup

The instrument used in this work was a Vestec 2000, illustrated in Figure 2.1, linear time-of-flight instrument with an adjustable focussing lens for the laser. The Vestec 2000 has a single stage source that has a maximum acceleration voltage of 30 kV. In addition this instrument also has a guide wire in the flight tube to improve the transmission of ions. This instrument used stainless steel sample pins with a radius of 1 mm. These pins were mounted in a 24 pin carousel that could be rotated to select different samples. The movement of the carousel is controlled by pressing a joystick left and right. By moving the joystick up and down the laser power can also be controlled. In addition one of the joystick buttons is used to start the acquisition of a spectrum while the other button is used to download a spectrum to disk.

The laser used with this instrument is a VSL-337ND nitrogen laser (Laser Science Incorporated). This pulsed laser produces a 3 ns pulse of radiation at a

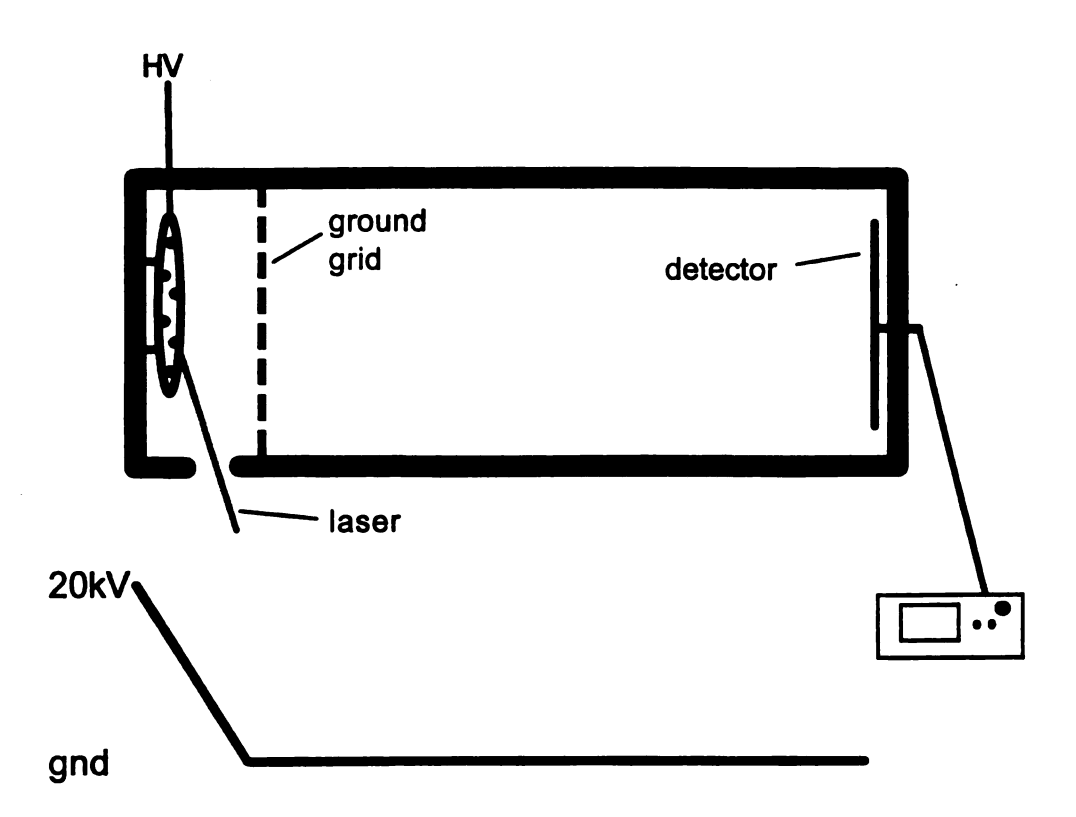


Figure 2.1 Diagram of the Vestec 2000, linear MALDI-TOF instrument

wavelength of 337.1 nm. The pulse energy of this laser varies from 150 to 250 μJ depending on the age of the nitrogen tube. The laser beam is passed through a 935-5-opt (Newport, Irvine, CA) laser atenuator, which controls how much radiation reaches the sample. The atenuator has been calibrated with the use of an 818j-09/DC (Newport, Irvine, CA) energy detector. A low laser power setting of 200 represents a laser power of 24 μJ. While a high laser setting of 5000 represents a laser power of 68 μJ. In this range the laser power varies linearly with the laser setting. For all of the results reported in this work only the laser setting will be reported, since the actual laser power was not measured for every experiment. An aproximation of the actual laser power could be calculated by interpolation. However the accuracy of these calculated values would be suspect since different laser cartridges were used over the course of this work and slippage was observed in the laser attenuation mechanism.

The standard sample preparation was done by placing 1 μ L of an analyte solution of 1:1 acetonitrile: 0.1% aqueous trifluoroacetic acid (TFA) on the sample pin. 1 μ L of 1:1 acetonitrile: 0.1% TFA saturated in matrix solution was than added to the sample pin. The solution was then allowed to air dry to form crystals.

The first step in a power titration is to pick a part of the sample to irradiate.

Typically I selected either the center or the left edge of the sample, since this laser position produces the greatest sensitivity, due to geometry of the ion source. Next a starting laser power is selected. The threshold of five samples is measured and the initial laser power is selected relative to the measured

threshold. Depending on how large of a range of laser powers are to be explored, a laser power increment is also determined. The number of acquisitions to be averaged together to produce a spectrum is then entered into the acquisition control software.

At this point the actual power titration experiment can be performed. The first spectrum is acquired by pressing the start button on the joystick. When the acquisition is completed the component spectrum is immediately downloaded to disk. While the spectrum is being transferred, the laser power is incremented. As soon as the spectrum is saved, another acquisition is started. This cycle is repeated 30 to 40 times to produce a complete power titration.

Once the acquisition is complete the separate data files are made into a multifile for display purposes. A multifile is a single file that contains a series of spectra that are sorted in the order they were acquired. Using the mfutil program, which is included with the acquisition software, creates the multifile. The resulting file is very hard to examine due to noise being present in a very complicated display. Smoothing all of the data can alleviate this problem. The entire multifile is then smoothed with the Savitsky-Golay smoothing algorithm. A smooth of 25 points is done on each trace, of 50,000 points, in the multifile. The smoothed multifile can now be displayed in a number of different ways. Typically a hidden 3-D format was used to make the data easy to interpret. This format stacks the spectra along a Z-axis, with the early spectra obscuring the later spectra.

A typical power titration

٩

An example of a typical power titration is shown in Figure 2.2. This figure shows results of a power titration of angiotensin (M.W. = 1296.5) in α -cyano-4-hydroxycinnamic acid. The sample was prepared by the standard method. For this sample the focusing lens was put in a position of 50 to provide a large laser spot. An initial power setting below threshold of 750 and a step size of 50 were selected. The number of acquisitions was set to 7, to provide a sensitive technique with a good signal-to-noise ratio.

This set of parameters led to a fairly typical power titration as shown in Figure 2.2. Power titrations are performed with time-of-flight spectra, so the x-axis is the flight time in nanoseconds. The y-axis is relative signal intensity based on the detector's current at a given time. The z-axis is the number of the spectrum as it is collected in the power titration experiment. As the spectrum number goes up, the laser power at which a given spectrum was acquired also rises. The laser power of any individual spectrum can be calculated by multiplying the spectrum number by the step size and adding the initial laser power. In this case spectrum number 20 would be $[20 \times 50] + 750 = 1750$. In addition the entire power titration is displayed with both a vertical and a horizontal offset. These offsets are used to make it easier to see as many of the peaks as possible.

The general trend that is illustrated by Figure 2.2 is that the matrix ions start forming at a lower power than the protonated analyte peak. At higher laser

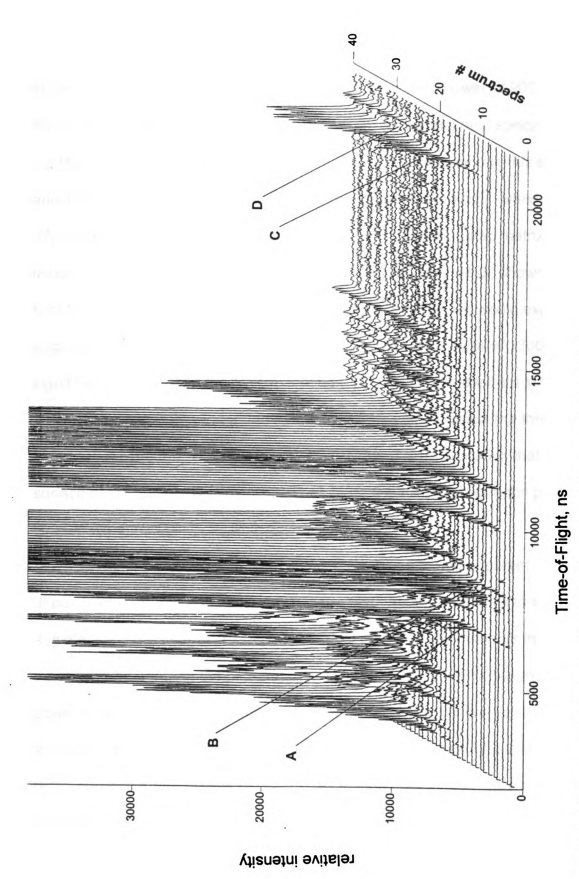


Figure 2.2 Power titration of angiotensin in $\alpha\mbox{-cyano-}4\mbox{-hydroxycinnamic acid}$

powers all of the peaks get more intense. The first 4 spectra that were collected in this power titration show virtually no signal. At a laser power of 900 the first few matrix peaks become visible, shown at point B in component spectrum number 6. The peaks which start at points A and B, correspond to m/z's of 172 and 189. The m/z 189 peak represents the charged intact matrix, while the m/z 172 peak represents the result of loss of H₂O from the protonated matrix. At a laser power of 1300 the protonated angiotensin produces a peak, shown at point C of Figure 2.2. From experience with this type of sample, we would expect angiotensin to have a threshold of about 1000. The laser power of 1300 is significantly higher than the typical threshold value from the standard MALDI data acquisition. Apparently extended irradiation of the sample below the threshold value causes the threshold value to rise. This trend is an indication that the surface of the sample is affected well before peaks are detected in the power titration experiment.

As laser power is increased, additional peaks become apparent. Shown at point D in Figure 2.2 at high laser power, 1750, an adduct begins to form with angiotensin. The time-of –flight of this adduct corresponds to an m/z that is 65 mass units higher than the protonated analyte peak. The matrix region of this power titration spectrum is displayed in Figure 2.3. Typically the adduct peaks are most often due to attachment of a metal ion. One possibility is that this peak is the result of a zinc adduct. However the isotopic distribution does not appear to be distribution that would be expected for Zn. Alternatively the peak at m/z 65 could be due to C₄⁺H₃N. This could be a fragment from the matrix or an impurity

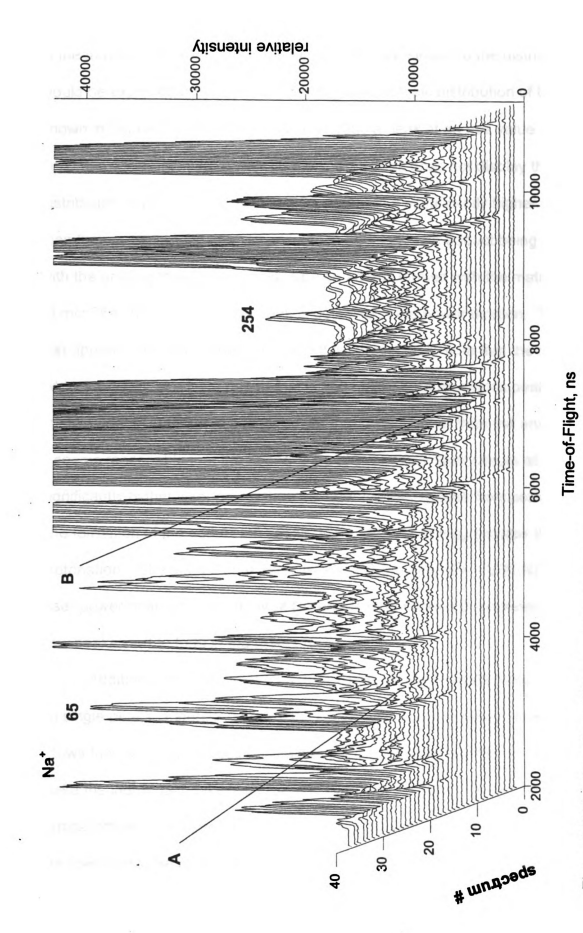


Figure 2.3 Matrix region of the power titration spectrum of angiotensin

in the matrix. The isotopic distribution seems to be similar to the distribution that would be expected for C₄H₃N⁺. The calculated isotopic distribution of C₄H₃N⁺ is shown in Figure 2.4. At a laser power of 1950 a peak at an m/z value of 65 becomes apparent in the power titration. This peak does not display the isotopic distribution of Zn. The signal at m/z 65 occurs at a significantly higher power than the corresponding analyte adduct. In addition to an adduct being formed with the analyte there also seems to be an adduct formed with the matrix itself. At m/z 254 [189 + 65] a large peak is detected in the power titration. This peak first appears at a laser power of 1250. It is interesting to note that the matrix adduct appears at a laser power that is 350 higher than the matrix peak while the analyte adduct appears at a laser power that is 450 higher than the analyte peak. It seems reasonable that the appearance of the adduct peak occurs at a significantly higher laser power than the cooresponding peak from protonation. The formation of the adduct ion seems to be a higher energy process than protonation. The adduct peak likely represents [angiotensin + C₄H₃N]⁺. At a laser power of about 1750 many of the matrix peaks become saturated and some new peaks start to form in the matrix region.

Additional information can be obtained from power titrations by zooming in on single peaks. Figure 2.5 shows the protonated analyte peak in detail. This shows the component spectra presented with no horizontal offset. In order to make the individual peaks easier to see the power titration is viewed with a large vertical offset, so the spectrum is viewed from a perspective that is well above the spectrum. The peak at the lowest laser power has the best resolution of the

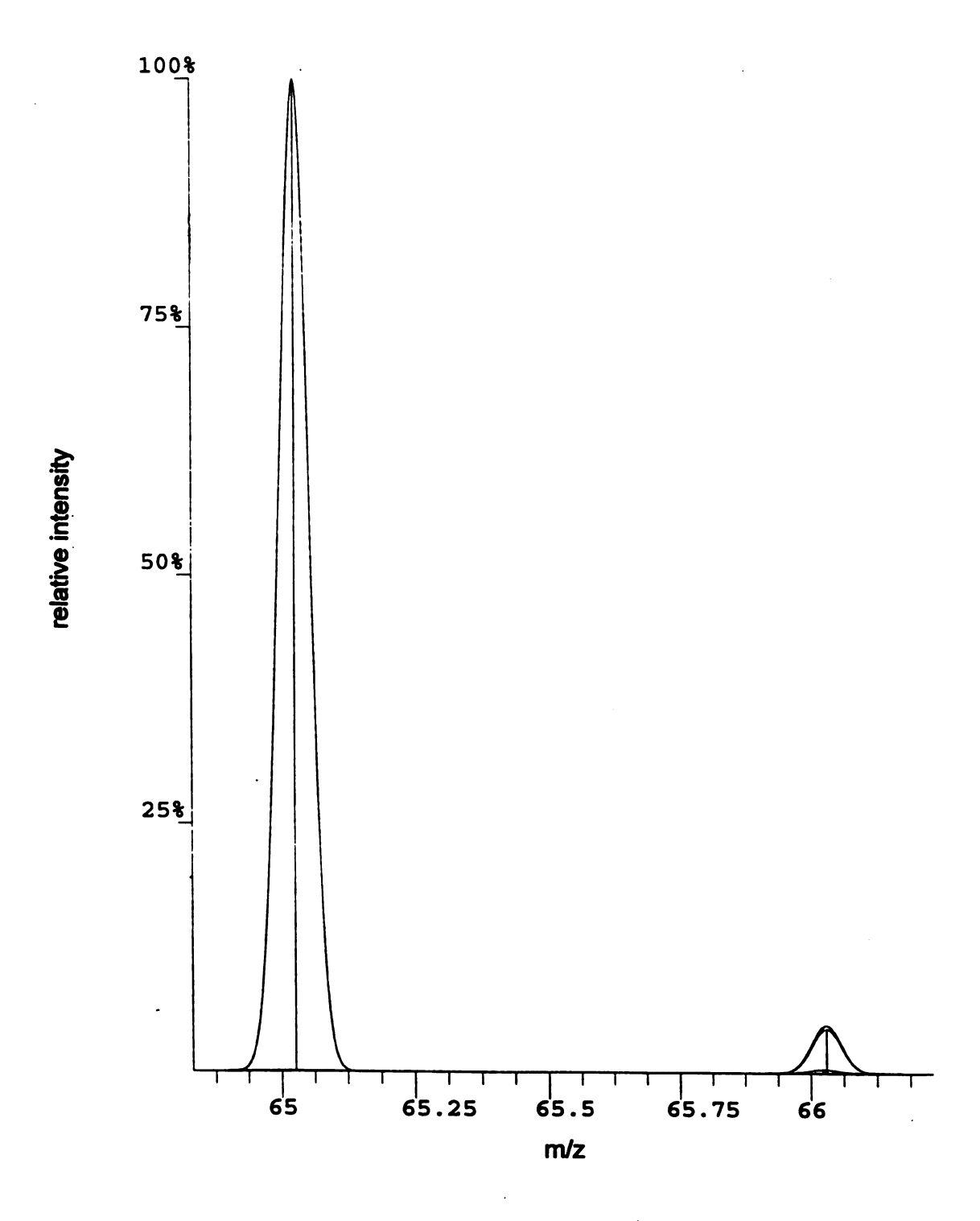


Figure 2.4 Theoretical spectrum of C₄H₃N⁺

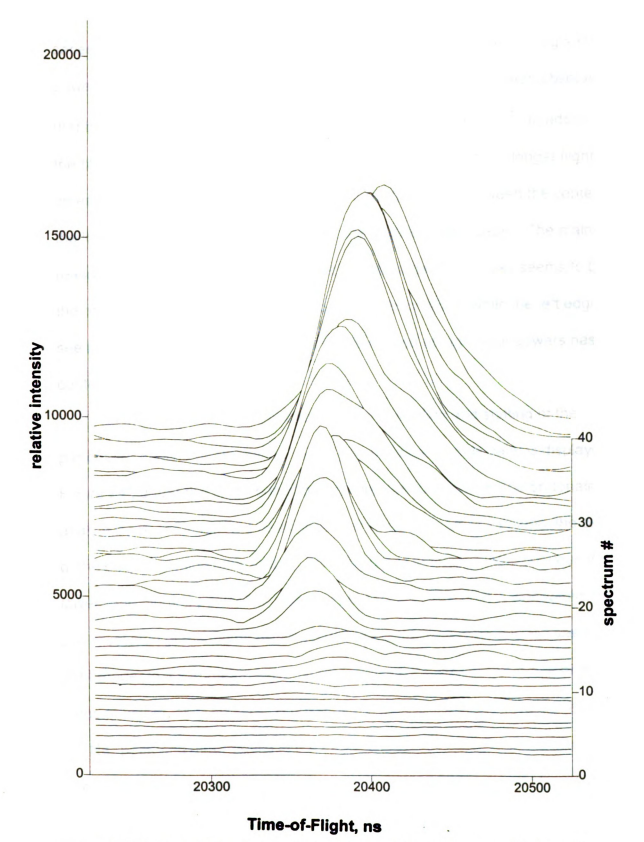
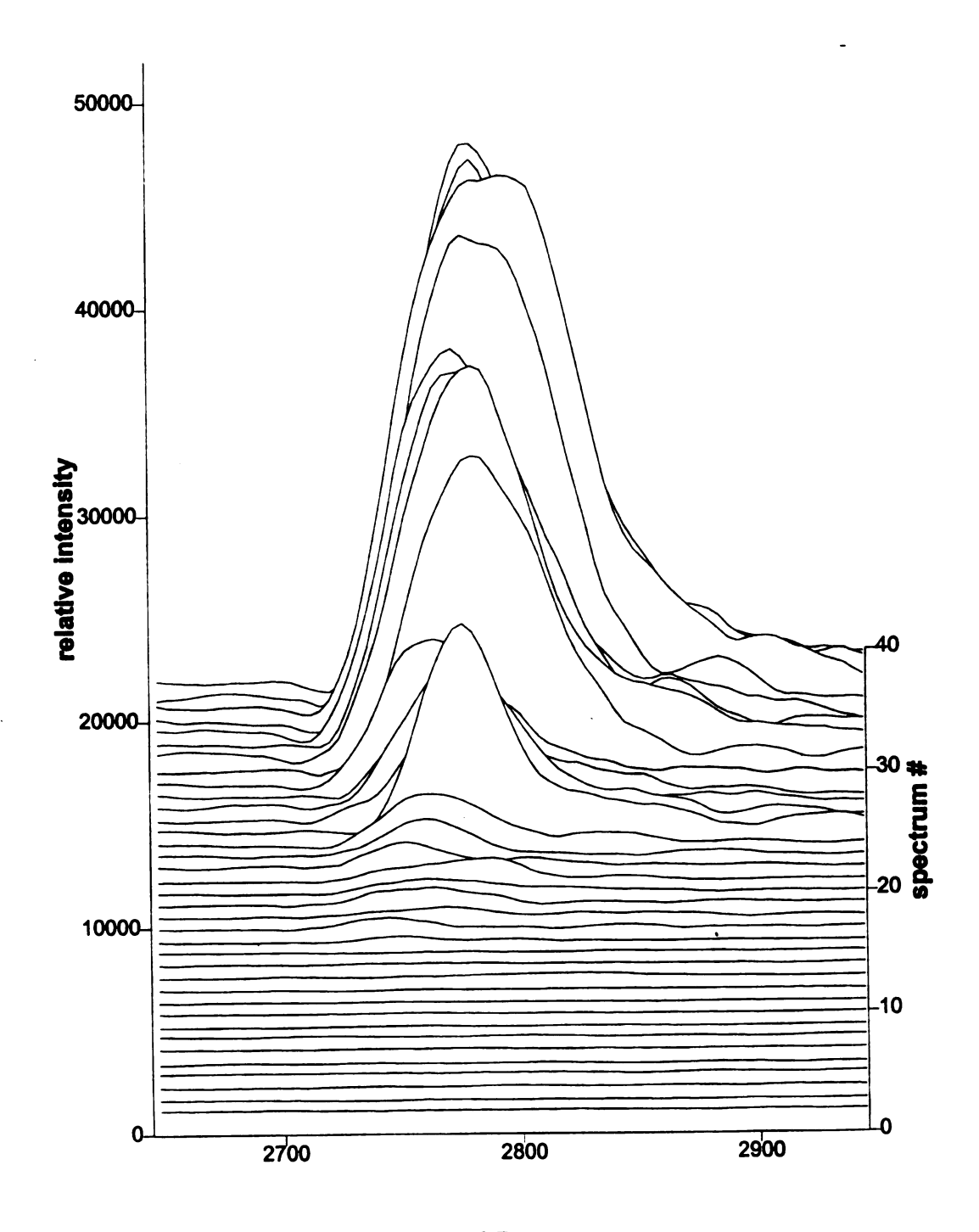


Figure 2.5 Region of the protonated analyte peak in the power titration of Angiotensin

series. In fact the low power peak has a resolution of 600, while the highest power peak has a resolution of 300 (FWHM). It has previously been observed that the best resolution in MALDI is obtained at low laser power ². In addition to the change in resolution the center of the peak is also moving to longer flight times at higher laser powers. There is a 45 ns difference between the center of the lowest power peak and the center of the highest power peak. The main reason that the center of the peak is moving to longer flight times seems to be the right edge of the peak is moving to longer delay times, while the left edge seems stable. The asymmetric peak that is formed at high laser powers has a center that is shifted to higher flight times.

In order to determine the cause of the spreading and shifting of the protonated analyte peak, the Na⁺ peak was examined. This peak is displayed in Figure 2.6, under the same conditions as were used to display the protonated analyte peak. Although the peak shapes show quite a bit of variation, the center of the peaks remains fairly stable. The difference in time-of-flight between the lowest and highest power Na⁺ peaks is about 1 ns. This shift is well within the 2ns resolution of the digital oscilloscope. The peak for the sodium ion seems to get broader in a symmetric way. Other matrix peaks also move to higher flight times at higher laser powers. A possible explanation for the difference between the Na⁺ peak and other peaks in the spectrum is that a reaction is necessary to form all of the other peaks besides the metal ions. Apparently the chemistry can take place over a longer period of time at higher laser powers. The delay in ion formation indicates that the ionization is occurring in the gas phase.



Time-of-Flight, ns
Figure 2.6 Region of the Na+ peak in the power titration of angiotensin

As another way to display the results of this power titration. Figure 2.7 displays some of the results from the power titration by an alternative method. In this figure the calibrated spectra acquired at three different laser powers are displayed on the same scale. For this figure each spectrum was calibrated, by time-of-flight to m/z values, individually using the Na⁺ and either the matrix peak or the [M+H]⁺ peak. In this series of spectra it is obvious how much of a difference laser power can make in the resulting mass spectra. The shape of the peaks is also strongly affected by the laser power used for a spectrum. At higher laser powers the major matrix peaks have a squared off appearance due to saturation of the 8 bit a/d converter of the instrument. Some of the major peaks that are seen in these spectra are the matrix peak at 189 Da. and the protonated dimer at 379 Da. In addition the peak resulting from the loss of water from the protonated matrix molecule is at 172 Da. At the laser power of 1650 the [M+65] peak is shown. In addition this same spectrum contains a peak from the matrix adduct at a m/z of 254.

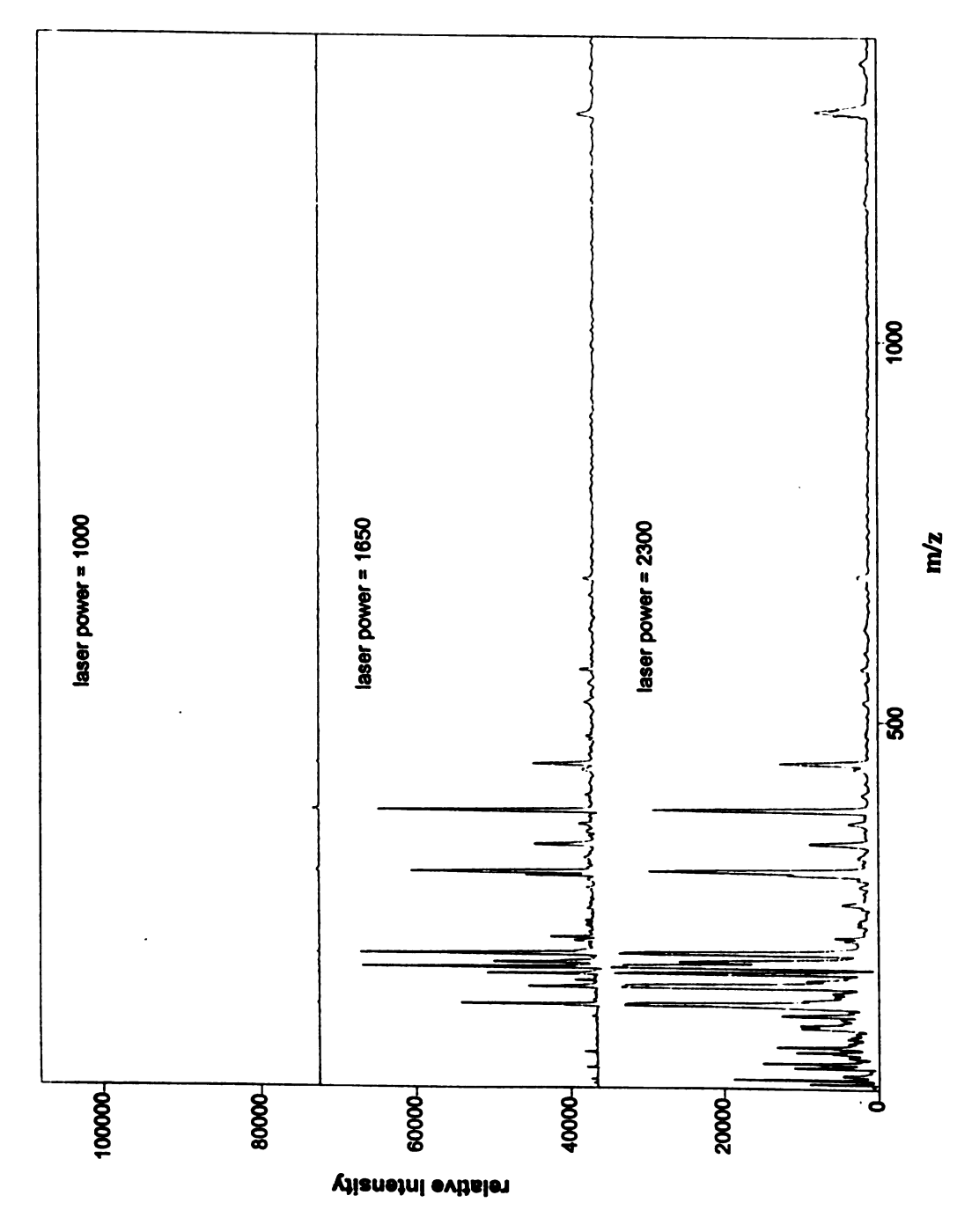


Figure 2.7 Three component spectra of the power titration of angiotensin in α -cyano-4-hydroxycinnamic acid

3. The Usefulness of Power Titrations

The utility of power titrations can be extended in several directions. By changing the laser powers that are used in the experiment a wide variety of conditions can be explored. Another parameter that can be varied is the increment in the laser power between the different acquisitions. The experiment can also be altered by irradiating the sample for a set period of time at a laser power that is well below the laser power at which the power titration is started. This type of experiment could determine if there are effects on the sample at low irradiation.

Unfortunately there are a couple of limitations on the use of power titrations. First power titrations can be difficult to interpret due to the large amount of data that are present. The low resolution and irregular peak shapes further complicate the interpretation since they make calibration more difficult. Finally the interpretation of power titrations is perhaps most difficult because of the irreproducibility of the experiment. Significant differences appear in power titrations of similar samples. These differences could be due to the fact that there is a significant amount of variation between samples prepared by the standard sample preparation method. For this reason power titrations are not useful for elucidating mechanistic details of the MALDI experiment or a standard method for comparison between different laboratories. In the next chapter, I will investigate the crystallization process, in an attempt to make the experiment more reproducible.

4. References

- 1)Dreisewerd, K.; Schurenberg, M.; Karas, M.; Hillenkamp, F. *International Journal of Mass Spectrometry and Ion Processes* **1995**, *141*, 127-148.
- 2)Ingendoh, A.; Karas, M.; Hillenkamp, F.; Giessmann, U. *International Journal of Mass Spectrometry and Ion Processes* **1994**, *131*, 345-354.
- 3)Westman, A.; Demirev, P.; Huth-Fehre, T.; Bielawski, J.; Sundqvist, B. U. R. *International Journal of Mass Spectrometry and Ion Processes* **1994**, *130*, 107-115.
- 4)Westman, A.; Huth-Fehre, T.; Demirev, P.; Bielawski, J.; Medina, N.; Sundqvist, B. U. R. Rapid Communications in Mass Spectrometry 1994, 8, 388.
- 5)Westman, A.; Huth-Fehre, T.; Demirev, P.; Sundqvist, B. U. R. *Journal of Mass Spectrometry* **1995**, *30*, 206-211.
- 6) Kaupp, G. Angewandte Chemie. International Edition 1992, 31, 592-595.

Chapter three. Evaluation of Sample Preparation Techniques

1. Introduction

The standard sample preparation technique for MALDI samples is the dried droplet method¹. This technique simply involves mixing a drop of a matrix solution with a drop of an analyte solution and allowing the solvent to evaporate. This method tends to produce irregular samples. The same sample may have many different shapes of crystals in it. In addition, samples can vary in the distribution of different size crystals and the overall density of crystals². The crystal surfaces also vary from highly reflective to dull.

The standard preparation procedure has many weaknesses to it.

Samples that have been prepared by the dried droplet method typically have only a couple of "sweet spots". These few selected areas of the sample produce much better signal at lower laser power than the rest of the sample. The standard method has also been found to be sensitive to some contaminants such as detergents³. In addition the dried droplet method displays different sensitivity for different analytes. All of these aspects of the experiment and the sensitivity for all analytes could potentially be improved with a more carefully controlled preparation procedure.

Before it is possible to improve upon the sample preparation procedure it is important to understand how the samples form. The first requirement is that both the matrix and analyte must be soluble in the solvent system that is used. The matrices are all small organic molecules which tend to be soluble in organic solvents. The analytes in this work are peptides and proteins, which are soluble

in aqueous solvents. The solubility of these analytes is typically enhanced in acidic solutions. For this reason the solvents that are typically used are a mixture of organic solvents and aqueous 0.1% trifluroacetic acid. Another factor that is important in the preparation of samples is that there must be a large excess of matrix relative to the amount of analyte. A typical ratio of matrix-to-analyte is 1000:1^{4,5}. The resolution of the experiment can be adversely affected by having too much analyte present in the sample. In addition, some samples can be difficult to detect when the matrix-to-analyte ratio is lower than 1000:1

By careful observation of the crystallization process, using a video microscope, it is observed that sample crystallization typically occurs in the following manner. After the sample is completely mixed and placed on the sample surface, the solvent begins to evaporate. The height of the drop first decreases as the solvent evaporates. The more volatile component of the solvent system evaporates first so that the composition of the solvent system is constantly changing. Over the course of 30 seconds or so the droplet is gone and all that is left are wet crystals. Once the crystals have started to form the majority of the analyte attaches to hydrophobic crystal faces⁶. Due to the inclusion process. the hydrophobicity of the analyte has been found to be a major contributor in the response factor for analytes. In addition the pH of the solution can affect this process, and pH has also been found to be important in the preparation of MALDI samples⁷. The last step that occurs is that the individual crystals dry out and once the crystals are completely dry they can be inserted into the instrument and the analysis can be performed.

By careful control of the crystallization process, it should be possible to develop an ideal sample preparation procedure. The crystals formed by this method should be very uniform, to produce a uniform response across the entire sample. This method should also be very reproducible so that the results from different experiments can be compared. In addition this technique should have high sensitivity and allow the detection of femtomoles of analyte. The ideal procedure would also allow for the experiment to be performed in the presence of high concentrations of contaminants typically present in the analysis of biological molecules. These contaminants include detergents and buffers such as sodium dodecylsulfate and urea.

Many alternative methods of sample preparation have been developed by myself and others. One technique that has been used is to prepare the sample by using two layers. The first layer provides seed crystals for the second layer which contains the analyte. The first layer can be a layer of crushed crystals or a layer formed by rapid evaporation of the matrix solution^{3,8}. Spin coating has also been used in an attempt to produce a uniform sample⁹. Additives such as fucose and nitrocellulose have also been evaluated for use in improving MALDI samples^{10,11}.

2. The Standard Method of Sample Preparation

As a way of evaluating the performance of the standard sample preparation technique a seven component mixture was analyzed. The analytes in this mixture were bradykinin (M.W. = 1060), angiotensin (M.W. = 1296), melittin

(M.W. = 2847), oxidized b-chain of insulin (M.W. = 3496), insulin (M.W. = 5734), cytochrome C (M.W. = 12, 384) and myoglobin (M.W. = 17,400) in a equimolar seven component mixture. This mixture represents a wide mass range of peptides and proteins. The experiment was performed two ways to determine if there was any difference between two similar methods. The first method was to put down a 1 μL drop of the mixture and then to place a 1 μL drop of matrix on top of the first drop. The results from this experiment are shown in Figure 3.1. While the signals from bradykinin, melittin and insulin are very strong, the signals from angiotensin, oxidized b-chain of insulin and myoglobin are weak. The second technique was to reverse this process by first placing a 1 µL drop of matrix solution followed by the 1 µL drop of the mixture. The result of this procedure is shown in Figure 3.2. By reversing the order the droplets are placed the signals for bradykinin and angiotensin are less intense. The signals from cytochrome C and myogloblin are at least 50% more intense than with the first technique. This simple change in technique can make a major difference in the spectra that are produced for a mixture. When the matrix solution is placed down first, the solvent begins to evaporate immediately. As the solvent evaporates the matrix can begin to start the crystallization process, so that when the analyte solution is added the analytes can more easily be incorporated onto the faces of the crystals that have already begun to form. This process can occur even though no crystallization is visible before the addition of the analyte solution.

In order to further study the effects of different sample preparation techniques, a two component mixture of 2 picomoles of bradykinin and

Figure 3.1 Power titration spectrum of the seven component mixture, prepared by the analyte first dried droplet procedure

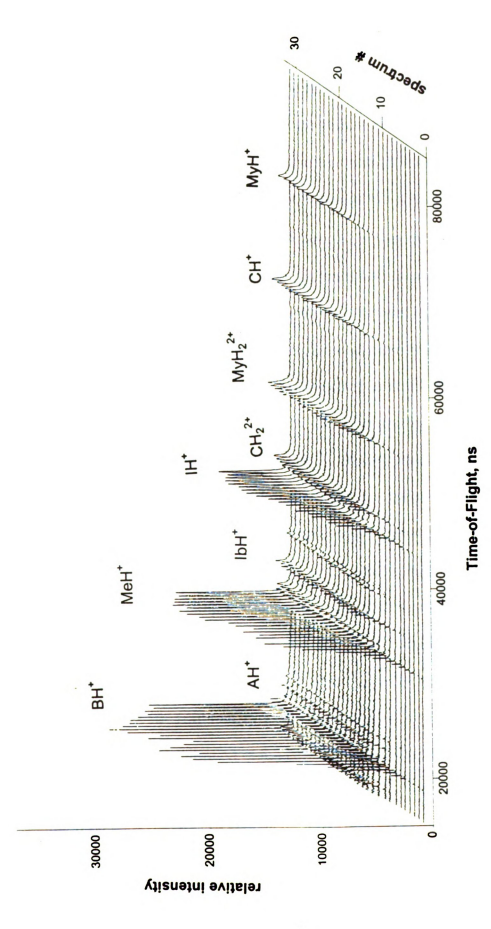


Figure 3.2 Power titration spectrum of the seven component mixture, prepared by the matrix first dried droplet procedure

2 picomoles of insulin was used. The samples were prepared by the matrix first dried droplet procedure. This mixture represents a best case mixture of two components that both have high response factors in the MALDI experiment. In addition, the structure of these two analytes is very different. Bradykinin is a single peptide chain while insulin is composed of two peptide chains that are connected by two disulfide bonds 12. As shown in Figure 3.3, the power titration of the two component mixture with the standard MALDI experiment produces strong signals for both bradykinin and insulin. However this technique does show some weaknesses. The most serious weakness is the intense copper ion adduct that forms with bradykinin. The copper that forms the adduct with bradykinin is most likely from trace amounts in the analyte and matrix. In addition it would be desirable to have equal intensity peaks representing bradykinin and insulin. With this simple mixture it is easy to observe that the insulin not only produces doubly protonated analyte ions but that there is also a small peak for the singly-charged insulin dimer. Most metal ions do not seem to be a problem with this sample preparation. The signals from Na⁺ and K⁺ are weak and the corresponding adducts are also weak. As shown in Figure 3.4 the metal ions are also weak in the matrix region. In addition, the region from 4000 to 6000 ns (~m/z 10- 100) has very little signal until high powers are used. The results from the power titration of the binary mixture prepared by the dried droplet method can now be compared with the results of other sample preparation techniques.

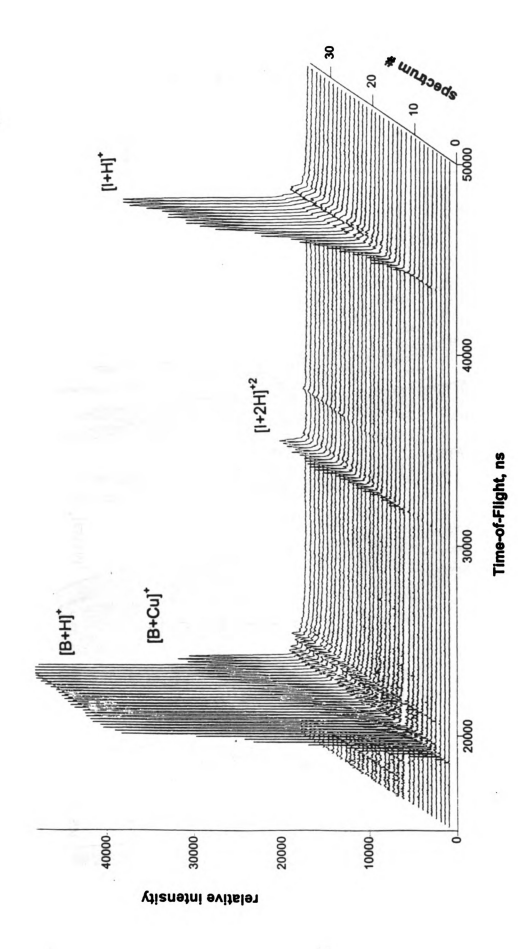


Figure 3.3 Power titration spectrum of the two component mixture, prepared by the dried droplet procedure

relative intensity

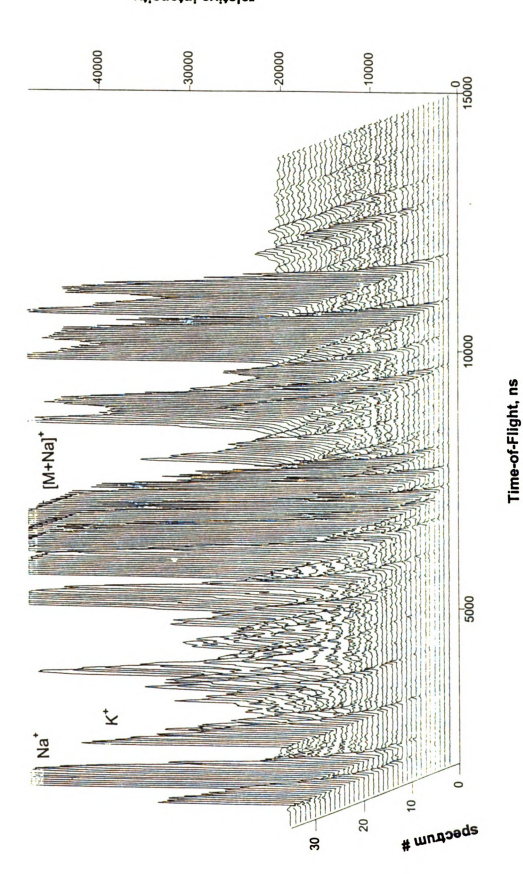


Figure 3.4 Matrix region of the power titration spectrum of the two component mixture, prepared by the dried droplet procedure

3. Alternative Sample Preparation Procedures

One alternative technique that was proposed by Vorm uses a two step sample preparation process⁸. In this technique a layer of matrix is first placed on the sample surface by placing a drop of the acetone saturated in matrix. The acetone dries quickly leaving a thin layer of matrix. A small amount of analyte solution with no matrix is then placed on top of the matrix layer. The idea is to only dissolve some of the first layer and use the remaining matrix as seed crystals. This technique does produce a homogeneous layer of crystals. This technique has also been reported to produce peaks that have a good resolution and sensitivity. In addition this type of sample is durable to being rinsed⁸.

The results for the analysis of the binary mixture are shown in Figure 3.5. The Vorm method produces a strong signal for bradykinin while producing a very weak, broad signal for insulin. Bradykinin forms strong adducts with both Na⁺ and K⁺. The Cu⁺ adduct does not seem to be present. The relatively crowded matrix region is shown in Figure 3.6. The metal ions of Na⁺ and K⁺ produce very strong signals throughout the power titation. In addition the [M+Na]⁺ peak becomes intense early in the power titration. There are three major peaks in the region of 4000-6000 ns. The most intense ion in this region is Ni⁺, while the other two ions are matrix fragments. No peak is present at the predicted flight time for the fragment at m/z = 65, from C₄H₃N⁺. The major features of the Vorm sample preparation procedure are that bradykinin produces a much stronger signal than insulin and that metal ions play a very prominent role with this technique. The intensity of metal ions could have been reduced by washing the

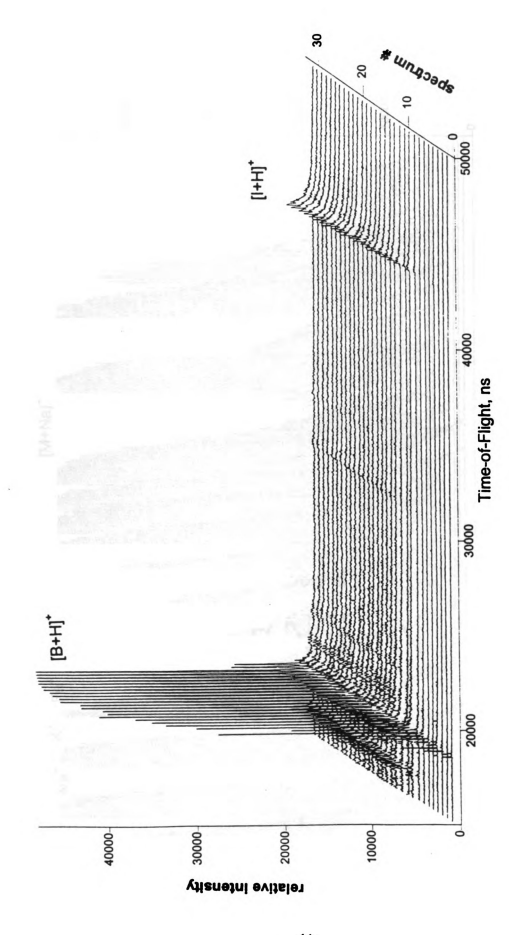


Figure 3.5 Power titration spectrum of the two component mixture, prepared by the Vorm procedure



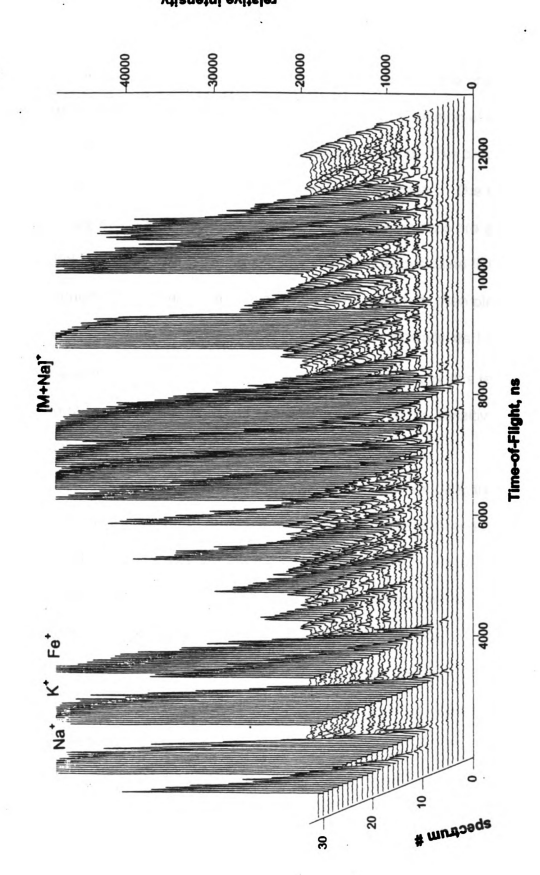


Figure 3.6 Matrix region of the power titration spectrum of the two component mixture, prepared by the Vorm procedure

sample, however this was not done so that affect of metal ions on the samples could be studied.

Another two step sample preparation procedure is the crushed crystal method. In this method a droplet of saturated matrix solution of a mixture of acetonitrile and water is placed on the sample surface. This droplet is allowed to dry completely to leave a collection of pure matrix crystals. The matrix crystals are crushed under a microscope slide and all loose crystals are wiped off of the sample surface. The crushing leaves behind a polycrystalline film. A droplet that is saturated in the matrix and also contains the analyte is then placed on the thin layer and allowed to air dry. The crystal formation typically start 15 seconds after the analyte droplet is deposited³. The main advantages of this technique, as reported by the developers of this technique, are that the sensitivity is increased and this sample can also be washed to remove salts.

Performing a power titration on the binary mixture using the crushed crystal procedure shows good response for both bradykinin and insulin. The power titration is shown in Figure 3.7. Using this sample preparation method bradykinin has a Na⁺ adduct that appears at low laser powers. In addition, at high laser powers bradykinin also forms an adduct with Cu⁺. The matrix region of this power titration, shown in Figure 3.8, is distinguished mostly by the fact that there are relatively few peaks in the matrix region. The metal ions do not appear until relatively high laser power. However the [M+Na]⁺ adduct is formed at low power. Using the crushed crystal sample preparation procedure a simple power titration is produced that has good response for both bradykinin and insulin.

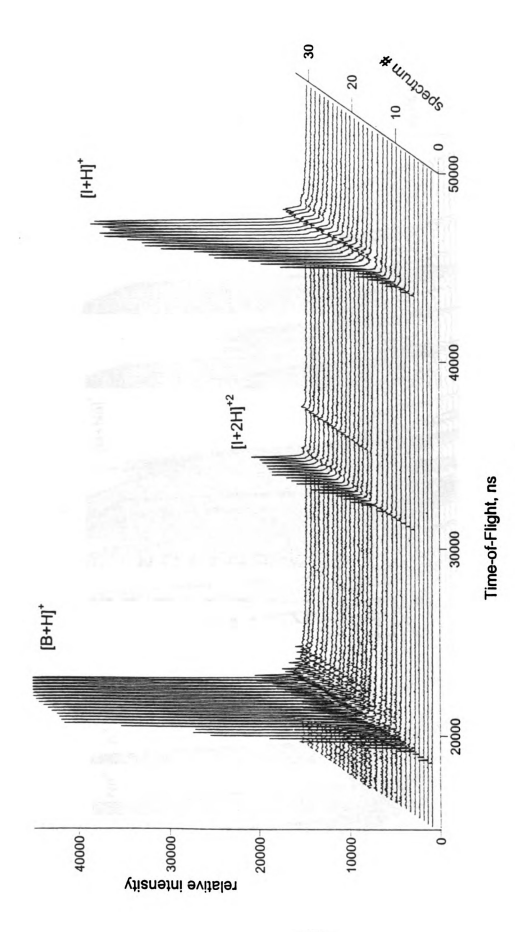


Figure 3.7 Power titration spectrum of the two component mixture, prepared by the crushed crystal procedure

relative intensity

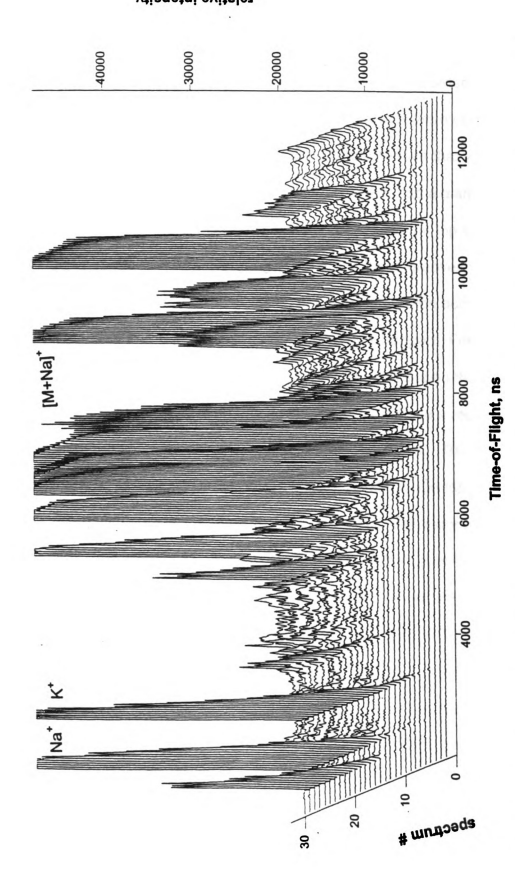


Figure 3.8 Matrix region of the power titration spectrum of the two component mixture prepared by the crushed crystal procedure

Careful observation of the crystallization, by light microscope, that occurred with the crushed crystal sample preparation method indicated that there was actually two separate types of crystallization occurring. In order to understand how these two different crystallization processes were occurring at the same time, it is important to understand the sample surface that was used. All samples were placed on top of a round sample pin that had a diameter of ~ 1mm. The pin had a series of concentric circular grooves in the top surface. Some of the crystallization was occurring at the top of these grooves where the thin film had been crushed. However, much of the crystallization occurred inside the circular grooves where larger crystals of matrix were trapped. For comparison another sample preparation procedure was developed that would isolate the bigger crystals. To meet this goal and still try to have a reproducible surface the Vorm and crushed crystal methods were combined. The first layer used is the saturated acetone droplet of the Vorm procedure. On top of this first layer analyte solution that is saturated in matrix is added. This sample preparation method was named "the combo method." When a power titration is performed on the binary mixture prepared by the combo method the results are similar to the crushed crystal results with good response for both bradykinin and insulin, similar to the results from the crushed crystal method. These results are shown in Figure 3.9. The biggest difference between the results from these two sample preparation techniques is that the Cu⁺ adduct of bradykinin is very intense. Bradykinin also seems to form a second adduct with two copper ions. In order for the charge on bradykinin to be +1 a hydrogen ion must be lost from

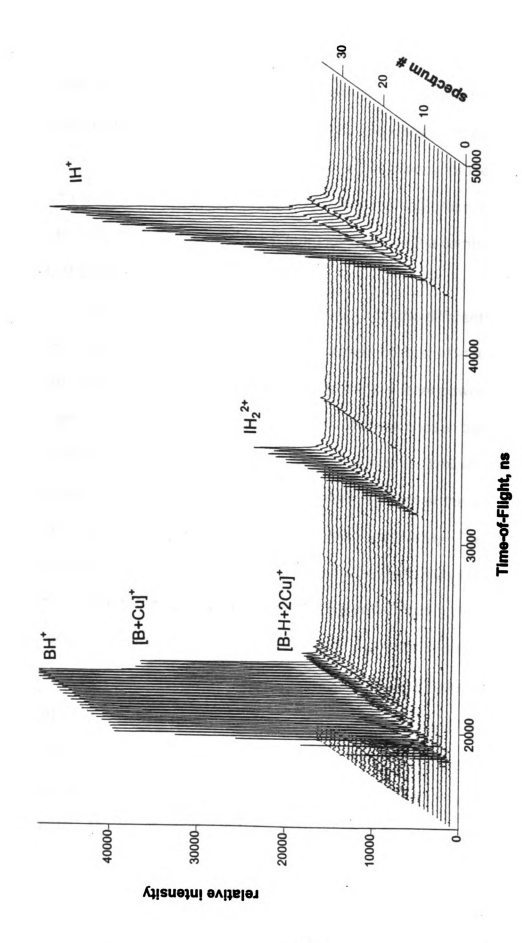


Figure 3.9 Power titration spectrum of the two component mixture, prepared by the combo procedure

the bradykin molecule. This type of hydrogen loss is rarely observed. The matrix region of the power titration, shown in Figure 3.10, is similar to the matrix region produced by the crushed crystal procedure. One difference between these two procedures is that the signal for [M+Na]⁺ is more intense for the crushed crystal sample preparation procedure than the combo method. Also, the peaks in the high mass matrix region are much more intense with the combo method than the crushed crystal method.

In order to directly compare the results from the different sample preparation procedures, calibrated spectra were compared at a low and a high laser power. The component spectra acquired at a laser power of 1450 are shown in Figure 3.11. The laser power of 1450 was chosen because it is near the threshold for the insulin peak. This laser power is a typical condition that may be used to detect both of the analytes. At this laser power the peak for bradykinin is saturated with both the standard and combo procedures. The crush procedure provides the most even response with the bradykinin/insulin mixture. For the three methods that produced a significant signal for insulin, the resolution is directly proportional to the height of the peak: the higher the peak the lower the resolution. This observation follows a general trend that has been observed for MALDI¹³. An expanded view of the region around the bradykinin peak is shown in Figure 3.12. For every method except the combo method a Na⁺ adduct is present. Both the standard method and the combo method have a large Cu⁺ adduct. The Vorm method is the only technique that produces a K⁺ adduct.

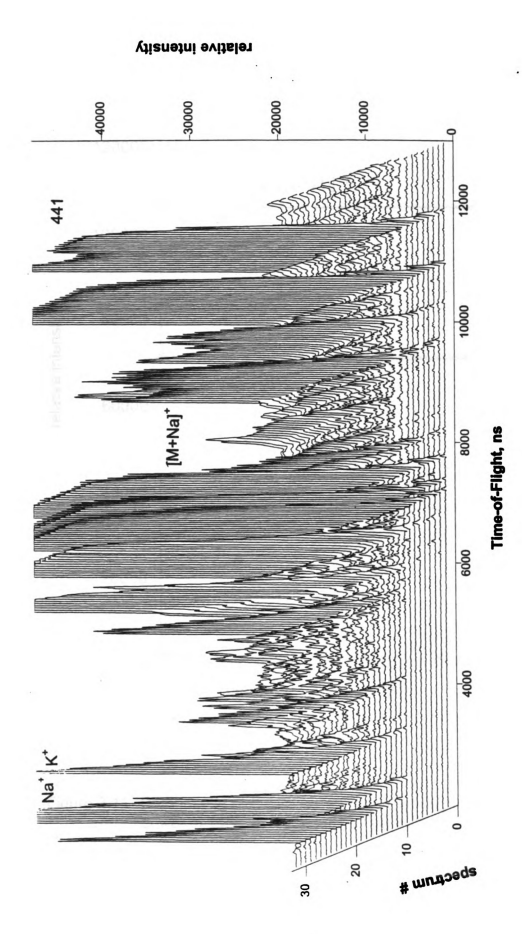


Figure 3.10 Matrix region of the power titration spectrum of the two component mixture, prepared by the combo procedure

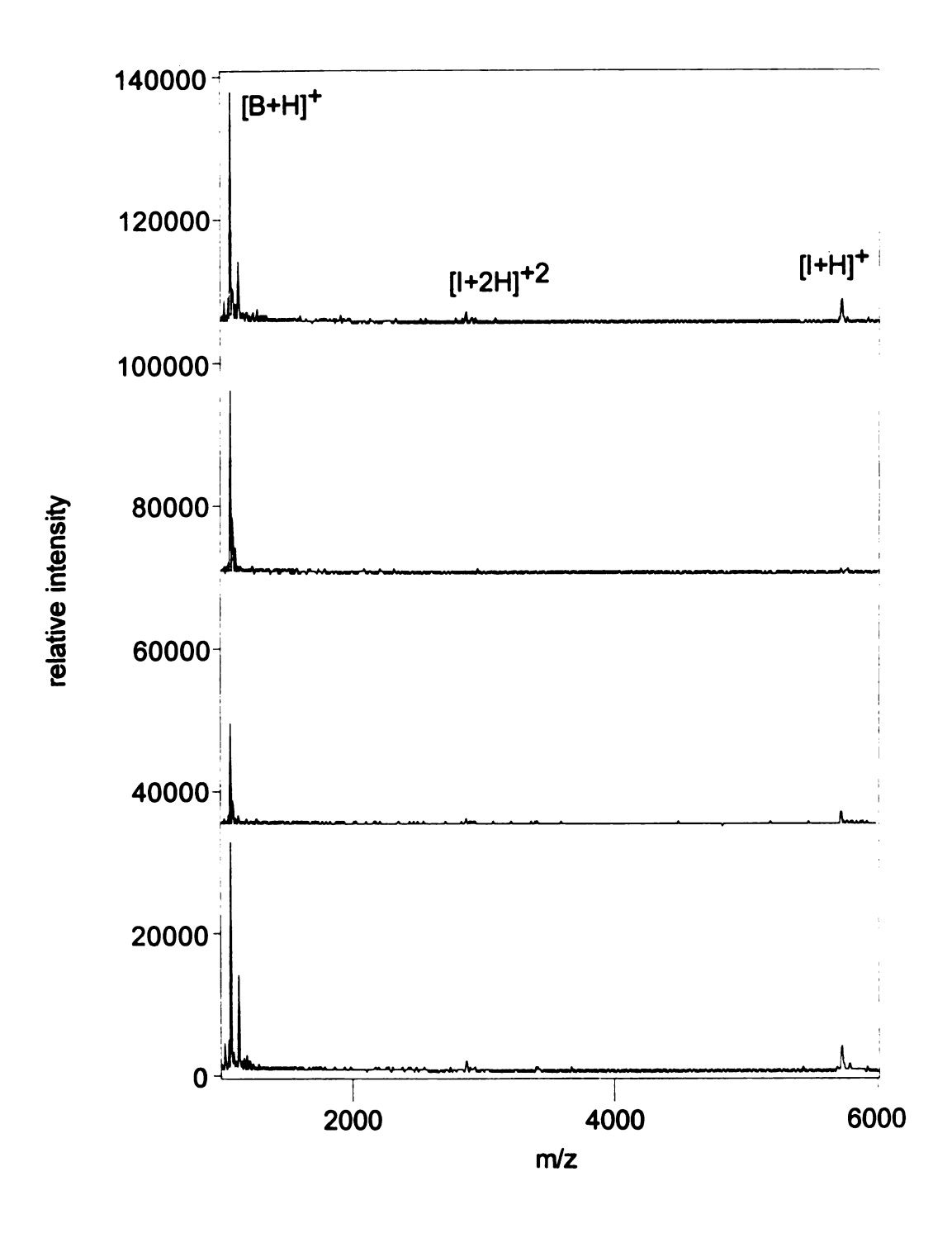


Figure 3.11 Comparison of the component spectra taken at a laser power of 1450 for the different preparation procedures

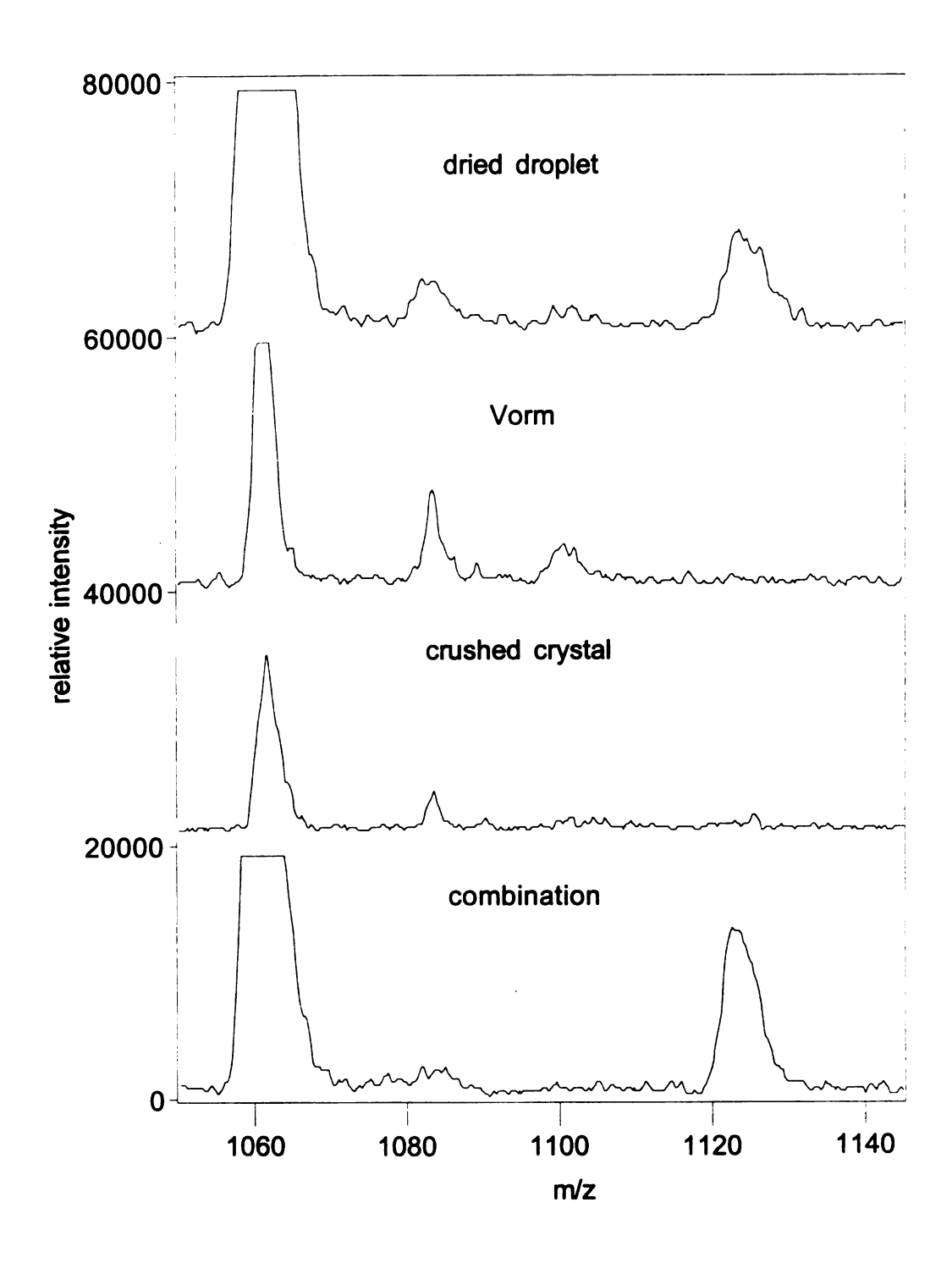


Figure 3.12 Expanded view of bradykinin peak in the comparison of the component spectra taken at a laser power of 1450 for the different preparation procedures

The spectra that were taken at the very high laser power of 2500 have two additional features. These spectra, shown in Figure 3.13, have intense peaks representing the doubly protonated insulin molecule. The intensity of the doubly protonated molecule scales well with the intensity of the singly protonated molecule. In addition a contaminant can be detected at m/z 3500. This is most likely some b-chain of insulin from the insulin sample. Based on the expected response factor of the b-chain of insulin, the amount of this contaminant must be well below 2 pm. This contaminant can provide some measure of the relative sensitivity of the preparation procedures for a minor component. Both the crushed crystal method and the combo method produce a detectable peak for the contaminant. At this high laser power all of the sample preparation methods except the Vorm method give a strong signal for insulin. However the resolution of these peaks is low. Adducts due to Na⁺ and K⁺ fall within the mass range of the large insulin peaks. However the Cu⁺ adduct be seen as a high mass shoulder to the insulin peak, since the resolution of the spectrum is just high enough to allow the two peaks to be differentiated from each other. In all of these sample preparation procedures insulin also has some high mass adducts. These adducts are formed by components of the matrix, such as the matrix itself, and the product of water loss from the matrix, complexing with an analyte molecule.

As mentioned previously the crushed crystal method that was evaluated included some large seed crystals in the circular grooves of the sample pin. In order to produce a pure crushed crystal preparation the metal surface that was

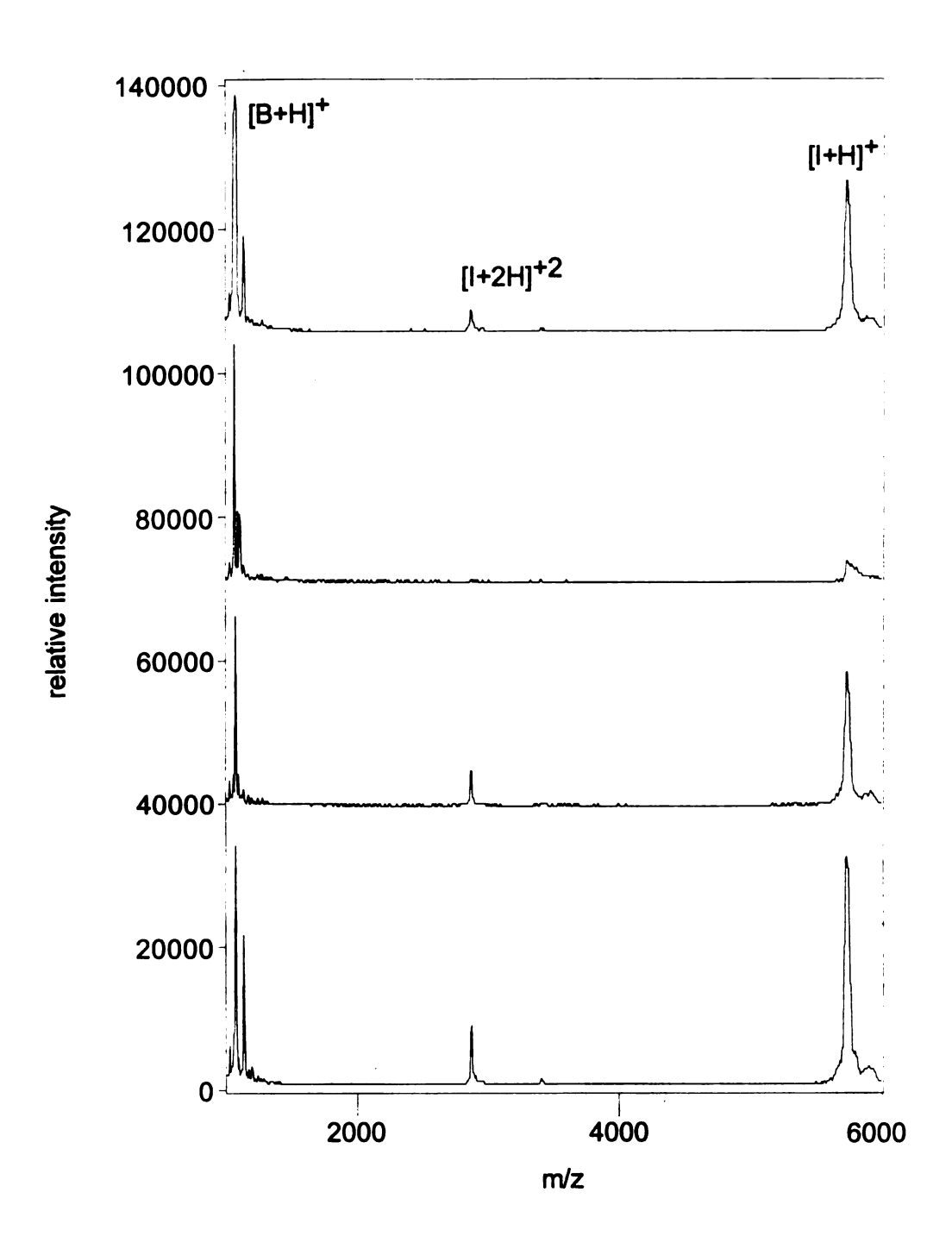


Figure 3.13 Comparison of the component spectra taken at a laser power of 2500 for the different preparation procedures

used for the sample preparation was smoothed so that no ridges were visible. When the procedure is done on this surface only one type of crystal was formed and the crystallization started very quickly. In order to further control the crystal formation the sample was heated with a hotplate to accelerate the evaporation of the solvents and make the sample preparation more uniform. The temperature of the sample block that the was used to hold the sample pins was monitored with a thermocouple (Omega Engineering, Stamford, CT). When the temperature equilibrated at the desired value, the droplet was placed on the prepared sample pin. One of the most outstanding characteristics of this type of sample preparation method is that two separate threshold fluences can be observed. To easily observe the two thresholds the power titration was started just above the first threshold value. The mixture used in this experiment is 2 picomoles each of angiotensin and insulin. The result of this experiment is shown in Figure 3.14. Evidence of the first threshold can be seen in the first spectrum of the power titration. This first spectrum contains both of the major analytes. Only a few laser shots can be acquired at these low powers before the products at the first threshold are depleted. The matrix region for this technique is shown in Figure 3.15. The most outstanding aspect of the matrix region is that there are few metal ions and virtually no signal from 4000-6000 ns. The relatively few peaks in the matrix region indicates that few reactions are occurring. However the reactions that are necessary for the protonation of analytes are still occurring. For the analysis of mixtures, the crushed crystal method produces the most even response for a mixture of peptides and proteins.

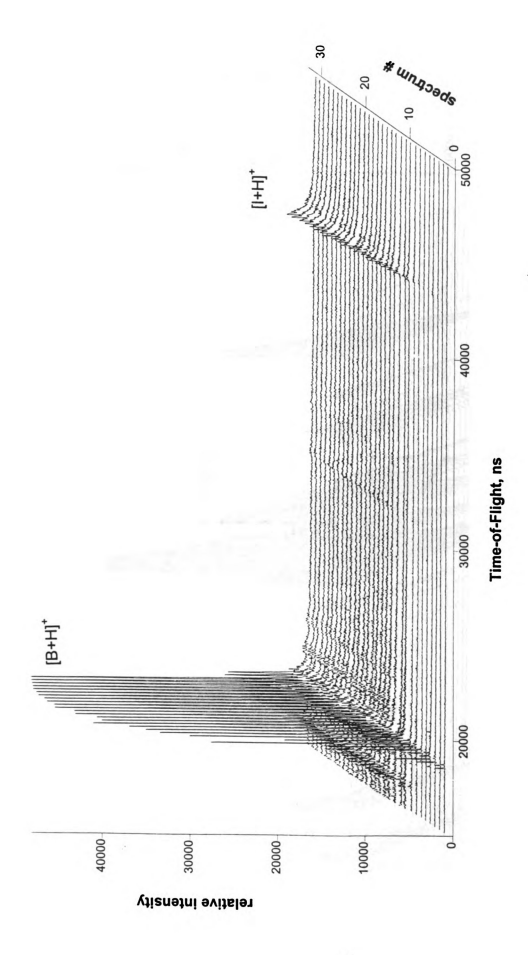


Figure 3.14 Power titration spectrum of the two component mixture, prepared by the pure crushed crystal method



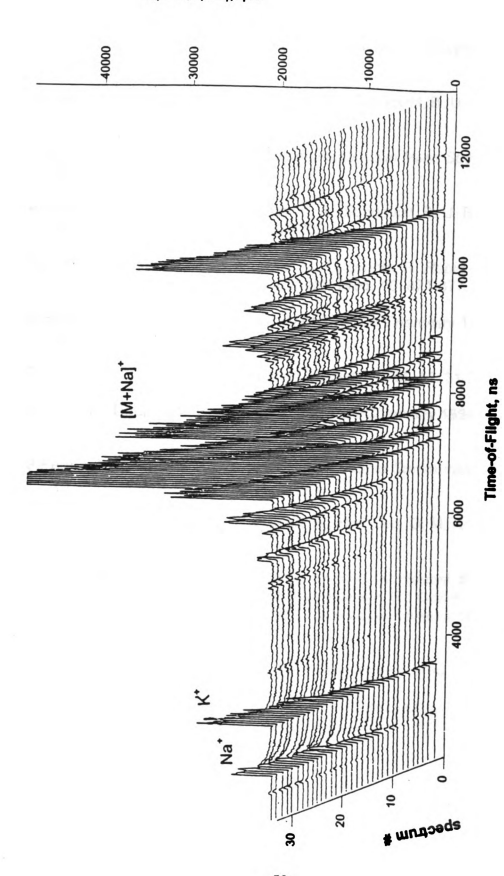


Figure 3.15 Matrix region of the power titration spectrum of the two component mixture, prepared by the pure crushed crystal method

4. References

- 1)Hillenkamp, F.; Karas, M.; Beavis, R. C.; Chait, B. T. *Analytical Chemistry* **1991**, *63*, 1193a.
- 2)Westman, A.; Huth-Fehre, T.; Demirev, P.; Sundqvist, B. U. R. *Journal of Mass Spectrometry* **1995**, *30*, 206-211.
- 3)Xiang, F.; Beavis, R. C. Rapid Communications in Mass Spectrometry 1994, 8, 199-204.
- 4)Medina, N.; Huth-Fehre, T.; Westman, A.; Sundqvist, B. U. R. Organic Mass Spectrometry 1994, 29, 207-209.
- 5) Knochenmuss, R.; Dubois, F.; Dale, M. J.; Zenobi, R. Rapid Communications in Mass Spectrometry 1996, 10, 871-877.
- 6)Beavis, R. C.; Bridson, J. N. Journal of Physical Chemistry 1993, 442-447.
- 7) Cohen, S. L.; Chait, B. T. Analytical Chemistry 1996, 68, 31-37.
- 8) Vorm, O.; Roepstorff, P.; Mann, M. Analytical Chemistry 1994, 66, 3281-3287.
- 9)Perera, I. K.; Perkins, J.; Kantartzoglou, S. *Rapid Communications in Mass Spectrometry* **1995**, *9*, 180-187.
- 10)Gusev, A.; Wilkinson, W. R.; Proctor, A.; Hercules, D. M. *Analytical Chemistry* **1995**, *67*, 1034-1041.
- 11)Kussmann, M.; Nordhoff, E.; Rahbek-Nielsen, H.; Haebel, S.; Larsen, M. R.; Jakobsen, L.; Gobom, J.; Mirgorodskaya, E.; Kroll-Kristensen, A.; Palm, L.; Roepstorff, P. *Journal of Mass Spectrometry* **1997**, *32*, 593-601.
- 12) Voet, J.; Voet, D. Biochemistry; John Wiley & Sons: New York, 1990.
- 13) Dreisewerd, K.; Schurenberg, M.; Karas, M.; Hillenkamp, F. *International Journal of Mass Spectrometry and Ion Processes* **1995**, *141*, 127-148.

Chapter four. Suppression Effects of Peptides and Proteins Using α -cyano-4-Hydroxycinnamic Acid as a Matrix for MALDI

1. Introduction

The technique of matrix-assisted laser desorption/ionization time-of-flight analysis has been vastly improved by the introduction of instrumental innovations. The rest of the studies in this work were performed on a Voyager Elite mass spectrometer with delayed extraction. The source regions of the Voyager elite is very different from the ion source on the Vestec 2000. One improvement ion source over the instrument that was initially used is that the sample is no longer placed on 24 sample pins in a carousel. Instead the samples are all placed on a single plate that has 100 spots on it. This plate not only allows many more samples to be run at one time, it also provides a much more uniform surface for the samples to be deposited on. The uniform surface increases the reproducibility between spectra acquired from different sample positions and makes external calibration much more reliable.

Another improvement to the technique of MALDI is the introduction of a reflectron. The reflectron was first introduced by Mamyrin¹. A reflectron is simply a device that has a voltage slightly greater than accelerating voltage. The gradient of the field is in the oppisite direction as the accelerating voltage gradient. The reflectron increases the resolution of the time-of-flight technique. The cause of poor resolution in time-of-flight analysis is the kinetic energy spread of the analyte ions. A reflectron provides a method to correct for this energy spread. The reflectron is placed at the end of the field free region. When the

packet of ions reaches this region the ions with high kinetic energies will reach the reflectron before ions of low kinetic energy. The high energy ions also penetrate farther into the reflectron field than the low energy ions. The high energy ions end up spending more time in the reflectron than the low energy ions. The ions are then detected at a plane in space, where the low energy ions and the high energy ions of the same m/z will arrive at the same time.

Recently the technique of MALDI-TOF has been further improved by the introduction of delayed extraction analysis. Delayed extraction is in part based on time-lag focussing, which was developed by Wiley and McLaren in the 1950's². This technique introduced a delay between ion production and ion extraction. During this delay the ions distribute in the ion source. When the accelerating voltage is applied, the different ions are at slightly different potentials. The ions are then detected at a plane in space where the ions are focussed together. An additional effect of the delay time is that neutrals from the desorption process diffuse, so that the ions encounter fewer collisions on their way out of the ion source. This technique was applied to MALDI by Brown *et al*³. Delayed extraction has been shown to significantly improve the resolution of the MALDI-TOF process⁴. In addition, delayed extraction can be used with a reflectron to give even higher resolution.

The technique of matrix-assisted laser desorption/ionization is well suited to the analysis of mixtures. MALDI has been used to analyze a wide variety of mixtures. These analytes include low molecular weight compounds⁵, oligosaccharides⁶ and mixtures of peptides and proteins^{7,8}. This work involves

the analysis of mixtures of peptides and proteins. A challenge in the analysis of mixtures by MALDI-MS is to produce uniform response for a wide range of analytes. Two different approaches have been recommended to optimize the analysis of mixtures of peptides and proteins. One approach involves modification of the sample preparation process^{9,10}. Another approach is to add a non-absorbing matrix additive to the sample¹¹. One type of mixture where a uniform response is very important is the mixture of an analyte and an internal standard for quantitation of the analyte. Two different methods, using additives, have been proposed for the quantitative analysis of peptides and proteins^{8,11}.

One matrix for the MALDI mixture analysis of peptides and proteins is α -cyano-4-hydroxycinnamic acid. This matrix has been found to produce intense signals for a wide variety of peptides with M.W.'s of less than 6000 Da. For proteins, this matrix produces a high degree of multiple charging, indicating that it is very efficient at protonation 12 .

A wide variety of analyte characteristics have been reported to influence the signal intensity in the MALDI experiment. In general, smaller analytes are more easily detected than large analytes 13 . Using α -cyano-4-hydroxycinnamic acid as the matrix it has been found that the degree of mass discrimination that is observed is dependent on the pH of the solution and the rate of crystal growth 14 . In addition the various analytes in a mixture often have different response factors. The sensitivity for a given analyte in the MALDI experiment is dependent on the hydrophobicity of the analyte as well as the basicity of the analyte.

Peptides that are both hydrophobic and have many basic sidechains are easily detected in the MALDI experiment.

In addition to the factors discussed above analyte suppression can also alter the signal intensity of an analyte in the MALDI experiment. Both matrix suppression and analyte suppression have been discussed in the MALDI literature. Matrix suppression describes when an analyte peak is observed with no matrix peaks in the low mass region. This effect occurs at low matrix: analyte ratios of 10:1 to 2000:1^{15,16}. One explanation for this effect is that there is a competition for available protons. When the matrix:analyte ratio is low enough the analyte(s) may be able to successfully scavenge all of the available protons. Another type of suppression that has been reported is analyte suppression. This effect occurs when the signal from a concentrated component actually suppresses the signal from a minor component 17. Competition for available protons from the matrix, can occur between different analytes. A large excess of matrix should prevent this competition from occurring. Preparing samples with a matrix-to-analyte ratio greater than 5000 has been reported to reduce analyte suppression 17. For the purpose of this work I define analyte suppression as the ability of one analyte or group of analytes to lower the signal intensity produced by a given amount of analyte from the signal intensity that is observed when the analyte is analyzed by the same preparation procedure with only matrix. In this work we examine some analyte suppression effects that occur at a high matrixto-analyte ratio.

2. Results and Discussion

Six Component Mixture

In order to evaluate how frequently analyte suppression occurs, a mixture analysis on a six component mixture of peptides and proteins that ranged in molecular weight from 1060 to 12600 Da. The analytes included bradykinin (M.W = 1060,B), angiotensin (M.W. = 1296,A), melittin (M.W. = 2848,M), b-chain of insulin (M.W. = 3495,lb), insulin (M.W. = 5735,l), and cytochrome C (M.W. = 12600,C). The results of this analysis at a low and a high laser power are shown in Figure 4.1. When a high laser power was used all the analytes could be detected. However the peaks for bradykinin and angiotensin are saturated while the peaks from the singly and doubly protonated cytochrome C are very weak. Figure 4.2 is a spectrum of 5 pm of cytochrome C with no other analytes. The peaks from cytochrome C are 3 times more intense when pure cytochrome C is analyzed. In addition analysis of the pure cytochrome C also produces peaks from the triply charged analyte. By using a much lower laser power none of the peaks are saturated, however cytochrome C can not be detected at all. The remaining analytes seem to fall into three classes. Bradykinin and angiotensin both produce intense peaks with the bradykinin peak being almost twice as intense as the peak from angiotensin. The peaks from melittin and insulin are about the same intensity. While the peak from the b-chain of insulin is about half of the intensity of the melittin and insulin peaks. These variations in the intensities of the peaks of these standards can not be fully explained by differences in hydrophobicity and amount of basic residues.

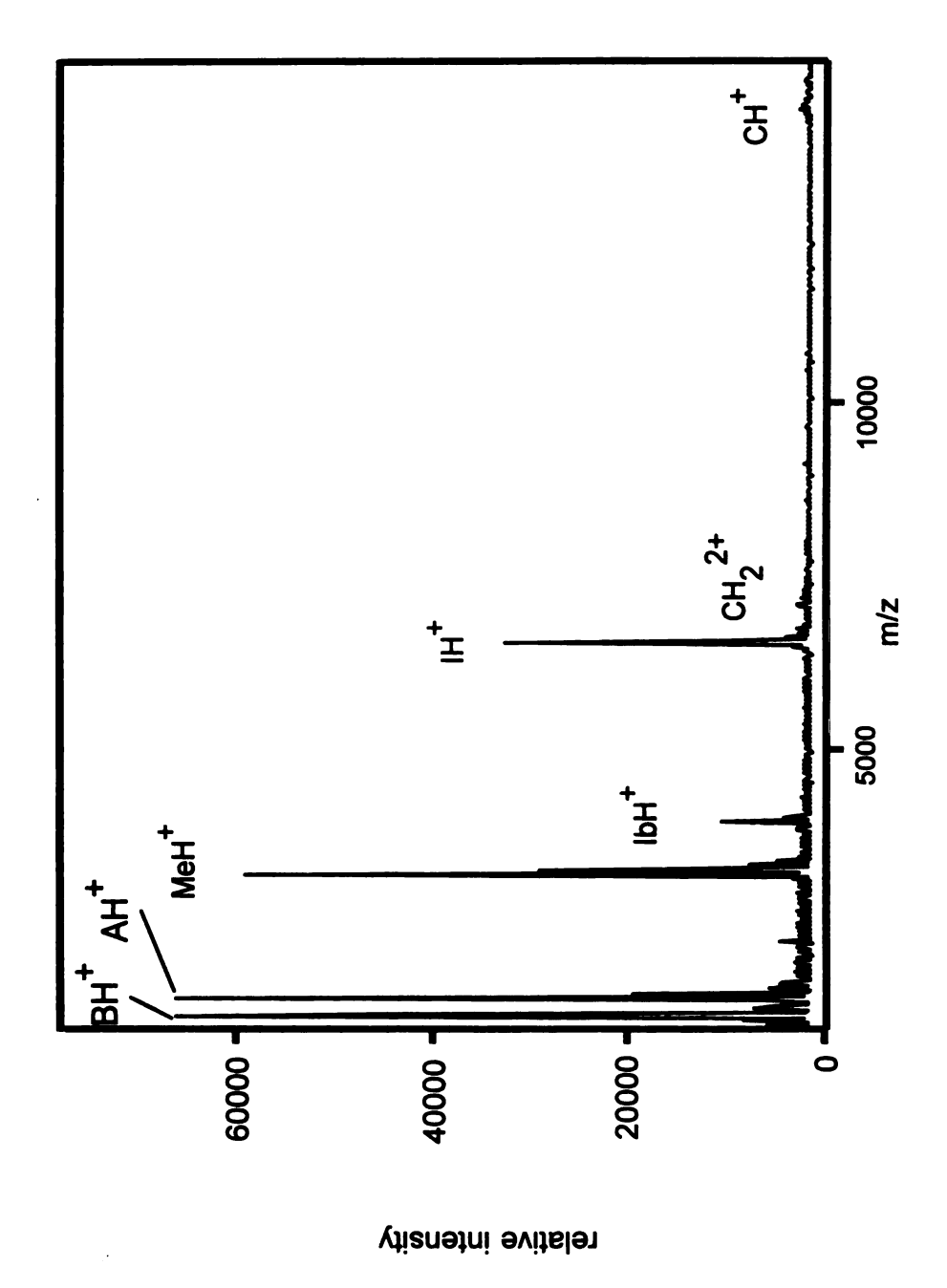


Figure 4.1 High power spectrum of six component mixture

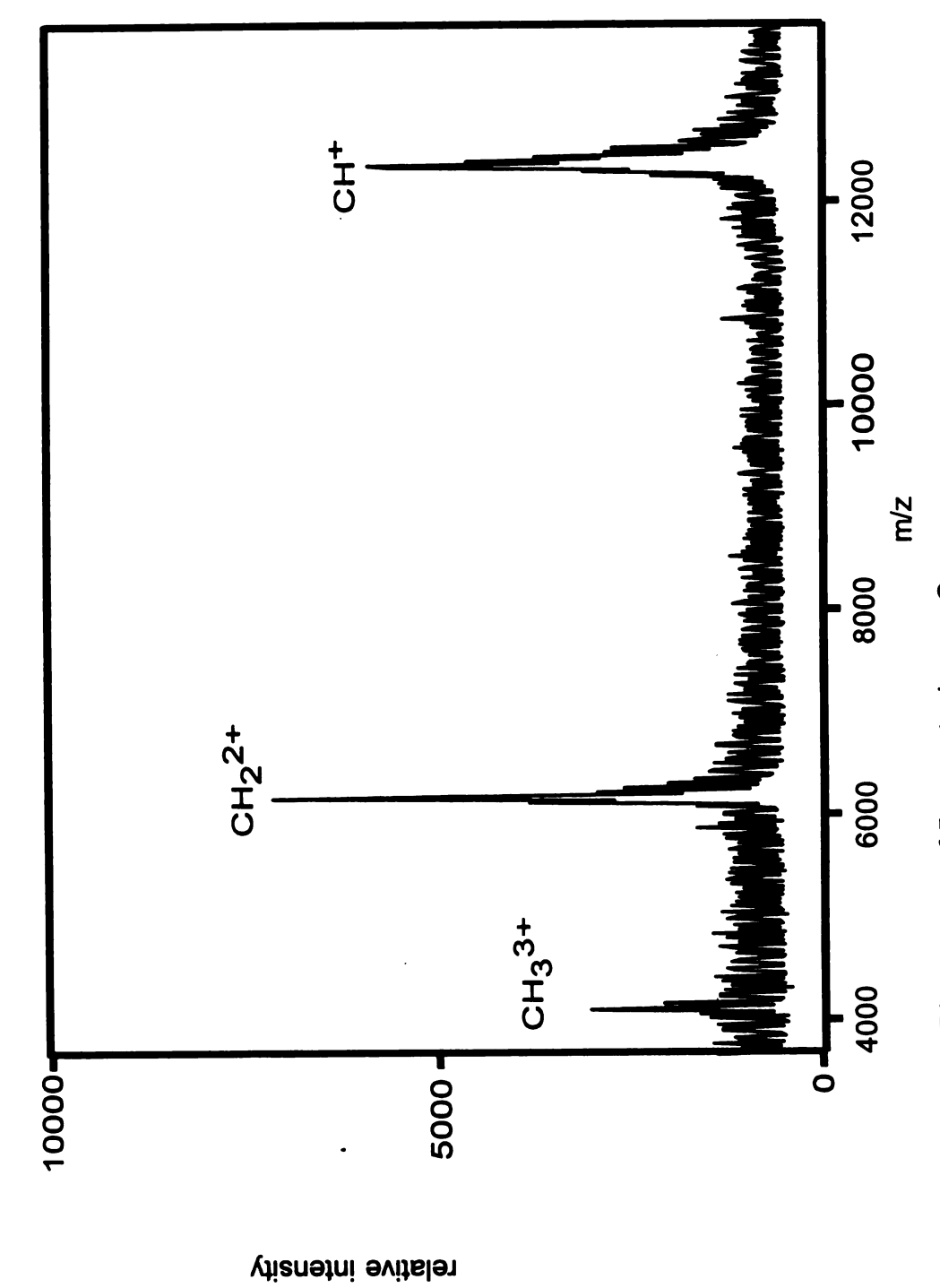


Figure 4.2 MALDI spectrum of 5 pm cytochrome C

Hydrophobicities can be compared by comparing analytes on the unitless Bull and Breese scale ¹⁸. The larger the Bull and Breese value the more hydrophillic a peptide. Peptides with positive Bull and Breese values are hydrophobic. All of these analytes have large negative Bull and Breese values and contain similar numbers of basic residues. In addition the subtle differences between these analytes in hydrophobicity and number of basic residues do not correlate to the different responses of the analytes. For instance melittin has the most basic residues and the second most negative Bull and Breese value of the six components in the mixture. In contrast angiontensin contains only a single basic residue and a greater Bull and Breese value than melittin. Yet angiotensin produces a much more intense peak than the peak that is produced from the same amount of melittin.

The conditions used for this work were optimized to study the possiblity of suppression in the absence of matrix saturation. In an attempt to eliminate the possibility of matrix saturation, matrix:analyte ratios of 15,000 to 60,000 were used. These ratios are well above the recommended minimum of 5000¹⁷. The other sample preparation parameters were chosen to mimic a routine sample analysis. A fast drying sample preparation method was used to produce reproducible results. A typical solvent system of 1:1 0.1% TFA:acetonitrile was used to for all of these experiments. The same experiment was also performed at a much lower laser power to eliminate saturated peaks. The most obvious results, shown in Figure 4.3, is the suppression of the signal from the b-chain of

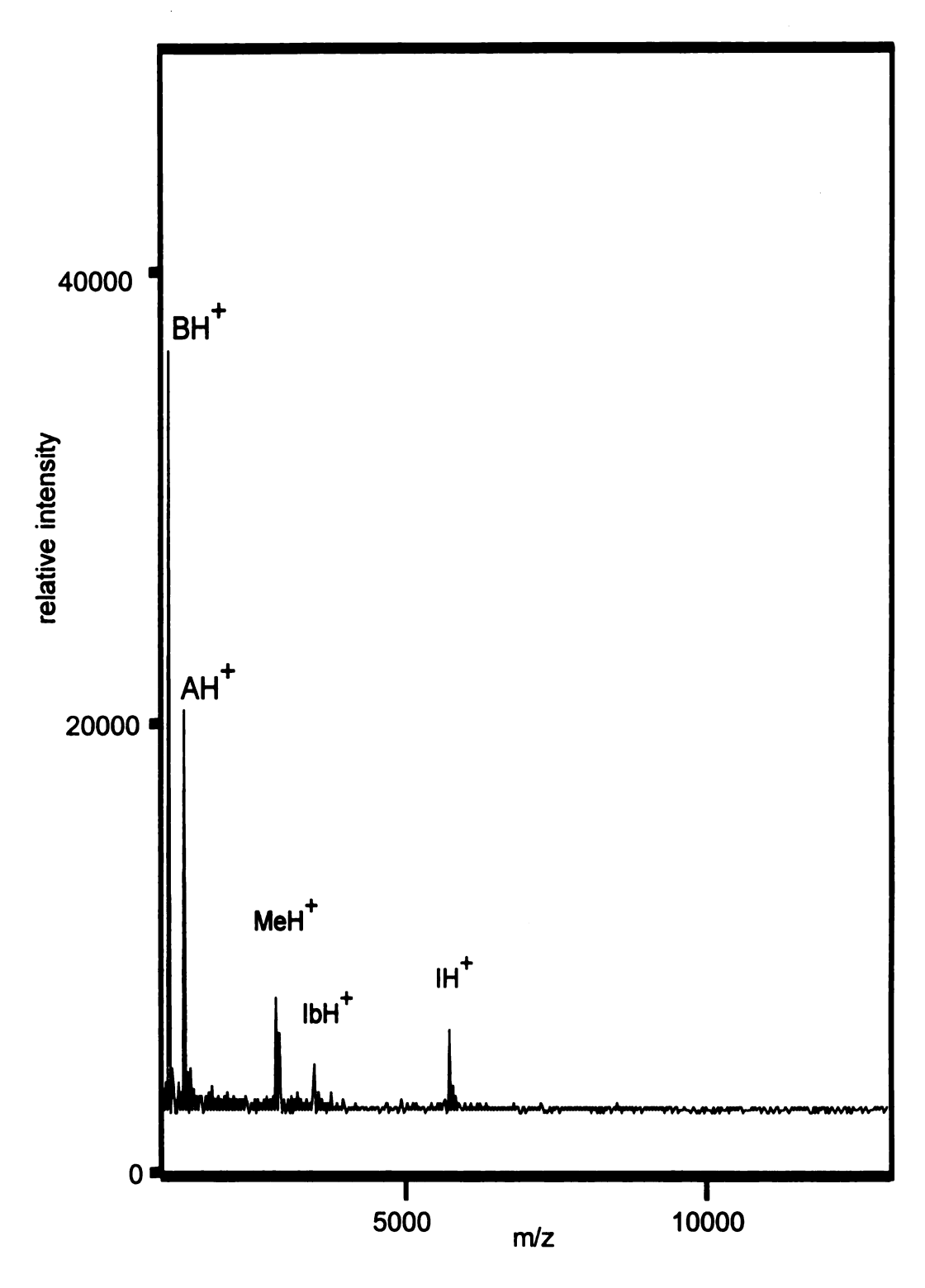


Figure 4.3 Low power spectrum of six component mixture

insulin. The peak for the b-chain of insulin should be easy to detect due to the analyte's hydrophobicity and number of basic residues. The high m/z of the b-chain of insulin compared to bradykinin and angiotensin could partially account for the lower single intensity. However, while the signal strength goes down significantly for peaks greater than m/z 6000, in the range of 1000-6000 m/z the response of analytes has been found to vary little 13.

For this mixture of six commonly used calibration compounds, there is significant variation in the responses of the analytes. Some of the discrepancies seem to be due to analyte suppression. In particular the signal from Cytochrome C has been shown to be suppressed by other components of the mixture. In addition it appears the signal from the b-chain of insulin is also being suppressed. The analyte suppression that I have observed could be due to only a limited number of protons because of saturation of the matrix. It is reasonable to expect that when the MALDI process is limited by the number of protons available, very slight differences in the analytes could be critical in the sensitivity of the various analytes. In addition, the fact that MALDI on cytochrome C as a single component produces a triply protonated molecule, could be an indication that more protons are available for protonation of cytochrome C when it is pure then when it is in a mixture. The variations of the analyte responses are such that minor components of a mixture could not easily be detected.

Binary Mixture

In order to determine the extent of the suppression of the b-chain of insulin signal by bradykinin, I examined a mixture of bradykinin and the oxidized b-chain of insulin. These two analytes have similar basicity since in each case about twenty percent of the ratios are basic. In addition these analytes are also both hydrophobic. The b-chain of insulin is a little more hydrophillic since the cystine residues are oxidized. Bradykinin has a Bull and Breese value of –940. Bradykinin and the b-chain of insulin are also similar in size in comparision to the large range of molecular weight values that are analyzed by MALDI.

This work was done at a low laser power that did not cause any of the analyte peaks to saturate. This experiment was performed with equimolar amounts of bradykinin and the oxidized b-chain of insulin. The experiment was done with total analyte concentrations of 5 pm and 20 pm. Under both of these conditions the spectrum is dominated by the bradykinin peak as shown in Figure 4.4. When the ratio between the analytes was adjusted to 1:9 bradykinin:b-chain of insulin the spectrum was dominated by the peak from the b-chain of insulin. This experiment, Figure 4.5, was also done with total analyte concentrations of 5pm and 20 pm. At the higher total concentration the peak due to the b-chain of insulin increased by 30% while the peak from bradykinin remained at about the same intensity. In addition the doubly protonated b-chain of insulin, detected at a m/z of 1740, also is more intense at the higher concentration. By comparing the peaks that are produced in these four experiments we can begin to draw some

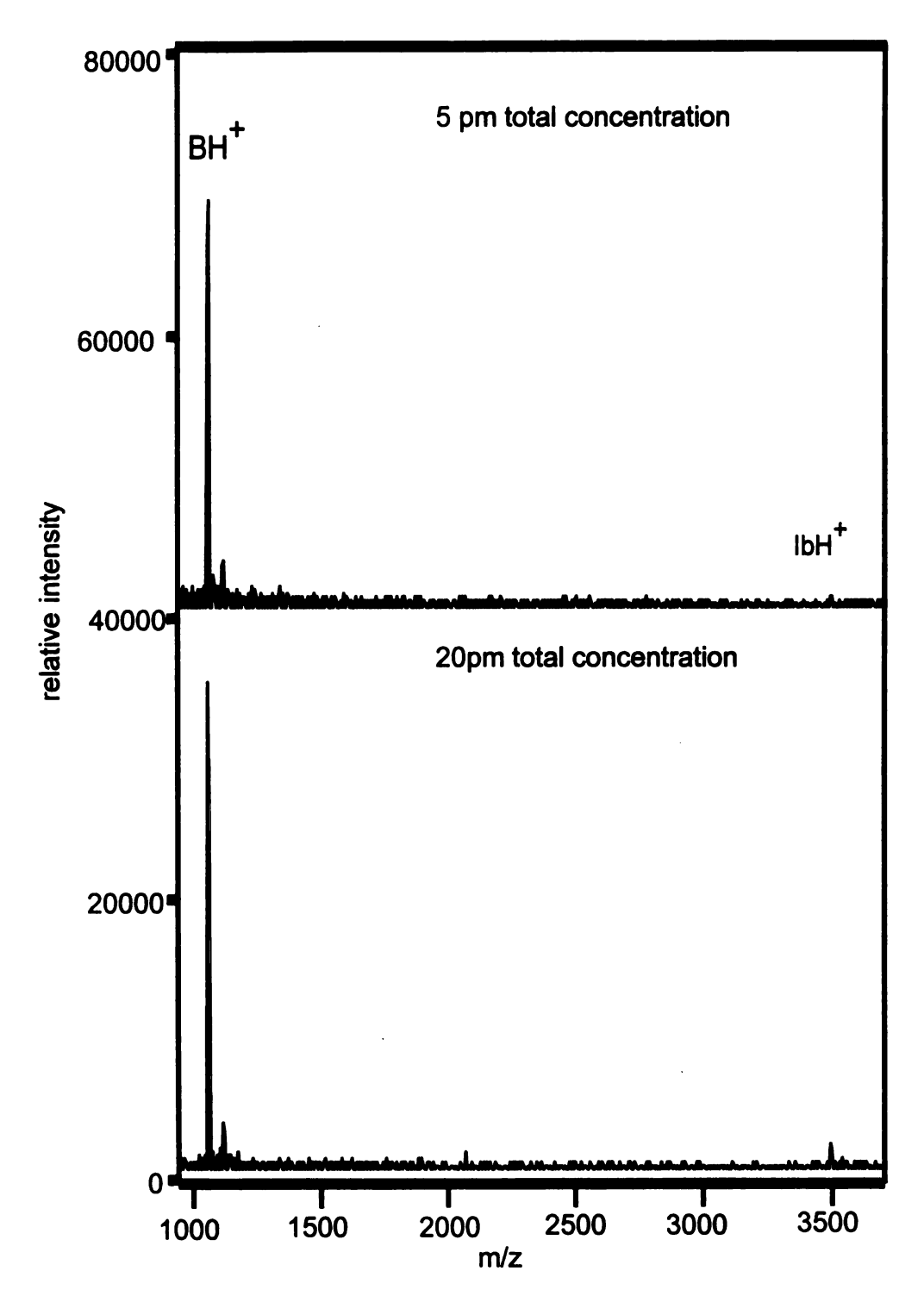


Figure 4.4 Spectrum of 1:1 mixture of bradykinin and b-chain of insulin

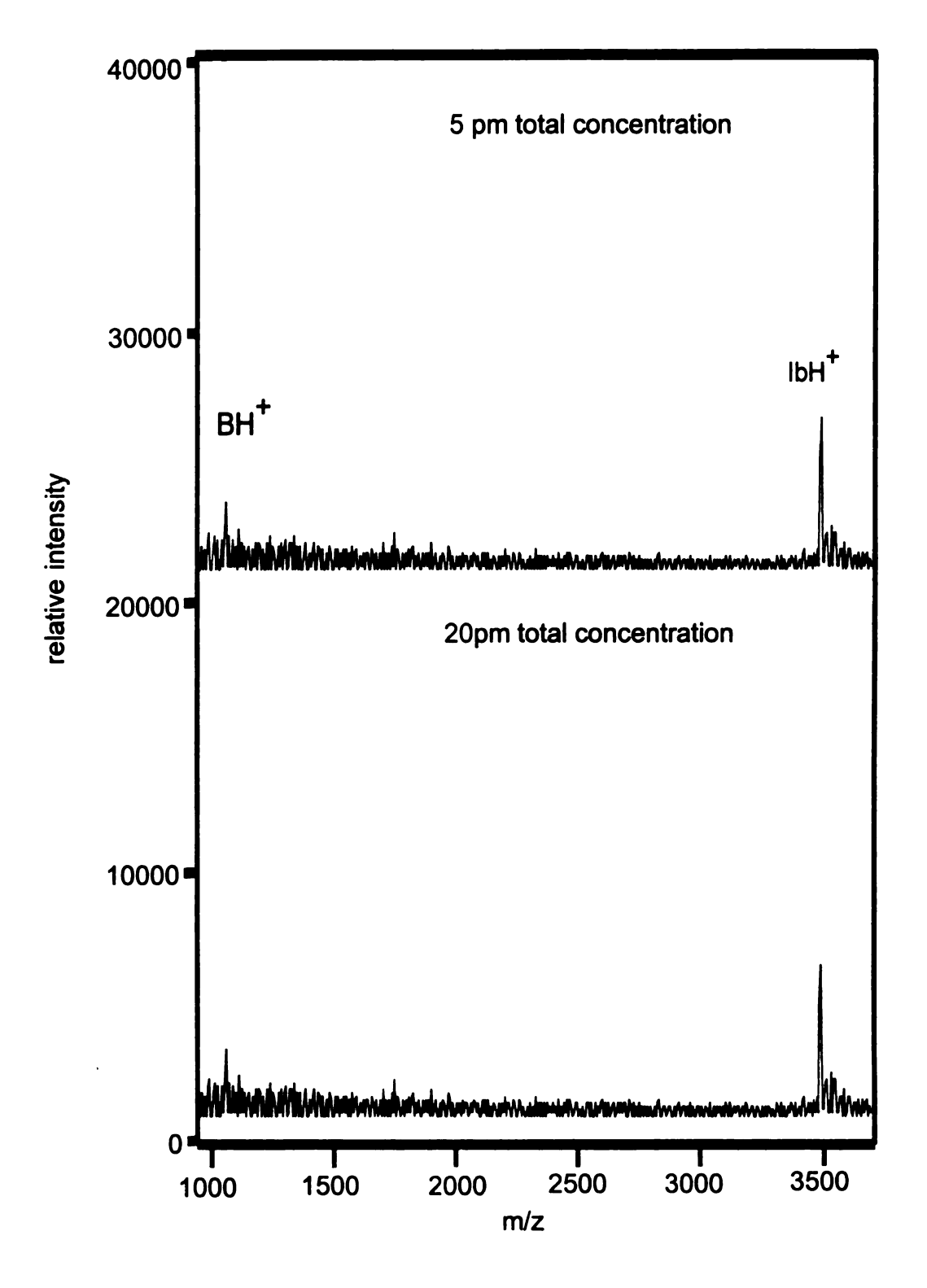


Figure 4.5 Spectrum of 1:9 mixture of bradykinin and b-chain of insulin

conclusions. The peak heights for bradykinin and the b-chain of insulin are listed in Tables 4.1 and 4.2.

ratio bradykinin: b-chain	[bradykinin] pmols	Peak height arb. units
Pure bradykinin	0.5	11405
1:1	2.5	29629
1:1	10	35409
1:9	0.5	3263
1:9	2	3181
6 comp. mix	5	34780

Table 4.1 Peak heights of bradykinin under different conditions

Ratio bradykinin: b-chain	[b-chain] pmols	Peak height arb. units
Pure b-chain	2.5	9260
1:1	2.5	1534
1:1	10	2576
1:9	4.5	6462
1:9	18	10957
6 comp. mix	5	2816

Table 4.2 Peak heights of the b-chain of insulin under different conditions

The peak that resulted from 4.5 pm of b-chain of insulin in the 1:9 mixture is twice as intense as the peak from 10 pm of b-chain of insulin in a ratio of 1:1. The signal from the b-chain of insulin seems to be suppressed by bradykinin. The signal from 2.5 pm of bradykinin in the 1:1 mixture is almost ten times as intense as the signal from 2 pm of bradykinin in the 1:9 mixture. The b-chain of insulin seems to be able to suppress signal from bradykinin when it is in excess. In addition the peak intensity of both of the analytes in the 6 component mixture seem to be similar to the peak intensities observed in the 1:1 mixtures. It appears the most intense analyte peak in the spectrum seems to be responsible for the majority of the suppression effects. Overall the results of these experiments seem to be very similar when the amount of total analyte is changed by a factor of 4.5. When the experiment is done with larger quantities of analytes both signals simply get a little more intense but the general trend remains the same, indicating that the suppression of the b-chain of insulin is not due to competition for protons. The large ratio of matrix:analyte seems to have been effective in preventing matrix suppression. It seems that the suppression that we are observing is occurring through some other mechanism than a competition for available protons. We do not seem to be at the proton supply limit for the experiments shown in Figures 4.4 and 4.5.

Analyte Suppression by an Undetected Analyte

It is commonly accepted that large peaks suppress small peaks in the MALDI experiment. A reasonable explanation for this trend is that there are a

limited number of protons available for the protonation of analytes. However it is possible to observe suppression effects from an analyte that is not even protonated. Some analytes are difficult to detect by MALDI. One of these analytes is bucalin (M.W. = 1053 Da). Bucalin is a peptide that has three acidic residues. However despite these acidic residues, bucalin is a hydrophobic peptide. This combination of properties is fairly rare in a peptide since acidic residues are very hydrophillic.

Spectra vary in the MALDI experiment so absolute intensity comparisons can be difficult. These comparisons are made even more difficult when there is no dominant analyte peak for reference. In this work I have chosen to look at series of multiple spectra for trends. In order to isolate significant trends from different sample it is important to have an even more homogenous sample surface than used in the previous work. A three layer sample preparation technique was used to produce reproducible samples. The first layer was $0.5~\mu L$ of acetone saturated with α -cyano-4-hydroxycinnamic acid. This forms a very thin, wide layer of matrix crystals. A $1.0~\mu L$ drop of the analyte in distilled water was placed on top of the first layer. This droplet would dissolve some of the matrix to create a well In the first layer. A second $0.5~\mu L$ drop of acetone saturated with α -cyano-4-hydroxycinnamic acid was then added to the analyte solution. This technique gave the most reproducible results as shown in the results.

The three component mixture of bradydinin, b-chain of insulin, and insulin was used to demonstrate this effect. Spectra from three consecutive spots are

shown in Figure 4.6. In these spectra bradykinin is always the most intense peak, while insulin is just slightly less intense. These spectra also have a large peak for the doubly protonated insulin molecule. In addition all of the analytes produce a significant amount of adduct peaks. The high incidence of adducts is most likely due to the type of sample preparation that was used.

When three equivalents of bucalin are added to the mixture the spectra change, shown in Figure 4.7. While the other analytes produce large peaks, bucalin is not detected at all. The bucalin (M.W. = 1053) peak would appear next to the bradykinin peak. It has been observed that peptides with acidic residues are harder to detect than peptide with basic residues 19. The other three components in the mixture all contain basic residues. In the spectra of the four component mixture bradykinin is still the most intense peak. However the intensity of the insulin peak is much reduced. The peak from the b-chain of insulin seems to be only slightly suppressed by the bucalin. It is interesting to note that the peak from the doubly protonated insulin is also suppressed to a significant degree. The protonation of insulin seems to occur in a sequential fashion. Apparently a critical number of protonated insulin must be formed to increase the rate of formation of the doubly charged insulin fast enough to make the doubly protonated insulin form in the time scale of the experiment. The bucalin is most likely competing with the b-chain of insulin and insulin for the hydrophobic crystal faces that are produced on the α -cyano-4-hydroxycinnamic acid crystals.

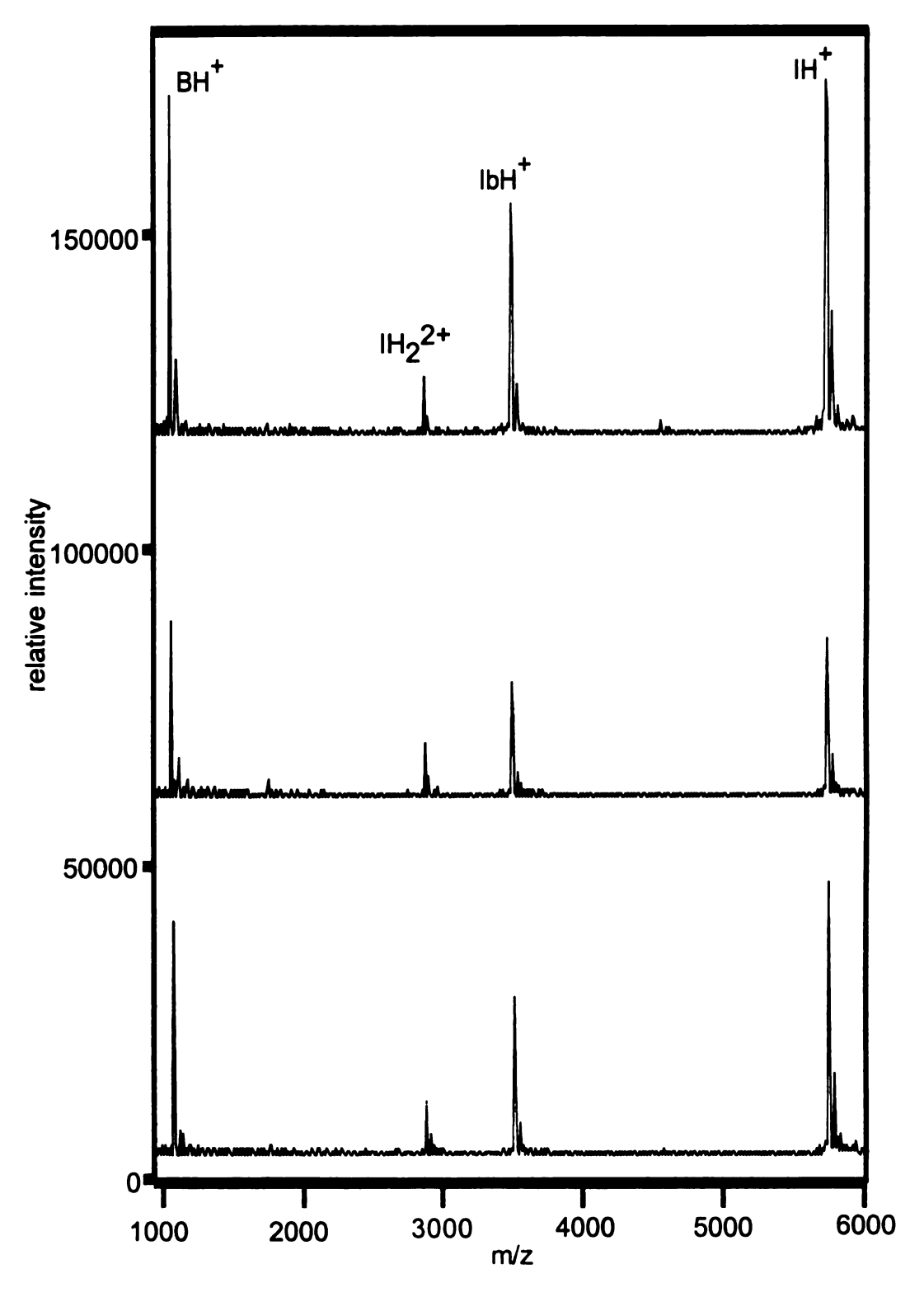


Figure 4.6 3 consecutive spectra of a 1:1:1 mixture of bradykinin, b-chain of insulin, and insulin

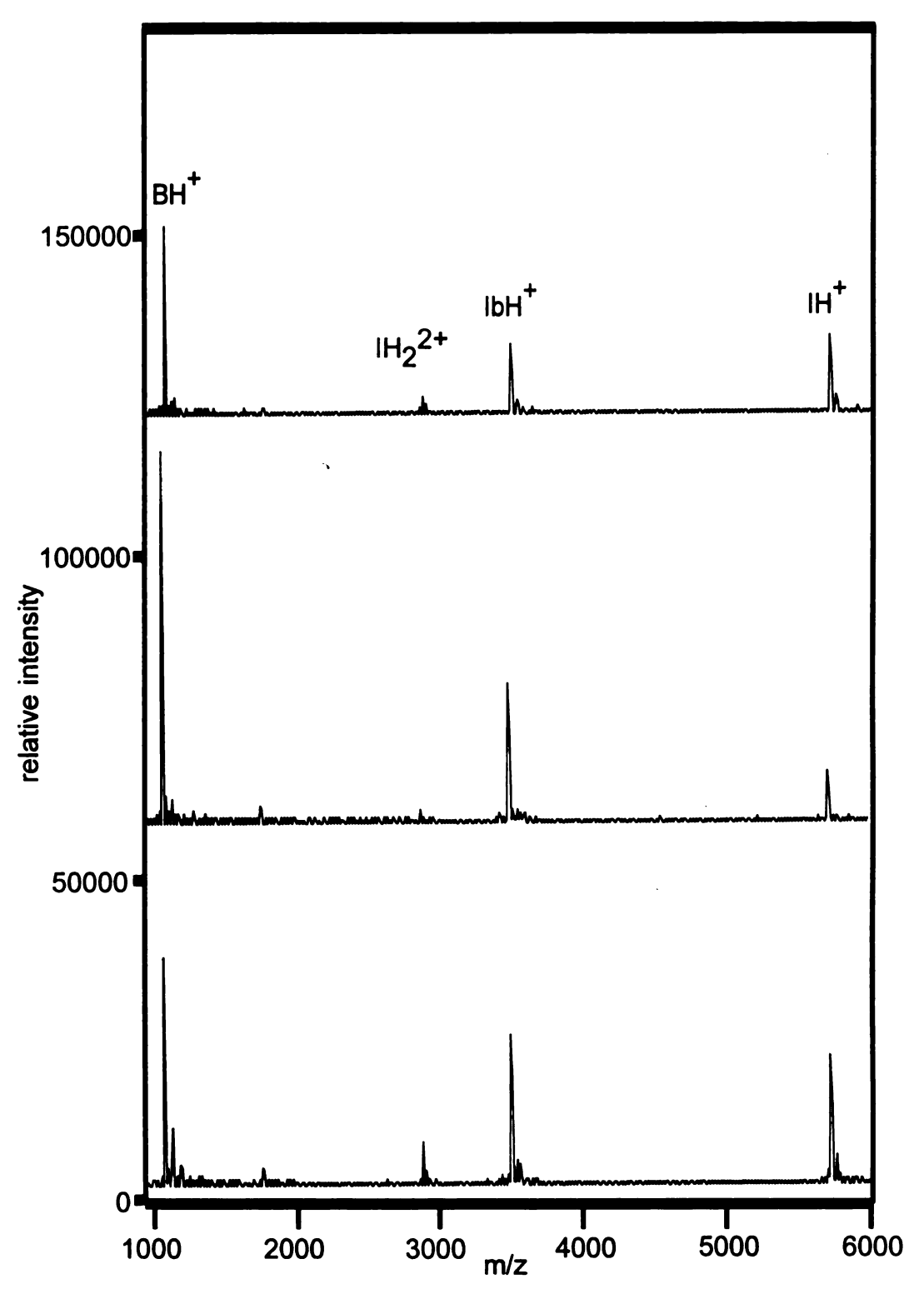


Figure 4.7 3 consecutive spectra of a 3:1:1:1 mixture of bucalin, bradykinin, b-chain of insulin, and insulin

The reason that a peak from bucalin does not appear in the spectrum may be that the peptide is too acidic to accept another proton at the energies achieved in this experiment. The effect that bucalin has on this mixture indicates a possible downfall of mixture analysis by MALDI.

3. References

- 1)Mamyrin, B. A.; Karataev, V. I.; Shmikk, D. V.; Zagulin, V. A. Sov. Phys. JETP 1973, 37, 46-48.
- 2)Wiley, W. C.; McLaren, I. H. Review of Scientific Instrumentation 1953, 26, 1150-1157.
- 3)Brown, R. S.; Lennon, J. J. Analytical Chemistry 1995, 67, 1998-2003.
- 4) Vestal, M. L.; Juhasz, P.; Martin, S. A. Rapid Communications in Mass Spectrometry 1995, 9, 1044-1050.
- 5)Lidgard, R.; Duncan, M. W. Rapid Communications in Mass Spectrometry 1995, 9, 128-132.
- 6) Harvey, D. J. Rapid Communications in Mass Spectrometry 1993, 7, 614-619.
- 7)Perkins, J. R.; Smith, B.; Gallagher, R. T.; Jones, D. S.; Davis, S. C.; Hoffman, A. D.; Tomer, K. B. *Journal of the American Society of Mass Spectrometry* **1993**, *4*, 670-684.
- 8) Billeci, T. M.; Stults, J. T. Analytical Chemistry 1993, 65, 1709-1716.
- 9)Xiang, F.; Beavis, R. C. Rapid Communications in Mass Spectrometry 1994, 8, 199-204.
- 10) Kussmann, M.; Nordhoff, E.; Rahbek-Nielsen, H.; Haebel, S.; Larsen, M. R.; Jakobsen, L.; Gobom, J.; Mirgorodskaya, E.; Kroll-Kristensen, A.; Palm, L.; Roepstorff, P. *Journal of Mass Spectrometry* **1997**, *32*, 593-601.
- 11)Gusev, A.; Wilkinson, W. R.; Proctor, A.; Hercules, D. M. *Analytical Chemistry* **1995**, *67*, 1034-1041.
- 12)Beavis, R. C.; Chaudhary, T.; Chait, B. T. Organic Mass Spectrometry 1992, 27, 156-158.
- 13)Farmer, T. B.; Caprioli, R. M. *Journal of Mass Spectrometry* **1995**, *30*, 1245-1254.
- 14) Cohen, S. L.; Chait, B. T. Analytical Chemistry 1996, 68, 31-37.
- 15)Chan, T.-W. D.; Colburn, A. W.; Derrick, P. J. Organic Mass Spectrometry 1991. 26, 342-344.

- 16) Knochenmuss, R.; Dubois, F.; Dale, M. J.; Zenobi, R. Rapid Communications in Mass Spectrometry 1996, 10, 871-877.
- 17) Gusev, A. I.; Wilkinson, W. R.; Proctor, A.; Hercules, D. M. Fresenius Journal of Analytical Chemistry 1996, 354, 4550-4563.
- 18)Bull, H. B.; Breese, K. Archives of Biochemistry and Biophysics 1974, 161, 665-670.
- 19) Dikler, S.; Kelly, J. W.; Russell, D. H. Journal of Mass Spectrometry 1997, 32, 1337.

Chapter five. Prompt Fragmentation (PF) MALDI

1. Introduction

Initially, MALDI was unique in that fragmentation did not appear to occur for the analytes that have dominated biological mass spectrometry (polypeptides). Subsequently, fragmentation products have been observed. Metastable processes were first detected, and the post source decay (PSD) experiment was developed. The PSD experiment is performed by lowering the reflectron voltage incrementally so that the products of metastable decay are focussed on the detector. The initiation of prompt fragmentation in peptide analysis is a new development, although it is notable that the process does occur to a large degree for other types of analytes such as oliglionucleotides 1. While conditions have been described with which prompt fragment ions can be generated, the technique of prompt fragmentation is not in widespread use 2. High laser powers are usually employed, which can increase chemical noise and lower mass spectral resolution in the linear time-of-flight (TOF) MS experiment. In MALDI, insource fragmentation must occur on a very short time scale in order to yield peaks in the resulting spectrum for which m/z values can be correctly assigned. If the ions slowly dissociate in the first region of a TOF-MS ion source, they will have a wide range of flight times, and will not be detected as a single peak. During the development of power titrations, it was observed that at very high laser powers there was some extra "noise" in the high mass region. This "noise" corresponded to fragment ions. The peaks for these fragment ions were very

broad and few in number. A large number of prompt fragment ions could be detected by delayed extraction (DE) TOF-MS, which has become an important development in the investigation of prompt fragmentation-matrix assisted laser desorption/ionization— mass spectrometry (PF-MALDI -MS). If prompt fragmentation is not really "instantaneous", occurring in a few vibrational periods, than DE will assist in the detection of prompt fragment ions by allowing fragmentation to occur within the first 350 ns or more of the experiment, under field-free conditions.

Further Fragmentation of Prompt Fragment lons

It is expected that prompt fragment ions would fail to further dissociate to yield abundant PSD fragment ions. If the energy available is all deposited in the desorption/ionization (D/I) event, that used for prompt fragmentation would not be available for PSD. Nonetheless, the combination would be a powerful one. If peptides undergo prompt fragmentation, and these prompt fragments could be analyzed in the PSD experiment, then MSⁿ-type experiments could be performed in a reflectron TOF-MS. As with other methods, collisional activated dissociation can be used to add additional energy to ions after extraction from the source. However collisions can alter flight times, scatter ions away from the ion-optical axis, and lower resolution in TOF experiments.

In this chapter a new matrix, bumetanide, is evaluated for its ability to induce the formation of prompt fragment ions of peptides in the linear MALDI-TOF experiment. Its use is compared to two commonly used MALDI matrices.

In addition, the use of burnetanide in mixed matrices will be presented. Using a mixed matrix, sufficiently intense fragment ions can be generated such that PSD spectra can be obtained. Thus, the MALDI/PF/PSD MS experiment is evaluated here as well. The data will be used to determine how PF and PSD spectra differ, and will lead to considerations of what factors influence the formation of prompt fragment ions.

2. Results and Discussion

Experimental Details

Peptide and protein samples of dynorphin, α -melanocyte stimulating hormone, and the b-chain of insulin were obtained from Sigma Chemical Co. (St. Louis, MO) and Bachem (Torrance, CA). All of these peptides were used without further purification. Dihydroxybenzoic acid (DHB), α -cyano-4-hydroxycinnamic acid (HCCN) and burnetanide (BMN) were obtained from Sigma Chemical Co. (St. Louis, MO) and used without further purification. All mass spectra were obtained on a Voyager Elite reflectron time-of-flight mass spectrometer (Perseptive Biosystems, Inc., Framingham, MA) equipped with a nitrogen laser (337 nm, 3-ns pulse). The acceleration voltage used was 20 kV for all of the experiments. Data were acquired with the data system provided and based on a transient recorder with 2-ns resolution. This mass spectrometer is equipped with delayed extraction. During the delay, a reverse bias of ~ 0.1 % of the accelerating potential is applied in the first region of the source. Due to the electronics used for the switching of the voltage on the acceleration grid the

minimum delay time is 170 ns. For all of the linear TOF experiments, the voltage on the accelerating grid was 95 % of the total accelerating voltage. The delay time was varied from 220-570 ns. For the experiments with the reflectron, the accelerating grid was set at 80% of the total accelerating voltage and the delay time was 650 ns. All experiments were done with the guide wire set at 0.250 % of the total accelerating potential.

All of the peptide-containing targets were prepared by a three-step preparation process. First 1 μ L of 3:5 acetonitrile: 0.1% TFA was placed on the sample plate. To this droplet 0.4-0.5 μ L of the analyte in 1:1 acetonitrile: 0.1% TFA was added. The droplet of analyte solution typically contained 80 pm of the analyte. One μ L of a saturated solution of the matrix in acetone was added to the droplet. The combination matrix was prepared by making separate solutions of the two matrices saturated in acetone. The two solutions were then combined in a ratio 4:1 BMN:HCCN (vol/vol). The resulting mixture was then used as the matrix solution. The cytochrome C sample was prepared by a dried droplet procedure outlined by Lennon 3 for proteins.

Maximizing Prompt Fragment Ions

We have been exploring matrices and approaches to increasing the amount of prompt fragment ions formed in MALDI, such that sequence information could be more easily obtained. An ideal matrix for sequencing by prompt fragmentation would produce the same types of fragment ions for a wide range of peptides and proteins with predictable relative intensities. The types of

fragment ions produced would include a series of N-terminal fragments and a series of C-terminal fragments. Both N-terminal and C-terminal fragment ions are necessary to elucidate an entire structure since prompt fragment ions can not be detected below an m/z of 700. In this best-case scenario, the fragment ions of the different types could be differentiated from each other. The sequence could be determined by the mass differences between the members of the various series. Another possible approach could make use of multiple matrices, some of which have more types of fragment ions than the others. By comparing and contrasting the fragment peaks that appeared in the various spectra the individual series could be identified. For instance, if one matrix produced c_n, y_n, and z_n fragment ions and another matrix produced c_n and y_n fragment ions, the z_n fragment ions could easily be identified by contrasting the spectra taken with the different matrices.

The work discussed here focuses on characterizing the different types of fragment ions that are produced with different matrices in the PF-MALDI experiment. We performed a survey of commonly used and new candidate matrix molecules. This survey included many "poor" matrix compounds, since a matrix that produces abundant prompt fragment ions may not be considered an ideal matrix for the standard MALDI analysis of peptides. The compound that gives sufficiently intense fragment ions such that it was selected for further investigation as a matrix is burnetanide. Burnetenide, 3-(aminosulfonyl)-5-(butylamino)-4-phenoxybenzoic acid (BMN), is a sulfur-containing diuretic with the structure shown in Figure 5.1. This compound has a local absorbance

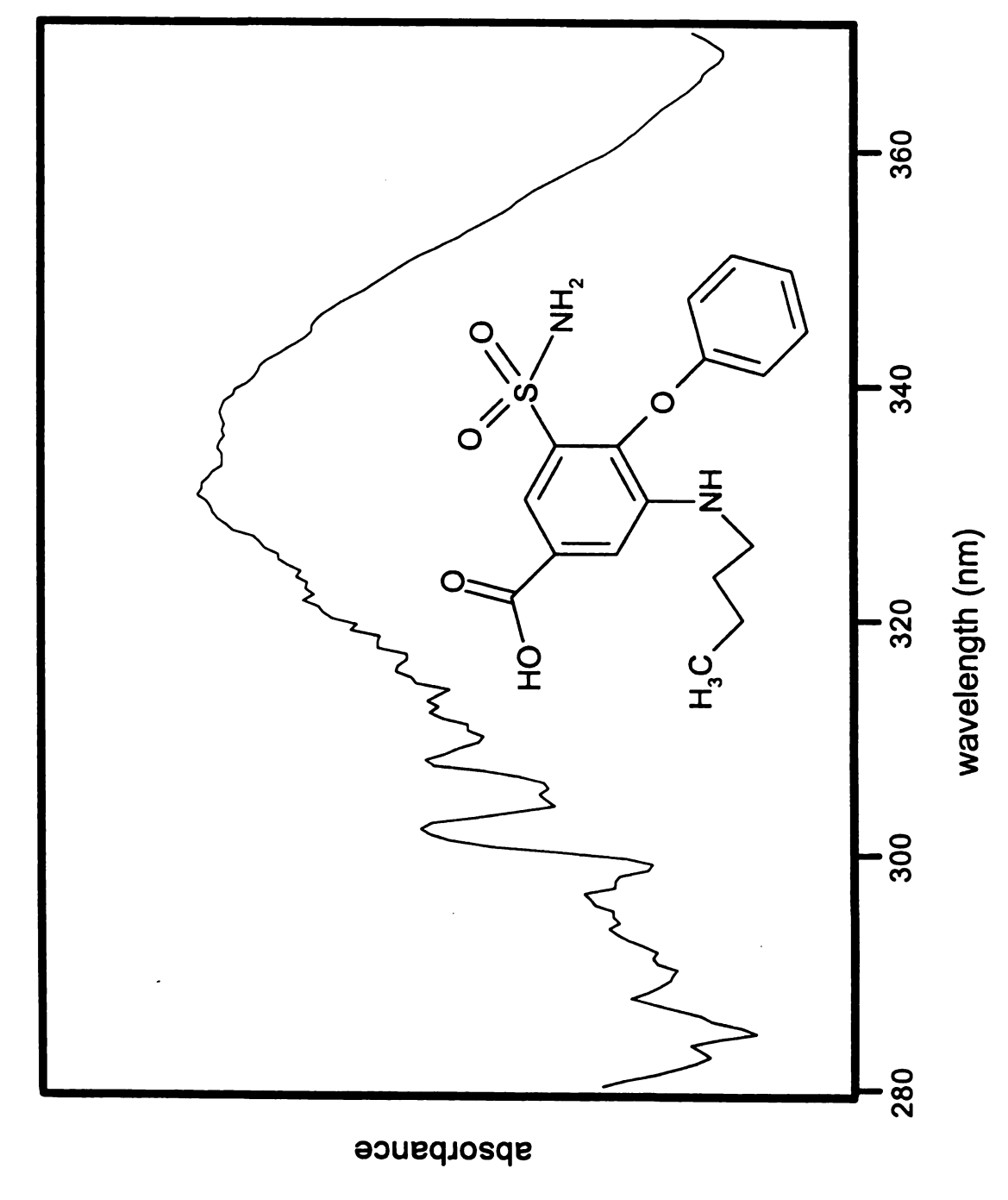


Figure 5.1 Structure and ultraviolet-visible absorption spectrum of bumetanide

maximum in the UV-Vis spectrum (aqueous) at 335 nm (Figure 5.1) At the laser wavelength of 337 nm the molar absorptivity of bumetanide is 5745 L/cm mole. This value is comparable to the molar absorbtivity of 2,5-dihydroxybenzoic acid (DHB) at the same wavelength, which is 4213 L/cm mole. However both of these values are fairly low compared to the molar absorptivity of α-cyano-4-hydroxycinnamic acid (HCCN) in methanol, at the same wavelength, which is 22,194 L/cm mole. Bumetanide also has a molecular weight of 364 Da, which is somewhat higher than that for most matrix molecules. For instance, the molecular weights of DHB and HCCN are both less than 200 Da. One characteristic that all three of these matrices have in common is that they have similar melting points, between 200-250° C.

The MALDI mass spectrum of BMN as a matrix has not been previously reported. The spectrum obtained at a laser power slightly above threshold is shown in Figure 5.2. The peak assignments were made by mixing KCI, NaCI and bradykinin into the BMN, and using peaks from these components for internal calibration. The m/z values measured in this experiment were then used to calibrate the spectrum of pure matrix, shown in Figure 5.2. The most intense peak represents the protonated molecule, [BMN+H]⁺, at m/z 365. The molecular ion region of the spectrum (Figure 5.2, inset) shows the formation of a relatively intense molecular ion, BMN⁺. at m/z 364, and an m/z 363 peak, [BMN+H-H₂]⁺. There is a typical collection of lower m/z peaks formed by elimination of small neutrals such as H₂O and CO₂ from the carboxylic acid group. There is a notable cluster of relatively intense peaks at around m/z 285, which appear to be formed

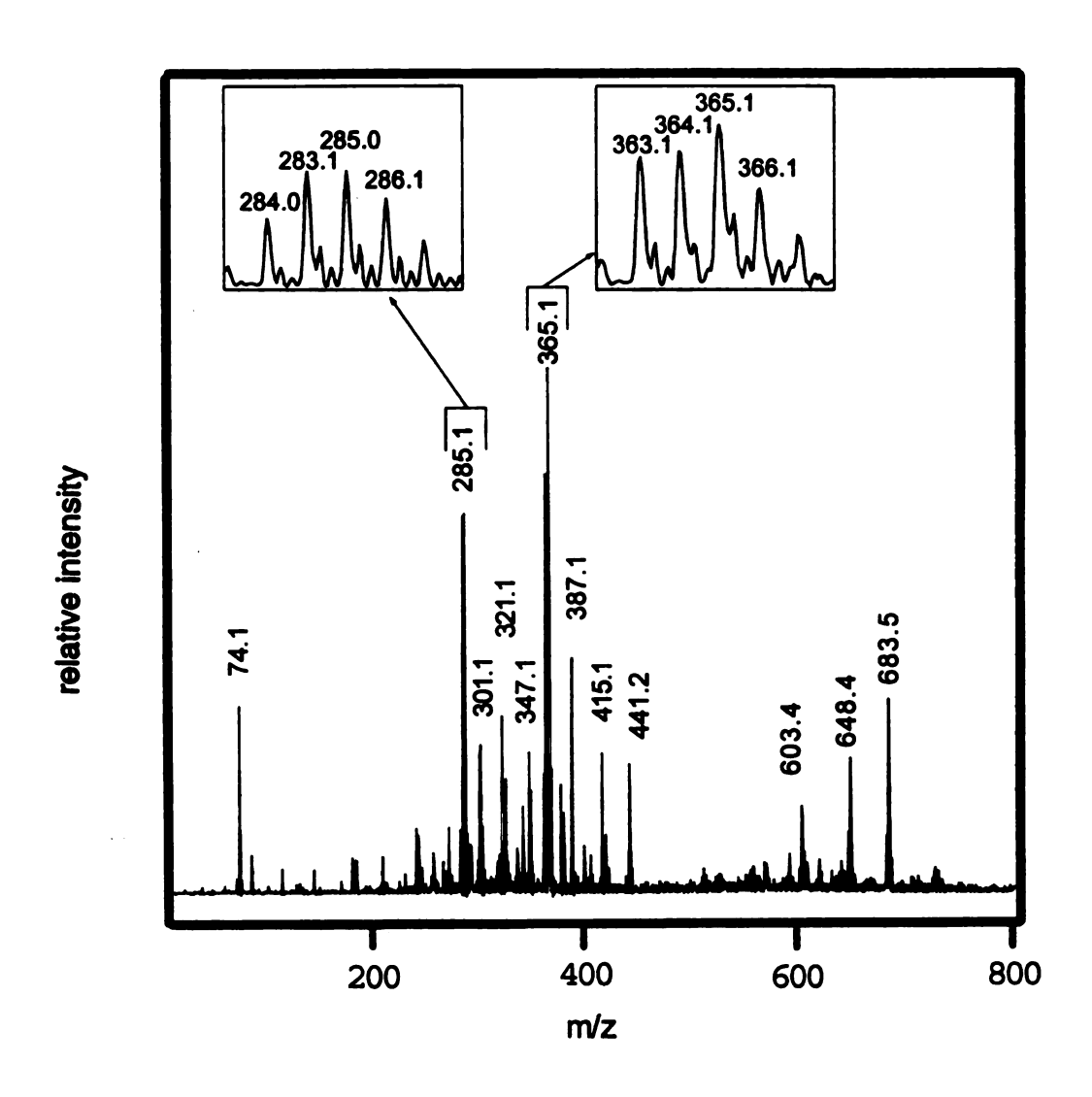


Figure 5.2 MALDI mass spectrum of burnetanide as a matrix

by elimination of the aminosulfonyl group from the various ionic forms of the intact molecule ([BMN+H]⁺, BMN⁺, etc.). For instance, the [BMN+H]⁺ ion eliminates an aminosulfonyl group to produce an m/z 285 ion [BMN+H-NH₂SO₂]⁺.

A low mass peak at m/z 74 is detected with some batches of BMN. This peak represents C₄H₉NH₃⁺, which could be formed via a 1,2-elimination of protonated butyl amine following protonation of the secondary nitrogen. The peak at m/z 74 could also represent an impurity in bumetanide. The matrix spectrum also exhibits peaks at m/z values greater than that for the [BMN+H]⁺ ions. Such higher mass peaks typically represent species such as the proton bound dimer of the matrix, and adducts of intense fragment ions with matrix molecules. This is not the case here. There is no peak representing [2BMN+H]+ (m/z 729), for example. These higher mass peaks appear to more likely represent ionized products of a covalent coupling of two matrix molecules, in which there are multiple reaction products. At higher laser powers, some products appear to be formed by the covalent coupling of three matrix molecules. Whatever their origin, it is important to understand the m/z values and relative intensities of matrixrelated ions in this experiment, since the utility of prompt fragmentation MALDI is in part determined by the useful low mass limit and the ability to calibrate accurately. This is established by the high m/z matrix peaks. In order for a matrix to be useful, it is important to understand the high m/z peaks formed from the matrix at higher laser powers - conditions at which PF MALDI experiments are performed. Spectra obtained at higher power exhibit the same high m/z peaks, and some at even higher m/z values. The major difference is that their

relative intensities increase. However, the working low m/z limit of PF MALDI using BMN is essentially m/z 780. Also of note is the fact that the peaks in Figure 5.2 representing the commonly observed metal ions (Na⁺, K⁺) and alkali ion adducts of the matrix are usually small and often not observed at all.

Prompt Fragmentation of Peptides with Different Matrices

In order to establish that PF-MALDI spectra can be very different when generated from different matrices, and to show how spectra obtained using BMN differ from those obtained using other common MALDI matrices, the results of PF-MALDI using BMN were compared with the results using DHB and HCCN. To produce prompt fragment ions, we deviate from the standard MALDI experiment in that a long delay time of 520 ns and elevated laser powers are used. One analyte used here to compare these three matrices is dynorphin. When dynorphin, a somewhat hydrophobic peptide, is used as an analyte, a high degree of fragmentation is produced in the PF-MALDI experiment as shown in Figure 5.3. The nomenclature of peptide fragment ions is illustrated in appendix 1. The prompt fragmentation of dynorphin also follows some consistent trends in the types of fragments formed in different matrices. Regardless of the matrix used, there seems to be more fragment ions that include the N-terminus than the C-terminus. All of the PF-MALDI spectra of dynorphin contain more peaks due to N-terminal fragment ions than C-terminal fragment ions. The fact that a greater variety of N-terminal fragments are detected indicates that the protonation of residues towards the N-terminus may be preferred. In addition, all of the spectra

16 15 14 13 12 11 10 9 8 7 6 5 4 3 2 1 xyz G-G-F-L-R-R-I-R-P-K-L-K-W-D-N-Q abc 1 2 3 4 5 6 7 8 9 10 11 12 13 14 15 16

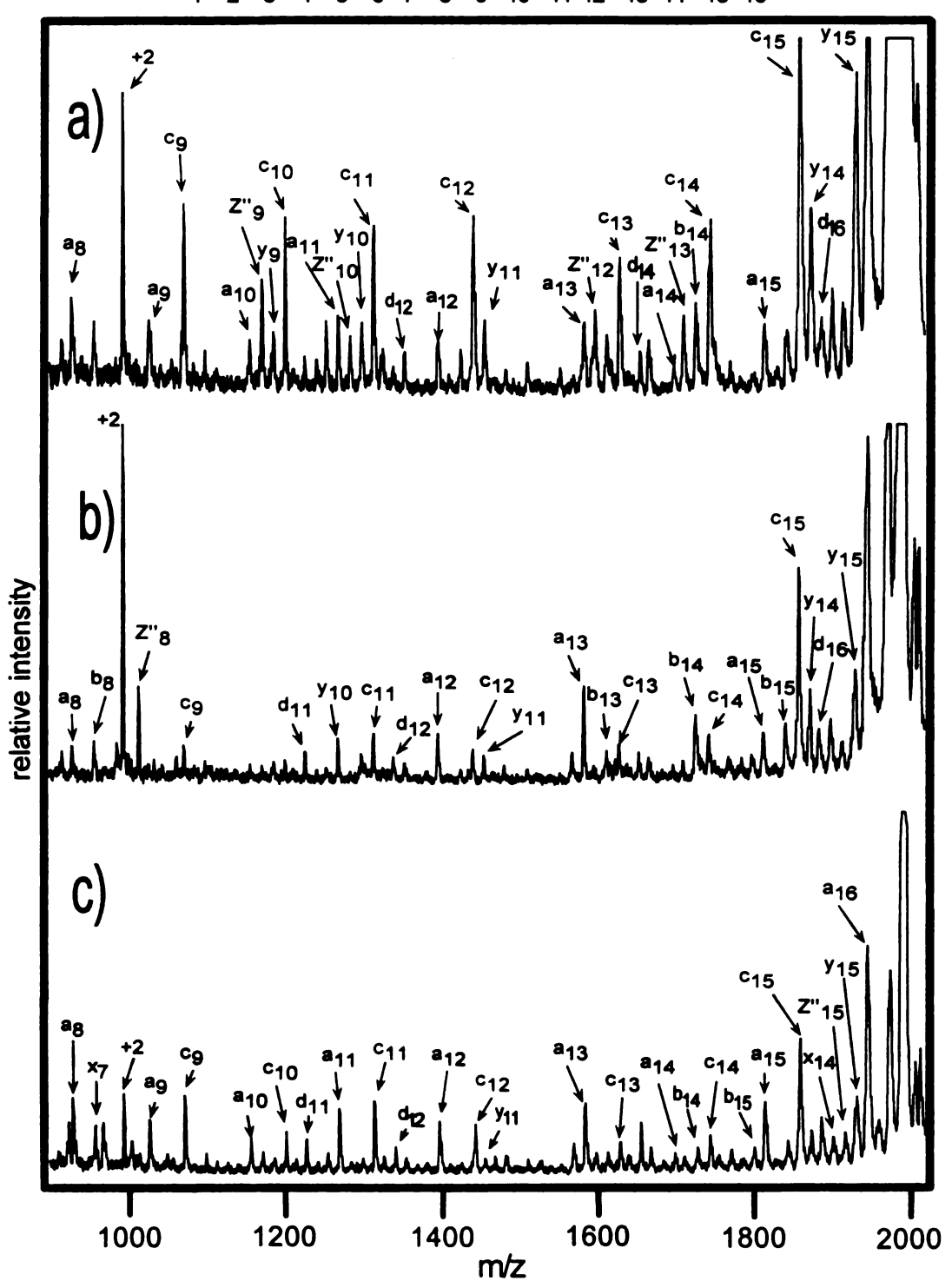


Figure 5.3 Prompt fragmentation spectra of dynorphin with a) DHB, b) HCCN and c) BMN

have peaks from fragment ions that are due to backbone cleavage with accompanying side chain losses, most commonly d_n ions.

There are some differences in the fragmentation that occurs for this peptide when each of these three matrices is used. When DHB is used as the matrix in the PF-MALDI experiment, Figure 5.3a, an intense series of c_n fragment ions and many y_n , $z_n + 2$, and a_n fragment ions are observed. Previously a_n fragment ions have not been observed with PF-MALDI performed with DHB and a variety of other matrices⁴. The spectrum obtained using DHB also has a large number of d_n and $z_n + 2$ fragment ions. The spectra that are acquired using HCCN and BMN as the matrices are very similar as shown in Figure 5.3 b, c. All of the matrices studied produce a doubly protonated analyte peak. It is interesting to note that while the +2 peak is very intense in both the spectra obtained with DHB and HCCN, the +2 peak is the same intensity as most of the other peaks in the case where BMN is the matrix. When PF-MALDI spectra are obtained for melanocyte stimulating hormone (MSH) (M.W. = 2662) as the analyte, Figure 5.4, the peak for the doubly protonated analyte is of medium intensity when DHB is the matrix, high intensity with HCCN and low intensity when BMN is used as the matrix. For this peptide, the prompt fragmentation of [MSH + H]⁺ seems to be particularly sensitive to the type of matrix used. The fragmentation spectrum of MSH in DHB, Figure 5.4a, contains exclusively c_n, y_n, and zn fragment peaks, as previously reported for prompt fragmentation fragment ions⁴. In contrast, MSH produces an intense peak from the doubly protonated

21 20 19 18 17 16 15 14 13 12 11 10 9 8 7 6 5 4 3 2 1 XYZ
A--E-K--K--D--E-G--P--Y--R--M--E--H--F--R--W--G--S--P--K--D

abc 1 2 3 4 5 6 7 8 9 10 11 12 13 14 15 16 17 18 19 20 21

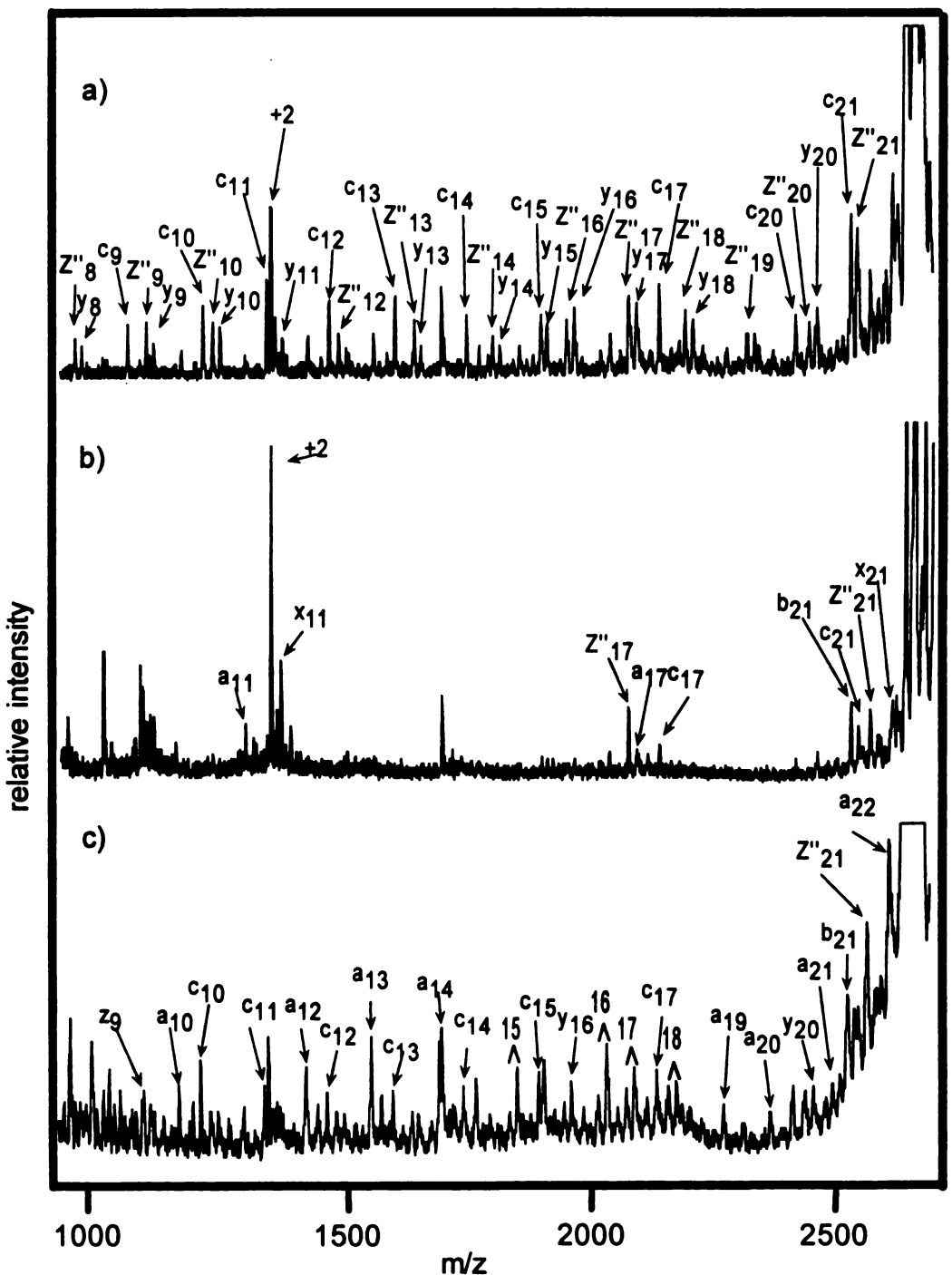


Figure 5.4 Prompt fragmentation spectra of MSH withe a)DHB, b)HCCN, c)BMN karat symbol above two peaks represents pairs of an and an - NH₃ ions)

analyte molecule with very few fragments when analyzed in HCCN (Figure 5.4b.).

When BMN is the matrix for this very hydrophilic peptide a series of a_n ions are apparent in addition to the c_n , y_n and z_n ions (Figure 5.4c.). Of the three matrices that were used in this work BMN produced a PF-MALDI spectrum with the most peaks from prompt fragment ions. In addition the signals due to prompt fragment ions are the most intense when BMN is used as the matrix. Using this matrix some internal fragment ions are also formed. In addition, a series of $[a_n - 17]$ ions are also observed. For each of the a_n fragment ions in the series a_{15} - a_{18} , there is a corresponding peak that is seventeen Daltons lower. These peaks are shown as losses from the appropriate a_n fragment ions in Figure 5.4c.

The PF-MALDI spectra that we have observed for MSH and Dynorphin differ from the expected results. The types of fragmentation ions that have been observed are different from previously reported results. In order to compare our results to the results obtained in other laboratories, PF MALDI was performed with the b-chain of insulin. This analyte has been characterized by Brown *et al.*⁴ using both DHB and HCCN as matrices. When DHB is used in our instrument, at laser powers significantly above threshold, a portion of the spectrum obtained is shown in Figure 5.5a. In this spectrum the y_n and $z_n + 2$ ions are labeled as a pair when they appear, by the use of a bracket. The spectrum, both in terms of the m/z values and the relative intensities, is very similar to that reported by Brown. For both our results and the spectrum reported by Brown a number of prompt fragment ions are formed which appear to be predominantly c_n , y_n , and $z_n + 2$

30 29 28 27 26 25 24 23 22 21 20 19 18 17 16 15 14 13 12 11 10 9 8 7 6 5 4 3 2 1 xyz F-V-N-Q-H-L-B-G-S-H-L-V-Q-A-L-Y-L-V-B-G-Q-R-G-F-F-Y-T-P-K-A abc 1 2 3 4 5 6 7 8 9 10 11 12 13 14 15 16 17 18 19 20 21 22 23 24 25 26 27 28 29 30

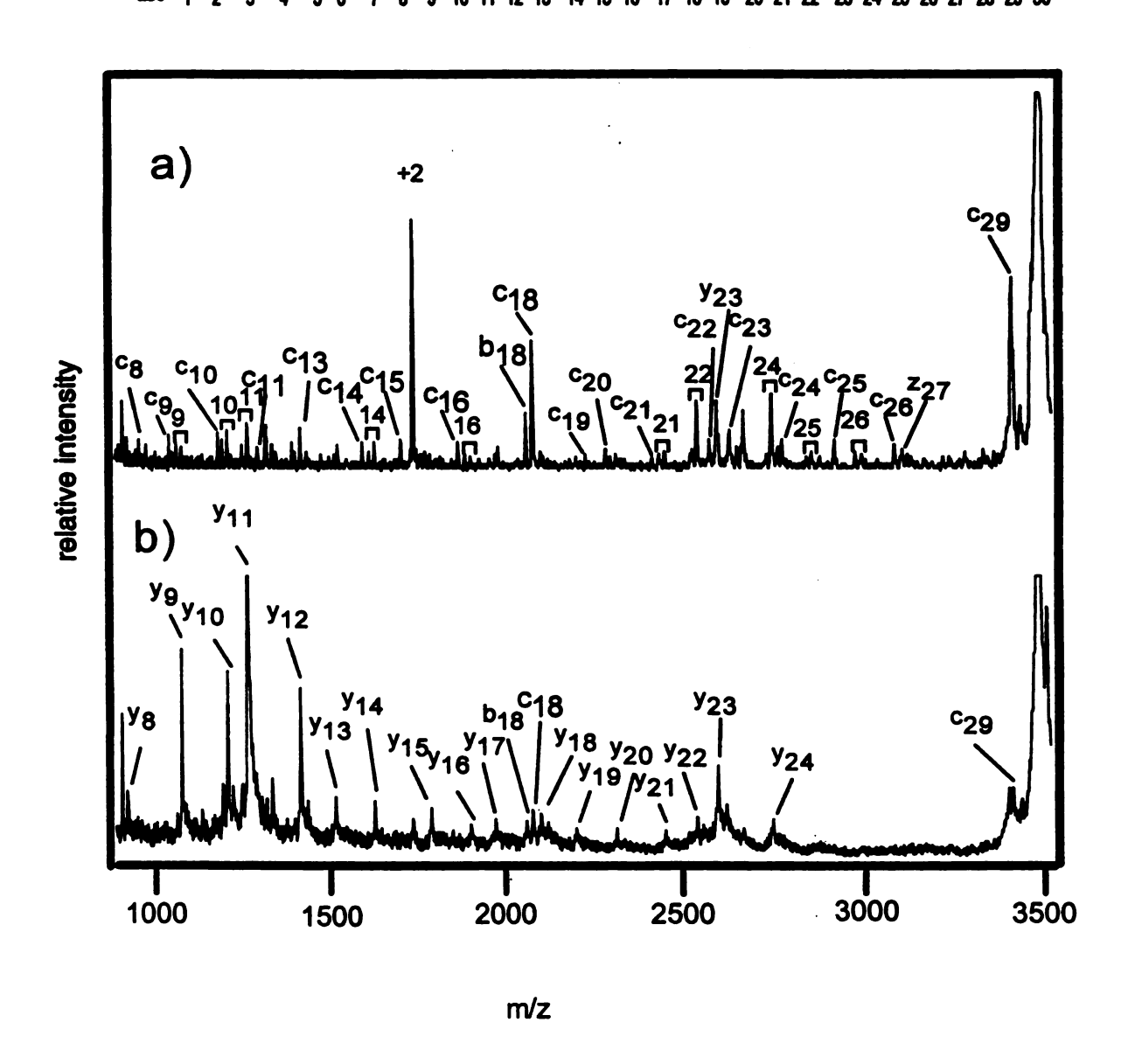


Figure 5.5 Prompt fragmentation spectrum of the b-chain of insulin in a) HCCN, b) DHB (square brackets represent pairs of y_n and z"_n ions)

fragment ions. The most intense peak in this spectrum is not a fragment ion at all, but the doubly charged [M+2H]⁺² peak. There are also two intense c ions. The c₂₉ fragment ion produces a very intense and broad peak. In addition the c₁₈ peak is also rather intense. All of these trends in the intensities of the peaks are very similar for the previously reported spectra and our own.

We obtained slightly different results when we used α -cyano-4-hydroxycinnamic acid as the matrix as shown in Fig. 5.5b. In this case we observed predominantly y_n fragment ions. This PF-MALDI spectrum included a series of y_n ions from y_8 - y_{24} . The spectrum contained only peaks from y_n ions unlike the previously reported result for the PF-MALDI spectrum of the b-chain of insulin in HCCN, which contained both a series of c_n and z_n+2 fragment ions as well as a series of y_n fragment ions. The most dominant feature of the PF-MALDI spectrum of the b-chain of insulin obtained using HCCN, is a very intense peak representing the y_{11} fragment. The intense peak from the y_{11} fragment is present in both the previously reported PF-MALDI spectrum and our results. While the results of our experiment are similar they are not identical. A speculation about why this may be due to differences in the hardware used. Brown's instrument maintains a field free region during the delay time². While our instrument maintains a 0.1% reverse bias during the delay time.

3. Chemistry of Fragmentation

Effect of Basic Residues

By examination of how different residues affect the fragmentation processes that occur, it should be possible to determine some of the mechanisms of fragment ion formation. One of the most important types of residues to understand are basic residues. Basic residues have been found to hinder the formation of fragment ions in the PSD-MALDI experiment⁵. The presence of basic residues does not seem to reduce the amount of fragmentation that occurs in the PF-MALDI experiment. All of the peptides studied have basic residues. Both dynorphin and melanocyte stimulating hormone have a high percentage of basic residues, yet they both readily undergo prompt fragmentation. In addition, the b-chain of insulin contains a small percentage of basic residues, yet it also produces many fragment ions in the PF-MALDI experiment. This result is the opposite of the trend that is observed in PSD 5. Basic residues actually seem to increase the amount of prompt fragmentation that is observed. Basic residues provide a preferred site for protonation on a peptide. When the basic residue is protonated, there is a suppression of the random backbone cleavages, that would otherwise occur⁶. The fact that basic residues do not reduce the amount of fragmentation indicates that charge initiated chemistry is not the only mechanism of prompt fragmentation. One product of the PF-MALDI experiment that is caused by basic residues are $[b_n +$ H₂O] fragment ions. These fragments are typically associated with basic

residues⁵. Examples of this type of fragmentation are observed in spectra of the b-chain of insulin and MSH which both contain a lysine residue immediately adjacent to the C-terminus.

Effect of Acidic Residues

Acidic residues in a peptide seem to have an effect on the type of prompt fragment ions that are formed, due to stabilization of transition states that can lead to additional fragment ions. One example is the prompt fragmentation that is produced by dynorphin, Figure 5.3. This analyte produces a series of a ions, $a_8 - a_{13}$ and $a_{15} - a_{16}$, when DHB is used as the matrix. An intense b_{14} and c_{14} fragment replaces the missing a_{14} fragment. The odd backbone cleavage in this series occurs when the n+1 residue is aspartic acid. This is the only acidic residue in the peptide. The same trend can be observed for the a_{14} ion when the matrix used is burnetanide or HCCN. This type of fragmentation has been observed in the PSD of charged derivatives 7 . The fragmentation of charged derivatives must occur through a charge remote process. In addition, the bulkiness of the charge derivatizing group may prevent the peptide from condensing into a distorted secondary structure.

Acidic residues also seem to effect the prompt fragmentation that occurs with melanocyte stimulating hormone. The effect can be seen most easily in the spectrum using HCCN as a matrix, Figure 5.4b. Since the PF-MALDI experiment typically produces the least fragmentation, it is reasonable to assume that HCCN produces only the lowest energy prompt fragment ions. The two most prominent

 c_n ions that are detected are the c_{11} and c_{21} ions. The c_{11} fragment occurs when the n+1 residue is glutamic acid and the c21 fragment occurs when the n+1 residue is aspartic acid. It is interesting to note in this spectrum that the two zn ions (z_{17} and z_{21}), both are formed via a skeletal cleavage of an acidic residue. A possible mechanism for the formation of the z₁₇ fragment ion could involve charge remote fragmentation with a hydrogen shift. In this mechanism the NH-CHR bond is cleaved, with an accompanying shift of the acidic hydrogen to the CHR group. Assuming that the initial protonation occurred at a site in between the cleaved bond and the C-terminus, a z_n+2 ion is produced. This mechanism only produces a product with the observed m/z of a z_0+2 ion if the fragmentation is a charge remote process. There seems to be no charge-initiated pathway available for a bond cleavage to produce this type of fragment ion. It is interesting to note that of the three glutamic acid residues in MSH, none of them form z fragment ions when HCCN is the matrix used, Figure 5.4b. The additional carbon present in the side-chain of glutamic acid produces a less stable 7 member ring transition state, compared to the six member ring that is formed with an aspartic acid residue.

The prompt fragmentation spectrum of the b-chain of insulin in HCCN, shown in Figure 5.5b, also is strongly affected by the presence of acidic residues. One of the few N-terminal fragments is a particularly intense c₁₈ ion. This fragment ion is the result of the cleavage of the peptide bond between cysteic acid and glycine. Cysteic acid is the oxidized form of the amino acid cysteine that contains the very polar sulfate group. PF-MALDI spectrum of the b-chain of

insulin in HCCN, also contains relatively intense y_{23} and y_{24} fragment ions, which represent cleavage of skeletal bonds involving a cysteic acid residue. A possible mechanism for this fragmentation is shown in equation 1.

In this mechanism a six-membered ring intermediate is formed with the sulfate group. The acidic hydrogen then shifts to the amide nitrogen on the C-terminal side of the side-chain and the amid bond is cleaved. The stable products of this reaction are SO₂ and CO₂ along with the peptide.

Analyte Structure

A closer look at the results of the PF-MALDI experiment with dynorphin and melanocyte stimulating hormone reveals that not all of the differences in the observed fragmentation are due to the matrix used. The PF-MALDI spectra of dynorphin with the three different matrices all have peaks from a_n and d_n fragment ions as well as peaks from c_n , y_n , and z_n fragment ions. The spectra of MSH in the same matrices do not seem to have nearly as many fragment ions and the fragment peaks are not as intense. The a_n and d_n fragments ions are

associated with charge-initiated high energy fragmentation processes⁸. This discrepancy is most likely due to the types of residues that are in these two different peptides. MSH contains nine large polar residues (arginine, lysine, aspartic acid, glutamic acid, glutamine, asparagine) and six small non-polar residues (glycine, alanine, and proline) of a total of 22 residues. Dynorphin contains eight of these large polar residues and three small non-polar residues out of 16 total residues. As shown in Table 5.1, the large polar residues appear to form a number of fragment ions by mechanisms similar to those already discussed. Small non-polar residues have been shown to restrict the fragmentation that can occur 3. Both glycine and proline have been observed to prevent the formation of c_n fragment ions that would result cleavage of the N-CHR bond. The residues with small non-polar sidechains are least likely to stabilize the transition state of a fragmentation process. Large polar residues have been observed to allow more fragmentation reactions to occur in the PSD spectra of N-terminal charged derivatives⁷. The observation that so much of the fragmentation that we observe occurs through the same type of process, instead of the processes observed in PSD of standard peptides, indicates that prompt fragmentation shares some characteristics of PSD fragmentation of charged derivatives. One possibility is that the fragmentation in PF-MALDI is not charge directed.

Peptide	# residues	% acidic	% basic	% polar	lons obsvd
MSH	22	23%	23%	46%	c _n , y _n , z _n
Dynorphin	16	6%	31%	37%	C _n , y _n , Z _n ,
b-chain of insuin	30	6%	0%	6%	c _n , y _n , z _n (weak)

Table 5.1. Effect of type of residues on fragmentation

The secondary structure of the analyte is also likely to be a factor to consider in the mechanism of prompt fragmentation. As already discussed the charged derivatives would have little secondary structure. The fact that so much stabilization seems to occur by neighboring sidechains, in a manner similar to that observed for charged derivatives, suggests that the secondary structure of the analyte during fragmentation is linear. In addition, the absence of a series of b_n ions indicates that there is no significant secondary structure. To form the typical b ion, significant secondary structure is necessary to produce a stable protonated oxazolone 9. Possible fragmentation mechanisms to produce c_n and v_n prompt fragment ions are shown in equations 2 and 3 respectively.

The c_n ion could be formed by a transfer of a hydrogen from the n+1 sidechain to the nitrogen at the N-terminus of the same residue. The N-CHR bond would then cleave. Although this mechanism is shown as a charge remote process it could also occur as a charge-initiated process. This mechanism takes into account the need for an n+1 residue that is not glycine or proline and the proposed linear

structure of the peptide at the time of fragmentation. The prompt fragmentation to form y_n ions could occur through a hydrogen shift from the alpha carbon to the nitrogen on the C-terminal side with an accompanying cleavage of the amide bond.

4. Combining Matrices

Only a limited amount of mechanistic information can be determined by analyzing the prompt fragmentation products of a few analytes with different matrices. If a prompt fragment could be selected for post source decay, then the structure of the prompt fragment ion could potentially be determined. Using the conditions that have been explored already, this experiment has not been possible. The method of combining matrices was explored as a means to make the prompt fragmentation – post source decay (PF-PSD) experiment possible.

Both HCCN and BMN have rather extreme characteristics as prompt fragmentation matrices. While BMN produces very good fragmentation for some analytes, it has a higher laser threshold and tends to produce noisy spectra. In addition BMN performs poorly for analytes that are over 3 kDaltons.

Alternatively, HCCN has a low laser threshold and has a higher mass limit but produces relatively little fragmentation. In an attempt to gain more control of the type of fragment ions that are formed in the PF-MALDI experiment, mixtures of the HCCN and DHB with BMN were explored. By combining these two matrices, unique results can be obtained. The combination that was found to be the most useful was 80% BMN and 20% HCCN. This combination of matrices produced

high mass ions and a large number of fragment ions. Figure 5.6a shows the results of using burnetanide for the analysis of the b-chain of insulin at low power. Only a few peaks from fragment ions are observed and their intensities are very low. Figure 5.6b shows the spectrum of b-chain of insulin in HCCN at the same laser power. This is a high laser power for HCCN and the spectrum is very noisy and contains relatively few peaks. The much improved results of using the combined matrix are displayed in Figure 5.6c. All of the peaks that were recognizable in Figures 5.6a and 5.6b are also present in this low noise spectrum. In addition the y₁₁ fragment peak is still very intense. The intensity of this peak makes it an ideal candidate for prompt fragmentation - post-source decay analysis.

5. Prompt Fragmentation-Post Source Decay

The combination matrix was used for the prompt fragmentation post source decay analysis of the y₁₁ fragment of the oxidized b-chain of insulin, Figure 5.7 Localized positive charges have been shown to produce simplified post source decay spectra. The spectra shown in Figure 5.7, have a great number of fragment ion peaks. The post source decay analysis of prompt fragment ions could be useful in determining the structure of the prompt fragment ions. The structure of the y₁₁ prompt fragment could have two different types of structures. The charge could be isolated on the N-terminal nitrogen. This structure should fragment to produce N-terminal fragment ions ⁷. Alternatively there could be a wide variety of structures with the proton residing on any of the

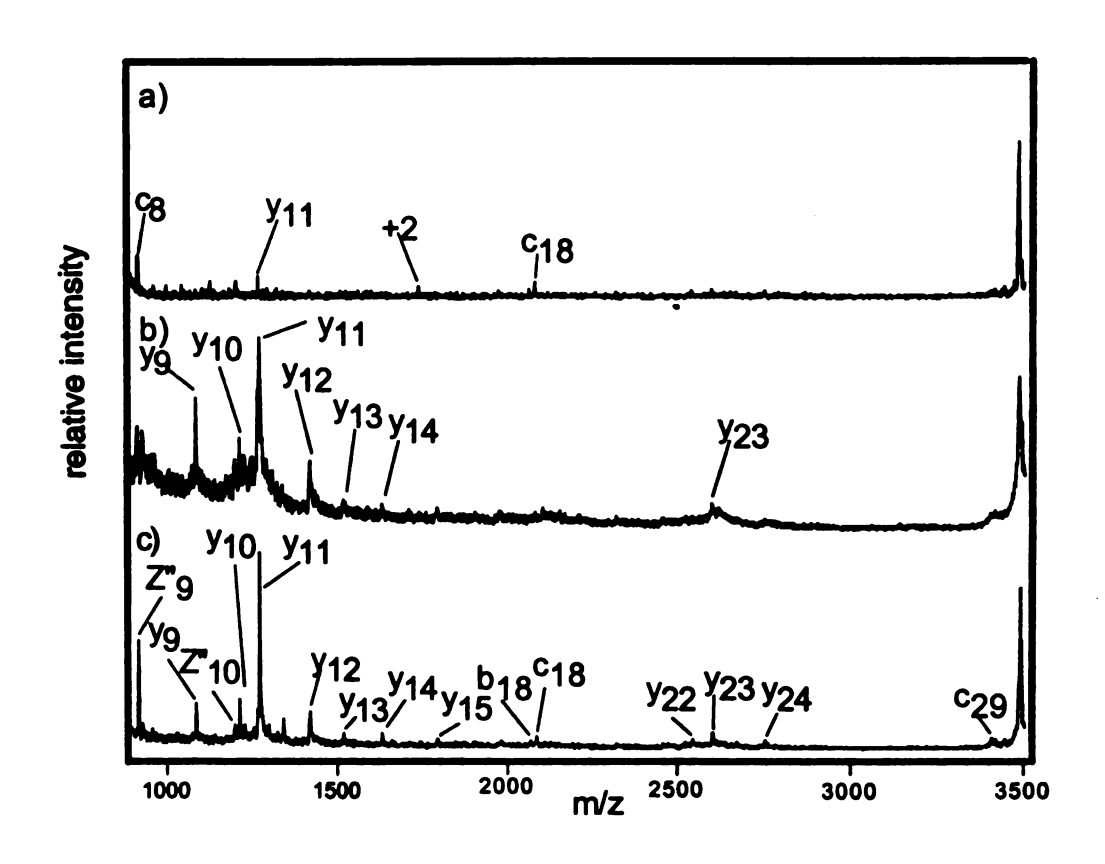


Figure 5.6 Prompt fragmentation spectra with BMN, HCCN and a mixed matrix

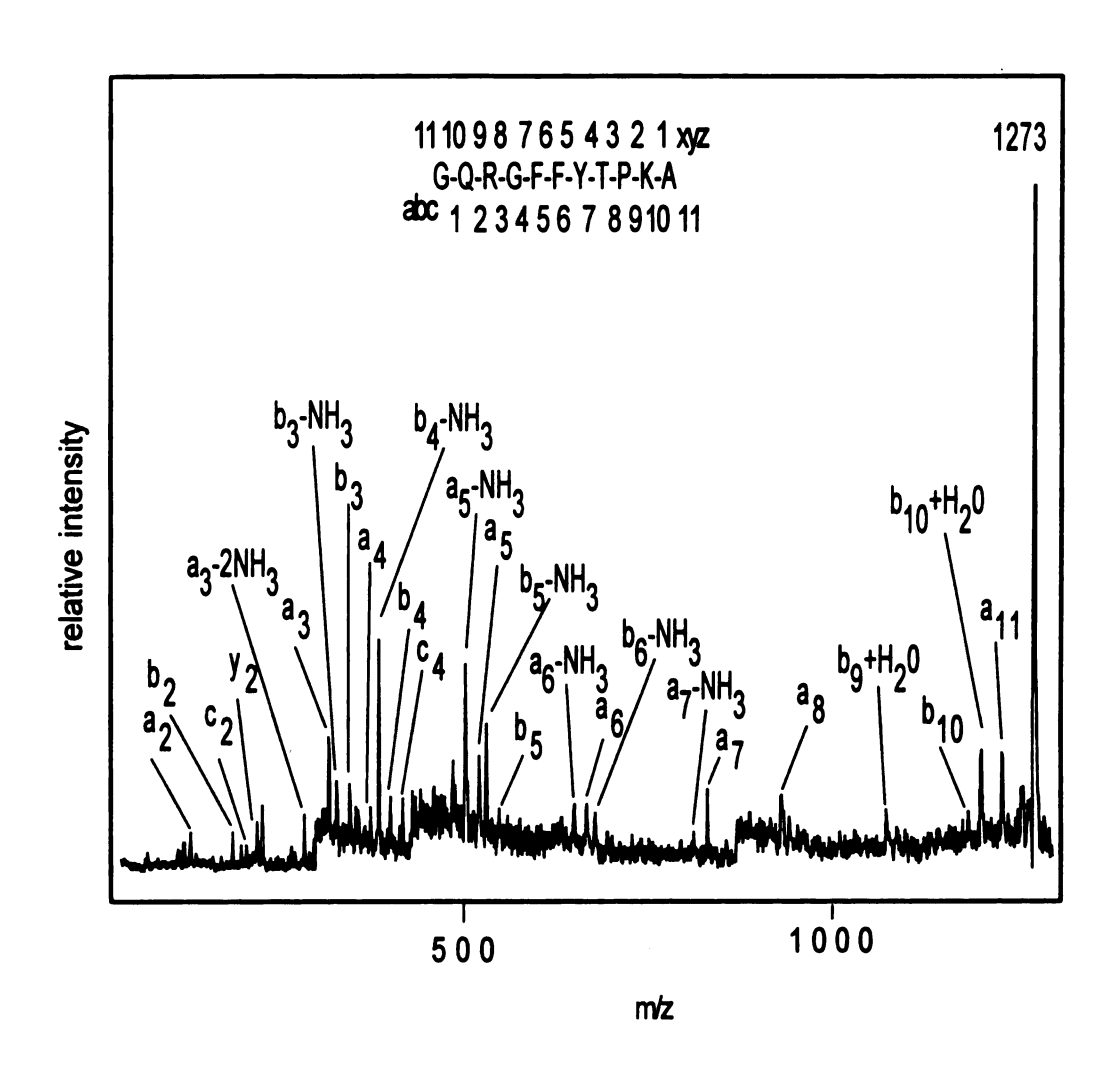


Figure 5.7 Post source decay of the y₁₁ prompt fragment ion of the b-chain of insulin

amide nitrogens. In fact the proton could be mobile during the decomposition process 6. Alternatively the charge could be isolated on the N-terminal nitrogen. In the prompt fragmentation post source decay spectrum shown in Figure 5.7. almost exclusively N-terminal fragments are observed. One surprise is that there are also many fragments that show a further loss of 17 Da corresponding to a loss of NH₃. In some cases there are 2 NH₃ losses for the same fragment. The second NH₃ loss must be from an arginine sidechain. None of the fragment ions that do not contain arginine show a loss of NH₃. However the a₃ fragment ion, which is the lowest mass N-terminal fragment ion that contains an arginine residue, produces fragment ions with both a loss of one and two NH₃ molecules. The a_5 fragment shows the same pattern of loss of NH₃ except that the $[a_5 - NH_3]$ peak is smaller than the a₅ fragment peak. It is interesting to note that the intensity of the peak from the a_4 ion is weak and there is no peak from $[a_4 - NH_3]$. There are many more fragment ions near the N-terminus than the C-terminus. Most likely this is due to the charge being isolated on the N-terminus. The charge is most likely not located on the arginine residue since no peaks are present to indicate a y_9 or y_{10} fragment ion. These peaks would most likely be intense is the charge was localized on the arginine residue. Two other peaks of interest are the $[b_9 + H_2O]$ and $[b_{10} + H_2O]$ fragment ions. This type of fragmentation is rare, however it has been observed with basic residues.5

6. Conclusion

In this work the use of burnetanide as a matrix for PF-MALDI has been demonstrated. Burnetanide produces a greater number of prompt fragment ions than other matrices that have been examined for PF-MALDI. In addition, burnetanide can be combined with HCCN to make the to make the PF-PSD experiment possible.

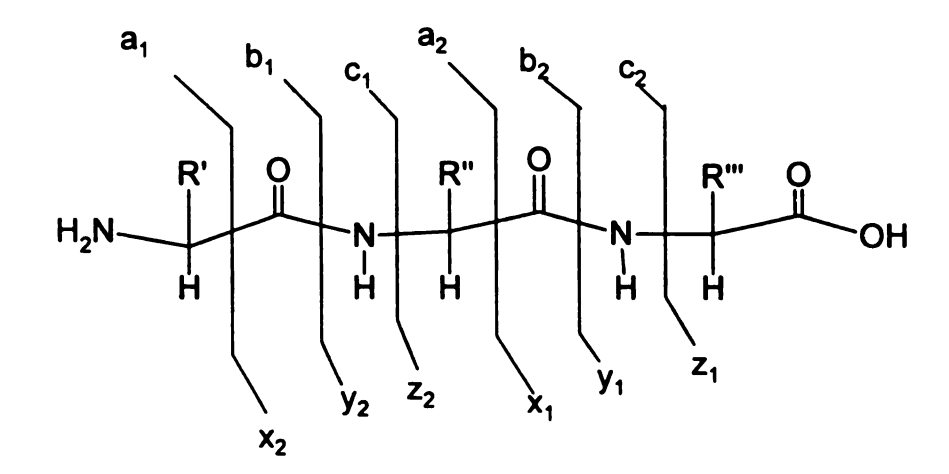
By analyzing the PF-MALDI spectra of a three peptides it has also been possible to make some mechanistic observations. In general both basic and acidic residues seem to increase the number of prompt fragment ions that are observed for a given peptide. It seems that large polar molecules increase the amount of prompt fragment ions while small non-polar residues hinder the process of prompt fragmentation. The large polar side chains are most likely stabilizing transition states that lead to peptide backbone cleavages, indicating that the peptides have a relatively linear secondary structure during the prompt fragmentation process. Finally the observation that all of the fragment ions produced in the PF-PSD of the y₁₁ fragment of the b-chain of insulin contain the N-terminus, indicates that the fragment's charge is isolated on the N-terminus. Apparently some prompt fragmentation can proceeds through a charge-initiated pathway.

7. References

- 1)Zhu, Y. F.; Taranenko, N. I.; Allman, S. L.; Taranenko, N. V.; Martin, S. A.; Haff, L. A.; Chen, C. H. *Rapid Communications in Mass Spectrometry* **1997**, *11*, 897-903.
- 2)Brown, R. S.; Lennon, J. J. Analytical Chemistry 1995, 67, 3990.
- 3)Lennon, J. J.; Walsh, K. A. Protein Science 1997, 6, 2446-2453.
- 4)Brown, R. S.; Carr, B. L.; Lennon, J. J. Journal of the American Society of Mass Spectrometry 1996, 7, 225-232.
- 5)Dikler, S.; Kelly, J. W.; Russell, D. H. *Journal of Mass Spectrometry* **1997**, *32*, 1337.
- 6)Dongre, R. A.; Jones, J. L.; Somogyi, A.; Wysocki, V. H. *Journal of the American Chemical Society* **1996**, *118*, 8365.
- 7)Liao, P.-C.; Huang, Z.-H.; Allison, J. Journal of the American Society of Mass Spectrometry 1997, 8, 501-509.
- 8) Rouse, J. C.; Yu, W.; Martin, S. A. Journal of the American Society of Mass Spectrometry 1995, 6, 822-835.
- 9) Yalcin, T.; Khouw, C.; Csizmadia, I. G.; Peterson, M. R.; Harrison, A. G. Journal of the American Society of Mass Spectrometry 1995, 6, 1164-1174.

Appendix

standard backbone cleavages occur as follows



$$H_2N$$
 H_2N
 H_3N
 H_4N
 H_4N
 H_5N

$$\begin{array}{c|c} & b_2 \\ & R' & O & R'' + \\ & & M & H & H \end{array}$$

$$C_{2}$$

$$H_{2}N \xrightarrow{R'} O \xrightarrow{R''} O \xrightarrow{I+} N-H$$

$$H_2N$$
 H_1
 H_2
 H_3
 H_4
 H_5
 H_5

R"b- partial sidechain

